Supplementary Information

Supplementary Methods

<u>Computational Techniques</u>

Overview of Anti-bZIP Design Using CLASSY

CLASSY is a computational design procedure for optimizing the stability of a particular structural state as a function of sequence, under an arbitrary number of constraints. It is compatible with many types of potential functions. Any linear analytical function of sequence variables can be constrained; examples include energy gaps towards other structures, or properties such as amino-acid composition or hydrophobicity.

CLASSY is based on two components: cluster expansion (CE) and integer linear programming (ILP) optimization. CE provides a way to express the energy of a sequence adopting a particular backbone structure as an algebraic function of the sequence itself[28]. The formal basis of the technique is briefly described in the next section, but two properties of a cluster expansion are important for CLASSY: (1) it makes the evaluation of sequence energies many orders of magnitude faster than with direct structural methods, and (2) its simple functional form renders a new set of computational approaches applicable to protein design. We used CE in conjunction with ILP as a way to incorporate information about undesired states into design calculations.

Theory of Cluster Expansion

We have previously shown that the conformational energy of a protein sequence in a specified fold, defined numerically using structural calculations and optimization, can be expressed as a direct function of sequence using the method of cluster expansion[28, 29]. For completeness, we briefly describe this method here. Let $E_{\min}(\vec{\sigma})$ be the energy of sequence $\vec{\sigma}$ in a given backbone fold (subscript *min* stands for minimization over side-chain degrees of freedom). Let $\vec{\sigma} = \{\sigma_1, ..., \sigma_N\}$, where σ_i is a discrete variable representing the amino acid at the *i*-th position of the sequence. For simplicity, and without loss of generality, assume that in our design problem there are *M* amino-acid possibilities at each position and σ_i can take on values from 0 to *M*-1. We can then express $E_{\min}(\vec{\sigma})$ as a cluster expansion of the form:

$$E_{\min}(\vec{\sigma}) = J_o + \sum_{si=1}^{N}\sum_{i=1}^{M-1} J_{si}^{i} \cdot \varphi(si,i) + \sum_{si=1}^{N-1}\sum_{sj=si+1}^{N}\sum_{i=1}^{M-1}\sum_{j=1}^{M-1} J_{si,sj}^{i,j} \cdot \varphi(si,i) \cdot \varphi(sj,j) + ...,$$

where $\varphi(si,i)$ is a binary function that evaluates as 1 if site *si* is occupied with amino-acid *i* and zero otherwise. The summations are over sites and amino-acid identities. A collection of sites is referred to as a cluster, and a cluster populated by a given set of amino acids is a cluster function (CF). Terms J are the effective contributions of each cluster function to the overall energy (effective cluster interactions, or ECI). The three terms shown correspond to the constant, point and pair cluster-function contributions. If the expansion is written out in its entirety (i.e. up to the N-tuple cluster functions), then by virtue of having exactly the same number of ECI as possible sequences (M^N), it is exact. If the expansion is truncated at a given point, an approximation of $E_{\min}$ can be derived by fitting the ECI to minimize the error between CE-estimated energies and structure-derived energies for a training set of sequence-energy pairs. Once this procedure is carried out, the process of estimating the energy of a sequence adopting the specified structure is made many orders of magnitude more efficient [28].

bZIP Models

To model parallel dimeric coiled coils, we employed two variants of the energy function HP/S/C that was previously shown to perform well in predicting human bZIP interaction specificity[26]. This function evaluates the relative stability of coiled-coil dimers primarily as a function of the amino acids at **a**, **d**, **e** and **g** positions, based on predicted structures of coiled-coil complexes. One of the key features of model HP/S/C is that core **a-a'** and **d-d'** terms derived from structure-based calculations are replaced with statistical weights from a machine-learning algorithm[26]. These terms can alternatively be replaced by experimentally determined thermodynamic coupling energies. However, these were only available for 15 amino-acid pairs at **a-a'** at the time of our earlier study[39], and using them gave inferior performance. Since then, Vinson and co-workers have measured coupling energies for 55 amino-acid pairs at **a-a'**[22]. Additionally, we recognized that almost all of the improvement upon replacing **d-d'** interactions with statistical weights can be attributed to Leu-Leu pairs, which are modelled as only slightly favourable in structure-based approaches, contrary to experimental data. As a result of these findings, we developed model HP/S/Cv. Structure-based **a-a'** interactions were replaced with **a-a'** coupling energies for 55 amino-acid combinations; the **d-d'** interaction for Leu-Leu was replaced with –2 kcal/mol (no experimental value is available), and the resulting model was expanded using CE. Because effective self contributions from our structural models and experimental coupling energies may be on different scales, point ECI values for the **a** position were adjusted such that 100 folding free energies measured by Acharya *et al*. were predicted optimally (in the least squares sense) by the overall CE model – see Supplementary Fig. 10.

As a way to account for pair-wise interactions in the reference state, both variant models used in this study ignored the energy of intra-chain side-chain interactions in the final predicted structure (see reference [26]). Note, however, that because the process of placing side chains for structure prediction does take into account all side-chain interactions, intra-chain interactions do make indirect contributions to the final energy, and corresponding ECI do emerge in cluster expansion.

Integer Linear Programming

Kingsford *et al.* have shown that the problem of finding the lowest-energy rotamer-based side-chain packing arrangement, in the context of protein design, can be expressed and solved as an ILP [27]. Given that CE provides the energies of the desired and undesired states as analytical functions of sequence, we introduced a similar approach for handling specificity in design. With notation as in Kingsford *et al.* [27], we represent the sequence space in our problem of designing a peptide of length *p* as an undirected *p*-partite graph with node set $V = V_1 \cup \ldots \cup V_p$. Set V_i contains one node for each amino-acid possibility at position *i*. For each state *S*, each node $u \in V_i$ is assigned a weight E_{uu}^S corresponding to its contribution to the energy of that state. If *S* is a heterodimer state (i.e. a state in which the design is complexed with a protein of fixed sequence), this individual contribution is simply the sum of the point ECI corresponding to *u* and pair ECI corresponding to pairs between *u* and all amino acids of the partner sequence. If *S* is the design•design homodimer state, then E_{uu}^S is the sum of point ECI corresponding to *u* and pair ECI of *u* and its image on the opposite chain. The edges of the graph $D = \{(u,v): u \in V_i \text{ and } v \in V_j, i \neq j\}$ are assigned weights E_{uv}^S. If *S* is a heterodimer state, then E_{uv}^S is the ECI of the corresponding intra-chain pair cluster function. If *S* is the design•design homodimer state, then additional contributions to E_{uv}^S come from the ECI between *u* and the image of *v* as well as *v* and the image of *u*. Given these definitions, the energy of the design sequence in any state *S* can be expressed as $\varepsilon^S = \sum_{u \in V} E_{uu}^S x_{uu} + \sum_{u,v \in D} E_{uv}^S x_{uv}$, where binary variables x_{uu} and x_{uv} determine which nodes and edges the sequence involves. Thus, the problem of optimizing the energy of state *S* can be expressed as an ILP seeking to minimize ε^S, under the constraint that the chosen nodes and edges correspond to one another. Further, because gaps between different states are also linear functions of decision variables x_{uu} and x_{uv}, arbitrary gap constraints can also be incorporated. Finally, any additional function of these decision variables, such as a PSSM score, can also be incorporated. With *T* as the target state and U_i representing undesired states, the ILP we used in this study is (where $V\backslash V_j$ stands for the set difference between *V* and V_j):

$$\text{Minimize}: \varepsilon^T = \sum_{u \in V} E^T_{uu} x_{uu} + \sum_{u,v \in D} E^T_{uv} x_{uv}$$

subject to:

$$\sum_{u \in V_j} \mathrm{x}_{\mathrm{uu}} = 1 \quad \text{for } j = 1,...,p$$

$$\sum_{u \in V_j} \mathrm{x}_{\mathrm{uv}} = x_{vv} \quad \text{for } j = 1,...,p \text{ and } v \in V \setminus V_j$$

$$\varepsilon^{U_1} - \varepsilon^T > gc_1, \text{ where } \varepsilon^{U_1} = \sum_{u \in V} E^{U_1}_{uu} x_{uu} + \sum_{u,v \in D} E^{U_1}_{uv} x_{uv}$$

...

$$\varepsilon^{U_k} - \varepsilon^T > gc_k, \text{ where } \varepsilon^{U_k} = \sum_{u \in V} E^{U_k}_{uu} x_{uu} + \sum_{u,v \in D} E^{U_k}_{uv} x_{uv}$$

$$\sum_{u \in V} W_u x_{uu} < pssmc$$

$$x_{uu}, x_{uv} \in \{0,1\}$$

Here k is the number of undesired states, gc_i is the gap constraint for i-th state, *pssmc* is the PSSM constraint and W_u is the PSSM weight corresponding to node u. We solved such ILPs with the *glpsol* tool from the GNU Linear Programming Kit (http://www.gnu.org/software/glpk/). Because of the simplicity of sequence-based expressions obtained through CE, solutions to these ILPs with as many as 46 undesired states were generally obtained within 1-5 minutes on a single 2.7 GHz CPU.

Note that although everything was formulated in this instance for energy functions that are pair-wise decomposable at the sequence level, in principle this approach can be easily generalized for higher-order terms. Clearly, the CE methodology is already capable of taking higher-order interactions into account, should there be a need [28]. The ILP formulation can be extended to handle higher-order terms by introducing additional decision variables. For example, x_{uvw} would be 1 if there is a triplet interaction between nodes u, v, and w. Constraints for these new decision variables would also have to be imposed to ensure that higher-order interactions occur only between those nodes that are chosen (e.g. in this case x_{uu}, x_{vv} and x_{ww} are 1). Note that these higher-order decision variables would have to be introduced only for those clusters of sites that do, in fact, participate in higher-order interactions. This allows the complexity of the ILP problem to grow naturally with the size of the system (i.e. the number of variables and constraints grows linearly with the number of interactions in the system).

PSSM Constraint

To constrain CLASSY designs to favour a leucine-zipper fold, we derived heptad position-specific amino-acid frequencies from the multi-species alignment of 432 bZIP leucine zippers described above. These frequencies were then used to score all of the sequences in the alignment (taking into account only **a**, **d**, **e** and **g** positions), from which a length-normalized score distribution was derived. Based on this distribution, a cutoff value of 0.247 was imposed in CLASSY such that all of the designed sequences had a PSSM score of at least 0.247. Although this is a stringent cutoff, with 84% of native sequences scoring below it, the sequence space remaining is still large. For example, for a six-heptad design sequence, where **a**, **d**, **e** and **g** positions are varied and 10 amino acids are allowed per position, the total sequence space is 10^{24}, whereas after applying the PSSM cutoff of 0.247 it is still ~10^{18} (calculated by convolving score distributions at individual positions to obtain the final distribution of scores and integrating it from 0.247 up).

Choosing b, c and f Positions

Positions **a**, **d**, **e** and **g** are assumed to encode most of the interaction specificity of the designed peptides[19, 40]. Thus, we chose the identities of the **b**, **c** and **f** positions such that they were appropriate for the already selected **a**, **d**, **e**, and **g** positions, given what is observed in the multi-species dataset of 432 bZIP sequences referenced above. Thus, for each **b**, **c**, and **f** position b_i we sought to optimize $P(b_i|a_1,...,a_n)$, where $a_1 \ldots a_n$ are the identities of the selected **a**, **d**, **e**, and **g** positions. We expressed this quantity in terms of probabilities we could measure from the dataset:

$$
\begin{aligned}
P(b_i|a_1,...,a_n) &= \frac{P(b_i,a_1,...,a_n)}{P(a_1,...,a_n)} = \frac{P(a_1|b_i,a_2,...,a_n)\cdot P(b_i,a_2,...,a_n)}{P(a_1,...,a_n)} \\
&= \frac{P(a_1|b_i,a_2,...,a_n)\cdot P(a_2|b_i,a_3,...,a_n)\cdot ...\cdot P(a_n|b_i)\cdot P(b_i)}{P(a_1,...,a_n)} \\
&\approx \frac{P(a_1|b_i)\cdot P(a_2|b_i)\cdot ...\cdot P(a_n|b_i)\cdot P(b_i)}{P(a_1,...,a_n)}
\end{aligned}
$$

The last step assumes that the pre-selected amino-acid decoration at positions **a**, **d**, **e**, and **g** represents well the natively observed decorations at these positions (i.e. probability $P(a_k|b_i)$ measured in the **adeg** context of the designed peptide and the probability averaged over all native contexts is the same). Quantity $P(a_1,...,a_n)$ is hard to estimate, but it is constant with respect to **b**, **c** and **f** and is therefore not important. Conditional probabilities $P(a_k|b_i)$ can be easily measured from the native bZIP dataset, and for each **b**, **c** and **f** position the amino acid that optimizes the above probability can be found. Using this approach, we were able to obtain **b**, **c**, **f** decorations of natural content and distribution. However, we found that infrequently this procedure resulted in sequences with large charge and/or helix propensity (mostly due to the fact that the pre-selected **a**, **d**, **e**, and **g** amino acids already had high values of charge or helix propensity). Thus, we expressed the problem of finding the optimal **b**, **c** and **f** combination according to the above equation as an ILP (by taking the logarithm of the probability it can be decomposed into a sum of pre-computed probability logarithms) and incorporated constraints on total charge, charge content (number of charged residues) and helix propensity. For each property, the range of acceptable values was defined as $\mu \pm \sigma$, where μ and σ are the mean and standard deviation of the corresponding property in the native bZIP dataset. In a few instances this resulted in no solutions (i.e. the selected **a**, **d**, **e** or **g** were already outside of the range for one of the properties) and for these cases more liberal intervals were allowed (either $\mu \pm 1.5\sigma$ or $\mu \pm 2\sigma$). Finally, because we wanted to rely on UV absorbance for determining concentration, we imposed the additional constraint that the **b**, **c**, **f** positions contain at least one Y or W residue (unless there was one already present at **a**, **d**, **e** or **g**).

Uncovering Specificity-encoding Features

We analyzed the 8 designs determined to be most specific using the arrays to identify specificity-encoding features. First, we compared each design•target complex with the corresponding design•undesired heterocomplexes. For each such comparison, we computed the contribution of each amino acid in the *i*-th position of the design sequence (aa_i) to the overall stability and specificity. This was done by computing the interaction of aa_i with the region of the target peptide from *i*-7 to *i*+7 (one heptad N- and C-terminal to aa_i) as well as the interaction of aa_i with the same region of the undesired partner. The first value corresponded to the stability contribution of aa_i and the difference between the two was the specificity contribution. To further isolate specificity determinants, this difference was decomposed into contributions from different positions on the target sequence and the corresponding positions on the undesired partner sequence.

We performed a similar analysis to elucidate features encoding specificity against the design•design homodimer, except the contribution of each amino acid aa_i to specificity was considered as the difference between interaction of aa_i with the residue opposing it in the target sequence and its interaction with itself in the design homodimer. The same analysis was repeated for pairs of amino acids at all position pairs (*i* and *j*) of the design sequence.

Dividing Human bZIPs into 20 Families

Human bZIPs were divided into 20 families based on the evolutionary analysis of Amoutzias *et al.* [41] with the exception of including CHOP and ZF as individual families, and condensing OASIS and OASISb into a single family based on the similarity of their interaction profiles [4]. The phylogenetic tree of human bZIPs shown in Supplementary Fig. 13 was made using only the leucine-zipper regions and was constructed with the PHYLIP (http://evolution.genetics.washington.edu/phylip.html) package using the Neighbour-Joining algorithm and the Jones-Taylor-Thornton (JTT) model of amino-acid replacements. TreeDyn (http://www.treedyn.org/) was used to visualize and annotate the tree.

How Many Unique anti-bZIP Profiles Are There?

Fig. 3A shows that our CLASSY designs exhibit many novel interaction profiles when binding human bZIPs, while the sequence diversity used to generate these profiles is rather limited (Fig. 3C). This suggests that there may be a very large number of different interaction profiles, of which our 48 designs have revealed only a very small portion. But how large is this number? To answer this question with high confidence we need either an extremely large number of designs and measurements or an extremely accurate model. At present, neither is available. However, if we have a good idea of a model's prediction accuracy and use this model to calculate the number of unique profiles that exist, we can then estimate a lower bound on the true number of profiles. Here, we used model HP/S/Cv for this purpose. Several steps were taken to ensure that our estimates were always below the true number of profiles.

The interaction profile of a peptide was defined as a binary vector indicating whether the peptide interacts (1) or does not interact (0) with each human bZIP. If two binary vectors are equal, the profiles are equivalent. In reality, there is a lot of space between such vectors, because interaction strength also plays a role in defining a profile. This is one way that we underestimated the total number of possible profiles. We also defined these vectors at the family level rather than the protein level – again, a significant underestimate of the real size of the profile space. We considered 19 out of the 20 families (due to difficulties assessing model performance on the ATF3 family), giving a total of 524,288 possible unique profiles. The following procedure was followed:

Compute the total number of unique profiles predicted by HP/S/Cv. For each human bZIP coiled coil P_i we defined a computational energy cutoff c_i to optimally discriminate interactions and non-interactions in the human bZIP interaction dataset (experimental interactions/non-interactions taken from Fong *et al.* [25]). To increase prediction confidence, we introduced a buffer parameter b, such that energy scores above c_i+b were considered non-interactions, below $c_i - b$ were considered interactions, and scores between $c_i - b$ and c_i+b were not considered as either (b was set to 3 kcal/mol by optimizing performance on the human bZIP interaction dataset). This parameter increases prediction confidence but reduces the number of peptides that can give rise to a profile, further reducing our final estimate. Next, we generated 1,000 random binary profile vectors and ran CLASSY to find the most stable sequence consistent with each profile (e.g. its interaction stability with each of the 40 bZIPs from the 19 considered families is either below $c_i - b$ or above c_i+b in accordance to the profile). The bZIP PSSM constraint was applied. Out of these 1,000 cases, 5 produced a solution. Given that there are a total of 524,288 possible binary profiles, this translates into ~2,600 unique profiles that can be achieved in design.

Estimate prediction rates. The rates of true positive (*TP*), true negative (*TN*), false positive (*FP*) and false negative (*FN*) predictions were estimated from anti-bZIP•bZIP interaction data. Performance is expected to be worse than for the human•human dataset for several reasons. First, the process of design tends to exacerbate errors in an energy function. Second, because designed sequences are different from native bZIPs in systematic ways, the ranges of HP/S/Cv scores for anti-bZIP•bZIP and bZIP•bZIP interactions will also be different, making cutoffs derived from the bZIP•bZIP dataset less applicable to anti-bZIP•bZIP interactions. Thus, although the prediction rates for the human•human interactions were $TP = 0.84$, $TN = 0.91$, $FP = 0.16$, $FN = 0.09$, they were worse for the anti-bZIP•bZIP interactions: $TP = 0.39$, $TN = 0.94$, $FP = 0.61$, $FN = 0.06$. The drastic difference between the two performance rates is a result of over-training optimal cutoffs to the case of human•human interactions, but since the most important goal here is not to over-estimate the performance rate, this approach is still valid. The performance predicting relative stabilities of two complexes of anti-bZIP•bZIP is much better than this.

Given two predicted distinct profiles, find the probability that they are in fact the same. This probability, *ps*, is a product of the probabilities that each individual element of the profile (interaction or non-interaction with each human bZIP) is the same. Formally,

$$ps = (TN \cdot TN + FN \cdot FN)^{zz} \cdot (TN \cdot FP + FN \cdot TP)^{oz} \cdot (TP \cdot FN + FP \cdot TN)^{zo} \cdot (TP \cdot TP + FP \cdot FP)^{oo},$$

where *oo*, *oz*, *zo*, and *zz* are the number of corresponding profile elements that are both 1, 0 and 1, 1 and 0, or both 0, respectively. Probability *ps* was estimated to be $2.0 \cdot 10^{-4}$ by averaging over 1,000 pairs of randomly generated profiles.

Calculate the probability distribution of the true number of profiles. We predicted that there exist ~2,600 unique profiles. The first one we consider is certainly unique. The second one is predicted to be unique, but it is actually unique with probability $1 - ps$. The third one is also predicted to be unique, but it is truly different from the first and the second with probability $(1 - ps)^2$. In general, if $P(k, n)$ is the probability of having *k* unique profiles after considering *n* predicted unique profiles, then we can give the recursive definition $P(k,n) = P(k,n-1) \cdot k \cdot ps + P(k-1,n-1) \cdot (1-ps)^{k-1}$. Using this we generated the probability distribution of the true number of profiles after considering 2,600 profiles. This distribution had a sharp peak around 1,900 profiles and quickly fell to essentially zero before and after that (integral between 1,785 and 1950 is 0.9999). Based on this, there should exist at least ~1,900 unique peptide•human bZIP interaction profiles, and probably there are many more.

A Picture of Multi-state Energy Phase Space

Specificity-sweep calculations predict that designs selected solely for optimal binding to the target are often not specific, and are especially prone to homodimerization (see Supplementary Fig. 2A). Many specificity problems can be eliminated by sacrificing relatively small amounts of stability (Supplementary Fig. 2C). However, it is not clear how severe the specificity constraint is and how much it restricts the choice of sequences. We investigated this in a simplified case where design•design homodimers are the only competing state. We constructed a 2D histogram of the entire design sequence space for several design problems, looking at the distribution of design•target energies versus design•design energies. In such a histogram, each 2D bin corresponds to energy ranges for the design•design and the design•target complexes and contains the number of sequences that satisfy these ranges.

If each amino acid at each site made an independent contribution to the total energy, this histogram could be built by convolving the 2D energy histograms of each individual site. However, amino acids at different sites interact with each other. To address this, we used the fact that amino acids more than a heptad apart do not interact in our CE energy expressions. As in the case for independent site contributions, sites were considered one-by-one and their histograms were convolved with the running total. However, at each step energy contributions from both single-residue and pair-wise interactions with residues in the preceding heptad were incorporated. In order to account for the pair-wise terms appropriately, individual histograms were maintained for each unique sequence combination in the preceding heptad. To limit memory usage, only 9 amino acids were considered at each site for this purpose. Note that because positions **b**, **c** and **f** were not explicitly considered in our models, there were a total of 9^4 = 6,561 possible heptad sequences and 6,561 running total histograms needed to be kept at each stage. In the last step these 6,561 histograms were added to produce the final 2D histogram.

The results for ATF-2 and MafG are shown in Supplementary Fig. 12 (other bZIPs produced similar results). The dashed lines show where the design•design and design•target energies are equal. Clearly, most stable sequences are even more stable as homodimers (i.e. are below the line; note log scale), indicating that destabilization of the design homodimer is an extremely severe constraint that limits sequence space by many orders of magnitude.

Experimental Characterization

Jun family constructs

The following peptides were used for the Jun family, which have more uniform length than those previously constructed by Newman & Keating[4].

cJun

MSYYHHHHHHLESTSLYKKAGSGSRKLERIARLEEKVKTLKAQNSELASTANMLREQVAQLKQKVMNHLE,

JunB

MSYYHHHHHHLESTSLYKKAGSGSRKLERIARLEDKVKTLKAENAGLSSTAGLLREQVAQLKQKVMNHLE,

JunD

MSYYHHHHHHLESTSLYKKAGSGSGSRKLERISRLEEKVKTLKSQNTELASTASLLREQVAQLKQKVMNHLE

Data Analysis

Scanned images of slides were analyzed using the program Digital Genome (Molecularware). For each probe the scan at the highest PMT voltage that did not show saturation was used for analysis. The signal in the red channel from the Alexa Fluor 633 hydrazide was used to identify the location of spots. The median signal and median background for each spot was determined, and signal less background for each spot was calculated. Missed spots and artifacts were manually flagged and removed from analysis; these represented less than 0.1% of all spots. For each pair of adjacent sub-arrays probed with the same labeled peptide, the average of 8 measurements for each protein on the surface was calculated and defined as *a*. These values are reported in Supplementary Tables 3 – 5.

Two other quantities were used in analyses. Because a small number of probes showed high background, a corrected fluorescence signal was defined as F = $a - \tilde{a}$, with $\tilde{a}$ the median of all signals measured using a common probe. The maximum of this quantity for a given probe was designated F_{max}. The quantity $-\log(F/F_{max})$ was used in Fig. 2, Fig. 3A, and Supplementary Figures 1 and 14 to indicate relative array signal differences.

To distinguish signal from noise, and thus put an approximate lower bound on the signal required as evidence for an interaction, we defined the quantity S_{array} as $S_{array}(a) = \frac{(a-\tilde{a})}{\sqrt{\sum_{i=1,\, a_i<\tilde{a}}^{N} (a_i-\tilde{a})^2 \Big/ N_{a<\tilde{a}}}}$, where $\tilde{a}$ is again the median of *a*, *N* is the number of unique printed proteins, and $N_{a<\tilde{a}}$ is the number of proteins producing *a* below the median. *N* and $N_{a<\tilde{a}}$ excluded other designed peptides on the surface when the solution probe was itself a designed peptide. S_{array} is a Z-score-like quantity, where the distribution of signals below the median was assumed to be primarily noise-driven and thus was used to correct stronger signals. S_{array} values are also provided in Supplementary Tables 3 – 5.

For the purpose of estimating the number of designs that homodimerize, and how many designs interacted with their target, the following criterion was used: A and B were judged to give signal above background, and thus to interact, if they produced an S_{array} score above 2.5 either when A was on the surface and B was the probe or when B was on the surface and A was the probe. This cutoff was chosen based on reported homodimerization of bZIP families as well as our solution measurements of stability[4, 42, 43].

Interaction-Profile Clustering

An interaction profile was defined using $-\log(F/F_{max})$ scores derived from microarrays, and profiles were clustered using Eucledian distance as the dissimilarity metric. Average linkage clustering was performed using the *linkage* command in Matlab 6.5.

Circular Dichroism

Circular dichroism (CD) spectra were measured on AVIV 400 and 202 spectrometers in 12.5 mM potassium phosphate (pH 7.4)/150 mM KCl/0.25 mM EDTA/1M GuHCl/1 mM DTT. All mixtures of peptides were incubated at room temperature for several hours before measurement. Wavelength scans were performed at 40 μM total peptide concentration and measured at 25 °C in a 1-mm cuvette. Scans were monitored from 280 nm to 195 nm in 1 nm steps averaging for 5 seconds at each wavelength. Three scans for each sample were averaged. Thermal unfolding curves were performed at 4 μM total peptide concentration and measured in a 1-cm cuvette. Melting curves were determined by monitoring ellipticity at 222 nm with an averaging time of 30 seconds, an equilibration time of 1.5 minutes, and a scan rate of 2 °C/min. All samples were measured from 0 °C to 85 °C unless otherwise noted. All thermal denaturations were reversible. T_m values were estimated by fitting thermal denaturation data to a monomer-dimer equilibrium, assuming no change in heat capacity upon folding. Specifically, we fit the derivative of the CD signal with respect to temperature to the equation:

$$\frac{d(signal)}{dT} = A \cdot \frac{\Delta H}{RT^2} \cdot \exp\left(-\frac{\Delta H}{R}\left[\frac{1}{T_m} - \frac{1}{T}\right]\right)\left[\frac{4\exp\left(\frac{\Delta H}{R}\left[\frac{1}{T_m} - \frac{1}{T}\right]\right)+1}{\sqrt{8 \cdot \exp\left(\frac{\Delta H}{R}\left[\frac{1}{T_m} - \frac{1}{T}\right]\right)+1}} - 1\right].$$

Here A, ΔH, and T_m were fitting parameters, with ΔH and T_m corresponding to the change in enthalpy upon folding and the apparent melting temperature, respectively. We fit the derivative of the CD signal to reduce the reliance of the fit on pre- and post-transition baselines [44]. For two-species mixtures AB, the difference between the melting curve of the AB mix and the average of melting curves of A and B (S_{AB-A-B}) was calculated and treated as the signal for the purposes of fitting the above equation. No fitting was performed for mixtures where S_{AB-A-B} was positive at any point during the unfolding transition (i.e. the signal from the average was stronger than the signal from the mixture), as it was not clear which species was being melted. Those mixtures with $S_{AB-A-B} > 0$ over the entire temperature range were assumed to show no evidence of interaction. Fitting was performed using the non-linear least squares method in Matlab 6.0. The 95% confidence intervals resulting from the fits are reported in Supplementary Table 2.

Comparing CD and Array-based Stability Ordering

Relative stability orders established by CD and microarray were compared conservatively. The arrays were only used to judge relative stabilities when two interactions involved the same solution probe interacting with partners on the same array surface. CD ranks were determined by visual inspection of thermal melts, with cases where the order was not clearly obvious being assigned the same rank. Array ranks for interactions sharing a common probe were established based on the S_{array} measure, with ranks differing by only one unit in normalized S_{array} considered the same. All possible pair-wise comparisons of CD and array ranks were made, a total of 41 comparisons, 35 of which gave the same order by CD and microarray.

Array Results were Highly Reproducible

The array measurements were highly reproducible over replicate experiments and a range of concentrations, as shown in Supplementary Fig. 14. The complete array data (averaged background-corrected signals as well as S_{array} scores) are given in Supplementary Tables 3, 4, 5 and 6. Proteins listed in columns were fluorescently labelled and used in solution as probes against proteins on the surface, which are listed in rows. All protein probes were at 160 nM unless otherwise noted. Duplicates are labelled. Supplementary Tables 3, 4, and 5 contain values from experiments in rounds 1, 2, and 3 respectively. Supplementary Table 6 contains experimentally determined S_{array} scores for 33 human proteins.

Supplementary Discussion

Beyond bZIPs: Requirements for Applying CLASSY to Other Systems

There are a variety of reasons that we selected bZIP transcription factors for this study. They comprise a biologically important class of proteins for which questions of interaction specificity are central to function. But also, interaction specificity is probably better understood for the bZIPs than for any other protein complex, and convenient properties of these proteins facilitate modelling and measurement. To what extent can CLASSY be applied to other problems in molecular recognition? To answer this it is important to distinguish between limitations that arise from CLASSY itself – of which there are few – and limitations that arise from our understanding of specificity in other protein complexes. The systematic study of protein interaction specificity is a new, expanding research area. There are already several complexes amenable to study using CLASSY, and this number will increase with advances in experimental screening technologies and computational modelling.

Below we outline three requirements that must be met to apply CLASSY to a specificity design problem. For each, we comment on how the bZIPs satisfy the requirement and discuss prospects for other complexes.

1. Application of CLASSY requires that sets of desired and competing states be defined.

To address interaction specificity explicitly, one must define the universe of relevant complexes. For many problems, competing states of particular interest can be identified as those that share structural and evolutionary similarity with the target. In our bZIP application, the competitors were other bZIPs. These can be detected easily by sequence similarity. Many related interaction specificity problems can be posed. In the design of peptides to activate specific integrins, the competitors would be other integrins; in the design of specific PDZ domains the competitors would be undesired protein C-terminal peptides; in the design of BH3 peptides that bind specific Bcl-2 family members, the competitors would be other Bcl-2 proteins. Although criterion 2 (below) may not yet be satisfied for these examples, at least one prior example of a successful design calculation in each of these cases illustrates progress in modelling and highlights the types of applications where CLASSY may prove fruitful[11, 12, 14]. Similar examples can be constructed for any set of paralogous interaction domains; zinc-finger and homeodomain transcription factors as well as SH2, SH3 and PDZ domains are discussed below.

2. A scoring function must provide information about the relative stabilities of the states under consideration.

Specificity can be designed using CLASSY only if a model captures information about the relative favourability of different states. CLASSY can use many types of scoring functions. Physical/structure-based models and empirical/statistical models are equally compatible with the requirements of the method. The only formal requirement is that the scoring function be expressed as a linear function of sequence variables (not necessarily limited to amino-acid pair terms). We have demonstrated that cluster expansion can accomplish this for complex structure-based energy functions and for several different protein folds[28, 29, 32]. Cluster expansion can in theory also be applied directly to large experimental datasets, where available, to generate a predictive expression in the appropriate computational form.

In designing anti-bZIPs, we took advantage of experiments that elucidated some of the determinants of interaction specificity; we captured these in a hybrid structure-based/experiment-based model, which was tested using available peptide array data[4, 26]. Specificity-scoring functions published for other protein domains can now be tested using CLASSY. For example, models based on fitting residue interactions to experimental data have been developed for PDZ domains and zinc fingers. Such scoring functions typically have the functional form required for CLASSY[1, 3, 34, 45]. Scoring functions based on structural modelling have the greatest potential to be general. RosettaDesign has been used for many applications, including the design of specific protein-protein interactions[8, 46]. Other structure-based specificity models have been tested for PDZ[12], SH2[33] and SH3[47, 48] domains. Structure-based models have also shown good performance for several transcription factor families[49-52]. Physical structure-based models face significant challenges, in particular capturing side-chain and backbone relaxation that can impact specificity. But as new methods for modelling structural relaxation are developed (and several groups report progress in this area [36, 53, 54]), there are no obvious barriers to employing them in conjunction with CLASSY. In fact, we recently demonstrated that cluster expansion works well when applied to models that incorporate backbone flexibility[32]. Finally, structural approaches that use atom-based or residue-based statistical potentials can give good predictions of binding energies and can capture some interaction specificity trends[37, 55, 56]; such models may prove especially useful for negative design.

How good do the scoring functions need to be? Our bZIP scoring functions, while capable of distinguishing strong interactions from non-interactions, do not provide quantitative predictions of relative stability (they do not correlate strongly with experimental ΔΔG estimates). Models can likely be effective for use in CLASSY if they (1) accurately capture some key specificity determinants and (2) are not under-defined. A model is under-defined if it has many missing or inappropriate weights; these can allow the design optimization calculations to proceed into non-sensible regions of sequence space. In our bZIP study, the experiments of Vinson and colleagues provided valuable data contributing to (1), though these experiments did not comprehensively assess all possible specificity determinants[19, 22]. To address (2), we used structural modelling to impose a physically realistic description of all amino-acid interactions that were not defined by experiments. A similar combined approach is likely to be appropriate for other domains. For example, for PDZ domains and zinc fingers, a small set of weights derived from experiments seem to predict much of the observed specificity[3, 45]. But structural modelling may be required to provide reasonable (even if not highly accurate) estimates for the many amino-acid interactions that are not constrained by experiments. Also important for addressing (2) is the ability of CLASSY to incorporate sequence property constraints (e.g. the PSSM constraint used in this study), which can be used to ensure that only the sequence space that is reasonably well described by the underlying model is considered in design.

Finally, energy gaps in CLASSY can be chosen according to the estimated accuracy of the underlying energy function. Thus, if errors in predicted energies are known to be large, the user can choose to impose large energy gaps as constraints, ensuring that any designs returned are predicted to have a significant preference for the desired state over others (at the risk of finding either no solutions or only poorly stable solutions).

In summary, while we do not yet know if breakthroughs in predicting specificity will come primarily from improvements in modelling or from fitting to large experimental data sets, this likely does not matter in terms of applying CLASSY. Designing specific PDZ/SH2/SH3 domains or specific PDZ/SH2/SH3 ligands, or zinc-finger transcription factors with specialized binding profiles, are already good candidate applications for testing this method more broadly.

3. An experimental assay appropriate for testing the specificity of the proteins under study is required.

It is impossible to know the quality of the scoring function, or the quality of CLASSY designs, without experiments that report on interaction specificity. Assessing specificity profiles generally involves testing many possible complexes. For the bZIPs, we took advantage of a previously validated peptide microarray assay[4]. Similar large data sets exist for SH2, SH3, PTB, and PDZ domains, as well as for many transcription factors[2, 57-61]. Exciting advances using SPOT arrays, protein microarrays, protein-binding DNA arrays, phage-display/phage ELISA, protein complementation assays and plate-based fluorescence assays expand the possibilities in this area, and suggest that many moderately sized binary complexes will be amenable to analysis[1-5, 59-63].

CLASSY Introduces Negative Design Using Familiar bZIP Features

CLASSY designs employed a range of strategies to achieve specificity, but some trends were evident. Designs optimized for stability alone often had **a** and **d** positions with medium-to-large hydrophobic residues[22], and CLASSY initially improved specificity by maintaining these cores and modulating electrostatic **g**-**e'** interactions in early iterations of the specificity sweeps (see Fig. 1C for definitions of coiled-coil heptad positions; a prime indicates a residue on the opposite helix). To achieve greater specificity (Δ), at a greater price in stability, CLASSY introduced core substitutions such as pairing of Ile with Ala (e.g. to destabilize homodimers using Ala-Ala pairs). The sequences selected for testing typically included additional elements, such as charged amino acids in core positions. Such interactions imparted large amounts of specificity but were also predicted to be quite destabilizing. They were chosen for analysis because we judged specificity to be relatively more important; generic strategies such as ACID extensions could be used to improve stability if necessary[64].

Our 8 most specific designs exhibit canonical bZIP specificity determinants (Supplementary Fig. 15A): there is a strong preference for Asn at an **a** position to be paired with Asn at the opposing **a′**, and electrostatic complementarity is exploited at **g**-**e′** positions[19, 26]. Interestingly, a less recognized complementarity between **g**-**a′** positions is predicted to make a comparable, if not larger, contribution to specificity; this feature was extensively used in our designs (Supplementary Fig. 15A)[65]. A strong preference for Leu-Leu over all other amino-acid pairs at **d**-**d′** positions was also exploited[66]. Finally, our model predicts that interactions between **a** and **d′** can contribute significantly to specificity. In particular, a beta-branched residue at an **a** position strongly prefers a non-beta branched residue at the next **d** position of the opposing strand. Similar effects have been noted in anti-parallel coiled coils[31].

Off-target Interactions May Form via Structures That Were Not Modelled

In our computational modelling, we considered only parallel coiled-coil dimer structures with a unique axial alignment of helices. For the designs that bound to their targets, it is likely that the interaction occurred as modelled because the designs were restrained to have leucine zipper-like sequences, frequently retained buried Asn and Lys residues to favour dimers over other oligomers, and retained paired Asn residues at **a**-**a'** positions to favour particular parallel alignments [67, 68]. These features were selected automatically by CLASSY in most cases, and where they were not present in all candidate designs, we imposed a bias for such solutions when choosing examples for experimental testing. Further supporting the formation of dimers, interactions of designs with their targets were observed to occur irrespective of which peptide was printed on the array and which was labelled in solution, which is unlikely for some alternate stoichiometries.

When unexpected design•off-target interactions occurred, it is less clear what the structures of those complexes were. In several instances, we suspect that the complex formed was not one that was modelled as an undesired state. For example, the strong interaction between anti-SMAF-2 and ATF-4 (Supplementary Fig. 1) was predicted to be very unfavourable relative to anti-SMAF-2•MafG (Supplementary Fig. 16A-B). However, because the SMAF family has an Asn in a different heptad than most human bZIPs, the alignment used to model anti-SMAF-2 paired with ATF-4 left two asparagines at **a** positions unpaired (see Supplementary Fig. 16A). Asn residues have a strong preference to occur in pairs in coiled-coil dimers [22], and it is unlikely that the anti-SMAF-2•ATF-4 interaction would occur in this way. More likely, the complex would adopt a shifted axial alignment (though this is also predicted to be unfavourable, Supplementary Fig. 16C), an anti-parallel helix orientation, or some other structure. Anti-BACH2-2, which showed strong homo-association on the array, illustrates another case where the complex formed may not be the one that was modelled as an undesired state. Anti-BACH-2 homodimer was predicted to be much less stable than anti-BACH-2•BACH1. However, although anti-BACH-2 has very strong anti-homodimerization features, they are heavily concentrated in the first two N-terminal heptads (see Supplementary Fig. 17). It is likely that this portion of the homodimer simply does not fold, and the rest of the sequence forms a stable association. Of course, if such problems can be anticipated, additional constraints can be incorporated into CLASSY, where alternative alignments, coiled-coil lengths and orientations can be explicitly considered.

Supplementary Figures

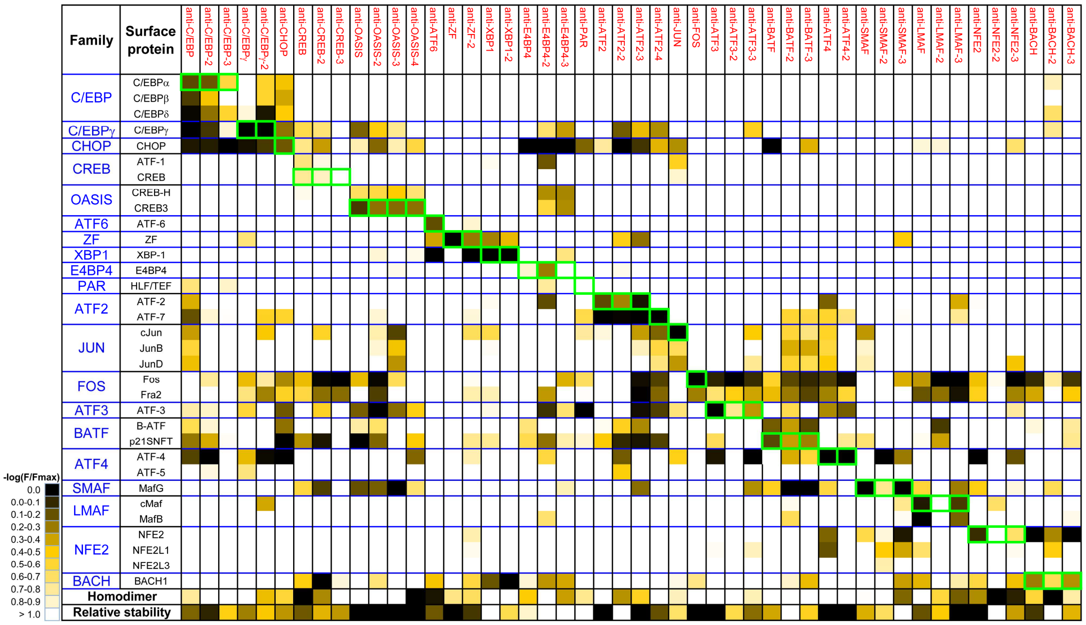

Supplementary Figure 1 Array measurements characterizing all 48 designs. Designs are in columns. Human bZIPs on the arrays are in rows. Family names are in blue, with families separated by blue lines. Shown as a heat map are interaction –log(F/F$_{max}$) scores (see section Data analysis), with lower scores (darker color) indicating stronger interactions. The "homodimer" row indicates the interaction of each design in solution with itself on the array, relative to the strongest interaction of that design with other partners on the array. The "relative stability" row indicates the interaction of each surface-attached design with its target in solution, relative to the target's strongest interaction (either the design or one of 33 human bZIPs on the same array). Green boxes indicate intended targets.

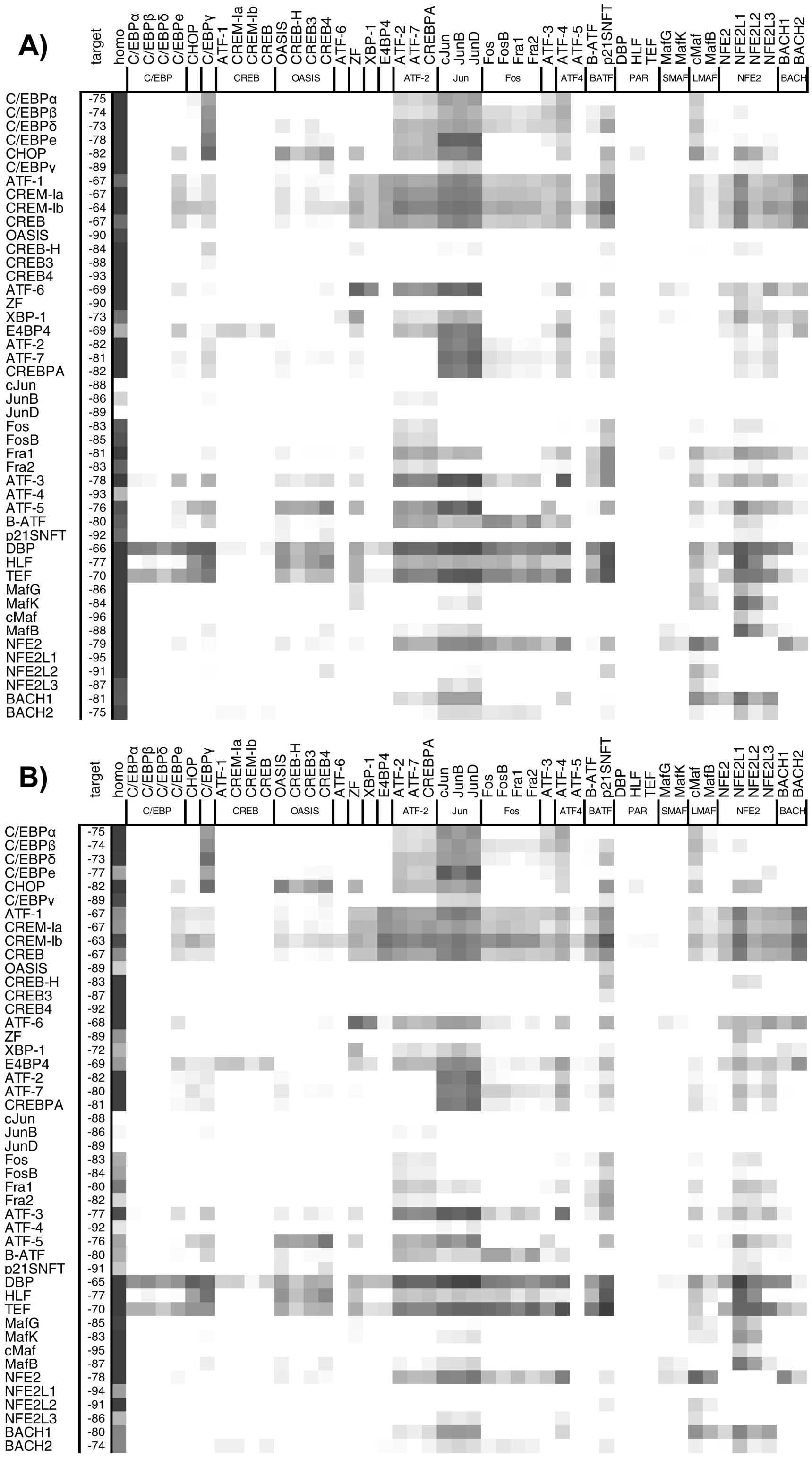
A)
target
homo
C/EBPα
C/EBPβ
C/EBPδ
C/EBPe
CHOP
C/EBPγ
ATF-1
CREM-Ia
CREM-Ib
CREB
OASIS
CREB-H
CREB3
CREB4
ATF-6
ZF
XBP-1
E4BP4
ATF-2
ATF-7
CREBPA
cJun
JunB
JunD
Fos
FosB
Fra1
Fra2
ATF-3
ATF-4
ATF-5
B-ATF
p21SNFT
DBP
HLF
TEF
MafG
MafK
cMaf
MafB
NFE2
NFE2L1
NFE2L2
NFE2L3
BACH1
BACH2
C/EBP
CREB
OASIS
ATF-2
Jun
Fos
ATF4
BATF
PAR
SMAF
LMAF
NFE2
BACH
C/EBPα -75
C/EBPβ -74
C/EBPδ -73
C/EBPe -78
CHOP -82
C/EBPγ -89
ATF-1 -67
CREM-Ia -67
CREM-Ib -64
CREB -67
OASIS -90
CREB-H -84
CREB3 -88
CREB4 -93
ATF-6 -69
ZF -90
XBP-1 -73
E4BP4 -69
ATF-2 -82
ATF-7 -81
CREBPA -82
cJun -88
JunB -86
JunD -89
Fos -83
FosB -85
Fra1 -81
Fra2 -83
ATF-3 -78
ATF-4 -93
ATF-5 -76
B-ATF -80
p21SNFT -92
DBP -66
HLF -77
TEF -70
MafG -86
MafK -84
cMaf -96
MafB -88
NFE2 -79
NFE2L1 -95
NFE2L2 -91
NFE2L3 -87
BACH1 -81
BACH2 -75
B)
target
homo
C/EBPα
C/EBPβ
C/EBPδ
C/EBPe
CHOP
C/EBPγ
ATF-1
CREM-Ia
CREM-Ib
CREB
OASIS
CREB-H
CREB3
CREB4
ATF-6
ZF
XBP-1
E4BP4
ATF-2
ATF-7
CREBPA
cJun
JunB
JunD
Fos
FosB
Fra1
Fra2
ATF-3
ATF-4
ATF-5
B-ATF
p21SNFT
DBP
HLF
TEF
MafG
MafK
cMaf
MafB
NFE2
NFE2L1
NFE2L2
NFE2L3
BACH1
BACH2
C/EBP
CREB
OASIS
ATF-2
Jun
Fos
ATF4
BATF
PAR
SMAF
LMAF
NFE2
BACH
C/EBPα -75
C/EBPβ -74
C/EBPδ -73
C/EBPe -77
CHOP -82
C/EBPγ -89
ATF-1 -67
CREM-Ia -67
CREM-Ib -63
CREB -67
OASIS -89
CREB-H -83
CREB3 -87
CREB4 -92
ATF-6 -68
ZF -89
XBP-1 -72
E4BP4 -69
ATF-2 -82
ATF-7 -80
CREBPA -81
cJun -88
JunB -86
JunD -89
Fos -83
FosB -84
Fra1 -80
Fra2 -82
ATF-3 -77
ATF-4 -92
ATF-5 -76
B-ATF -80
p21SNFT -91
DBP -65
HLF -77
TEF -70
MafG -85
MafK -83
cMaf -95
MafB -87
NFE2 -78
NFE2L1 -94
NFE2L2 -91
NFE2L3 -86
BACH1 -80
BACH2 -74

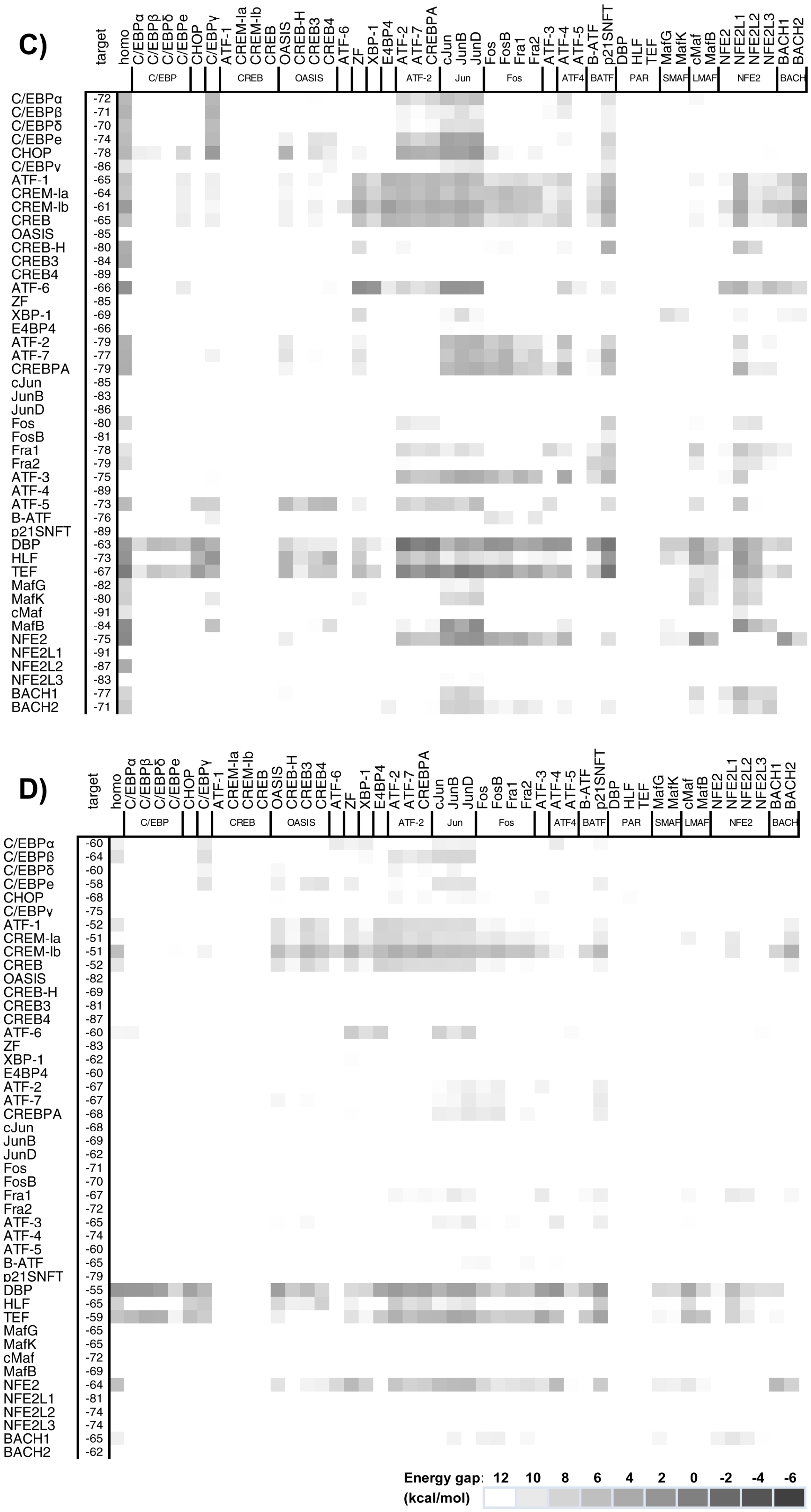
C)
target
homo
C/EBPα
C/EBPβ
C/EBPδ
C/EBPe
CHOP
C/EBPγ
ATF-1
CREM-Ia
CREM-Ib
CREB
OASIS
CREB-H
CREB3
CREB4
ATF-6
ZF
XBP-1
E4BP4
ATF-2
ATF-7
CREBPA
cJun
JunB
JunD
Fos
FosB
Fra1
Fra2
ATF-3
ATF-4
ATF-5
B-ATF
p21SNFT
DBP
HLF
TEF
MafG
MafK
cMaf
MafB
NFE2
NFE2L1
NFE2L2
NFE2L3
BACH1
BACH2
C/EBP
CREB
OASIS
ATF-2
Jun
Fos
ATF4
BATF
PAR
SMAF
LMAF
NFE2
BACH
C/EBPα -72
C/EBPβ -71
C/EBPδ -70
C/EBPe -74
CHOP -78
C/EBPγ -86
ATF-1 -65
CREM-Ia -64
CREM-Ib -61
CREB -65
OASIS -85
CREB-H -80
CREB3 -84
CREB4 -89
ATF-6 -66
ZF -85
XBP-1 -69
E4BP4 -66
ATF-2 -79
ATF-7 -77
CREBPA -79
cJun -85
JunB -83
JunD -86
Fos -80
FosB -81
Fra1 -78
Fra2 -79
ATF-3 -75
ATF-4 -89
ATF-5 -73
B-ATF -76
p21SNFT -89
DBP -63
HLF -73
TEF -67
MafG -82
MafK -80
cMaf -91
MafB -84
NFE2 -75
NFE2L1 -91
NFE2L2 -87
NFE2L3 -83
BACH1 -77
BACH2 -71
D)
target
homo
C/EBPα
C/EBPβ
C/EBPδ
C/EBPe
CHOP
C/EBPγ
ATF-1
CREM-Ia
CREM-Ib
CREB
OASIS
CREB-H
CREB3
CREB4
ATF-6
ZF
XBP-1
E4BP4
ATF-2
ATF-7
CREBPA
cJun
JunB
JunD
Fos
FosB
Fra1
Fra2
ATF-3
ATF-4
ATF-5
B-ATF
p21SNFT
DBP
HLF
TEF
MafG
MafK
cMaf
MafB
NFE2
NFE2L1
NFE2L2
NFE2L3
BACH1
BACH2
C/EBP
CREB
OASIS
ATF-2
Jun
Fos
ATF4
BATF
PAR
SMAF
LMAF
NFE2
BACH
C/EBPα -60
C/EBPβ -64
C/EBPδ -60
C/EBPe -58
CHOP -68
C/EBPγ -75
ATF-1 -52
CREM-Ia -51
CREM-Ib -51
CREB -52
OASIS -82
CREB-H -69
CREB3 -81
CREB4 -87
ATF-6 -60
ZF -83
XBP-1 -62
E4BP4 -60
ATF-2 -67
ATF-7 -67
CREBPA -68
cJun -68
JunB -69
JunD -62
Fos -71
FosB -70
Fra1 -67
Fra2 -72
ATF-3 -65
ATF-4 -74
ATF-5 -60
B-ATF -65
p21SNFT -79
DBP -55
HLF -65
TEF -59
MafG -65
MafK -65
cMaf -72
MafB -69
NFE2 -64
NFE2L1 -81
NFE2L2 -74
NFE2L3 -74
BACH1 -65
BACH2 -62
Energy gap: 12 10 8 6 4 2 0 -2 -4 -6
(kcal/mol)

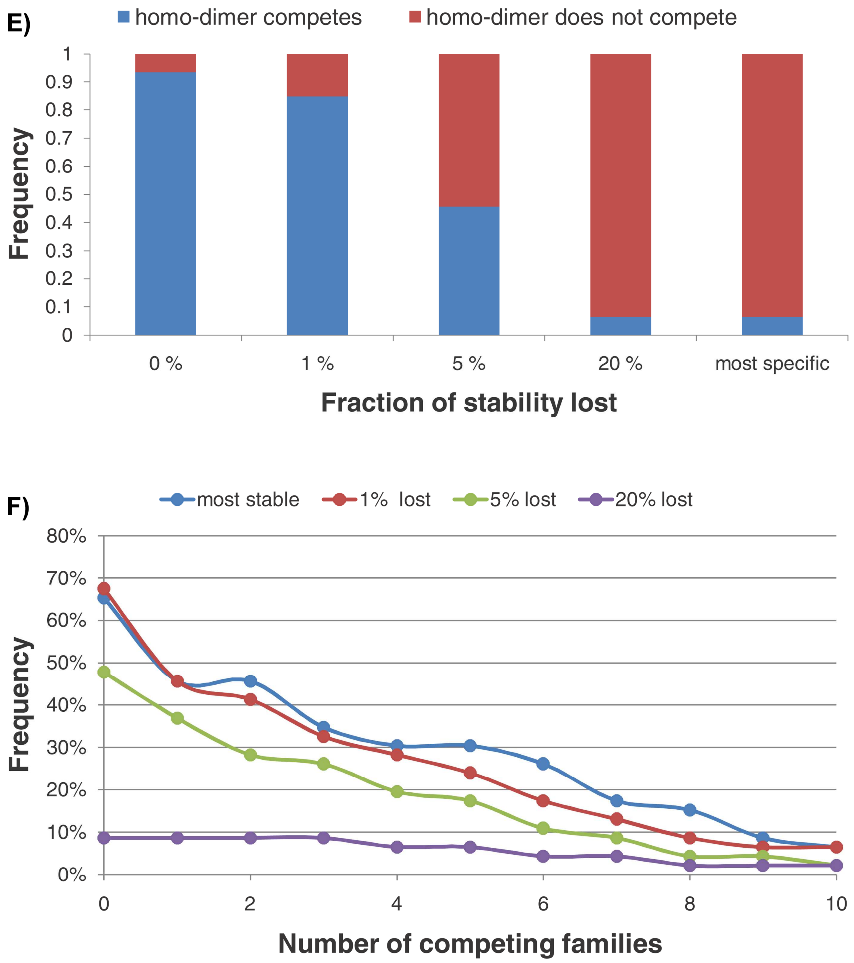

Supplementary Figure 2 A global view of specificity sweeps with each human bZIP coiled coil as a target. In each row, the protein indicated at left is the target. The first column contains the score of the optimal design•target complex, whereas each subsequent column contains the energy gaps between the design•target complex and the corresponding design•competitor complex, including the design homodimer in the second column. A positive energy gap corresponds to design•target being more favorable than design•competitor. The color bar gives the energy scale. **(A)**, **(B)**, **(C)** and **(D)** correspond to designs from different stages of specificity sweeps. In **(A)** the design producing the most stable complex for each target was used to compute energies (first iteration). In **(B)** up to 1% of the stability score was sacrificed to gain specificity. In **(C)** up to 5% of stability was sacrificed and in **(D)** the most specific designs were considered. In **(E)** and **(F)** the specificity data are summarized as a function of decreasing stability. **(E)** shows the proportion of anti-human designs for which the design•design homodimer has a gap of less than 6 kcal/mol, and **(F)** shows the proportion of designs predicted to compete with a non-target-family human bZIP by the same criterion. Energies were computed using model HP/S/Cv.

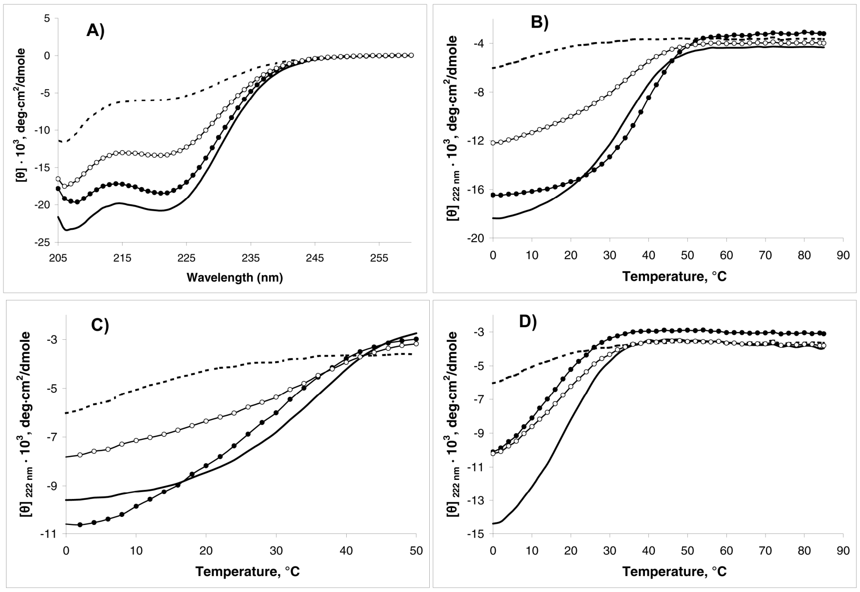

Supplementary Figure 3 Solution characterization of anti-ATF2 by CD. Format and presentation is the same as in Fig. **2**B-E for anti-SMAF. The target protein is ATF-7 (which is in the same family as ATF-2) (in **A** and **B**), the closest off-target competitor is p21SNFT (in **C**), and the bZIP related to the target by sequence is cJun (in **D**). T_m values are given in Supplementary Table 2.

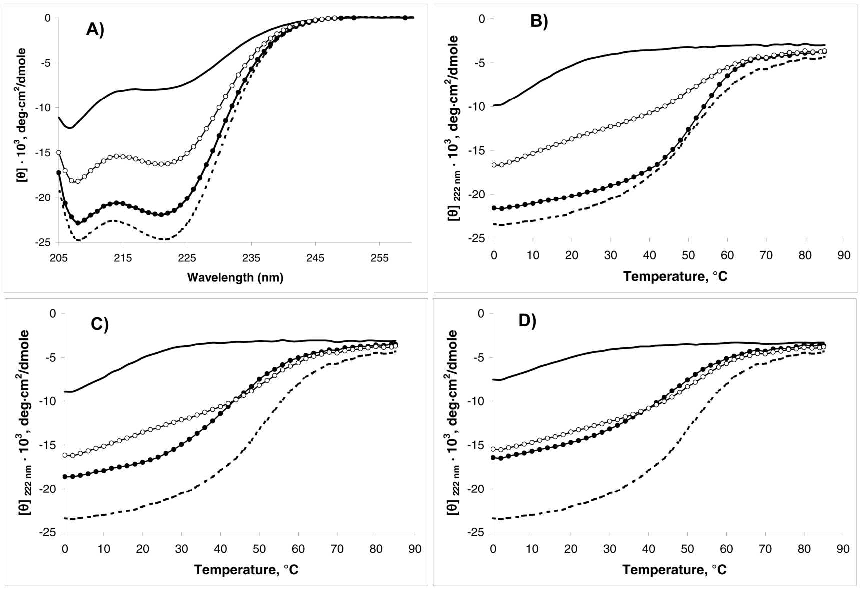

Supplementary Figure 4 Solution characterization of anti-ATF4 by CD. Format and presentation is the same as in Fig. **2**B-E for anti-SMAF. The target protein is ATF-4 (in **A** and **B**), the closest off-target competitor is Fos (in **C**), and the bZIP related to the target by sequence is ATF-3 (in **D**). T_m values are given in Supplementary Table 2.

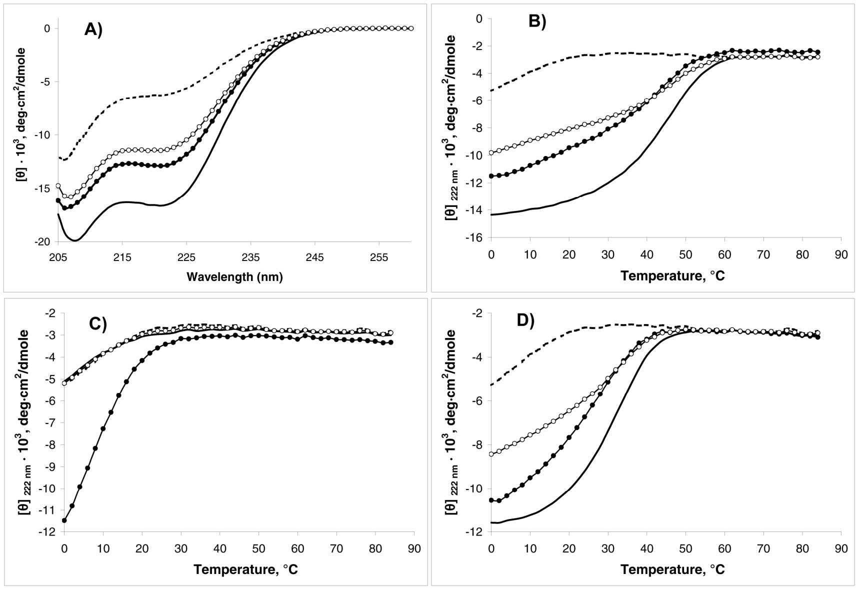

Supplementary Figure 5 Solution characterization of anti-LMAF by CD. Format and presentation is the same as in Fig. **2**B-E for anti-SMAF. The target protein is cMaf (in **A** and **B**), the closest off-target competitor is Fra2 (in **C**), and the bZIP related to the target by sequence is MafG (in **D**). T_m values are given in Supplementary Table 2.

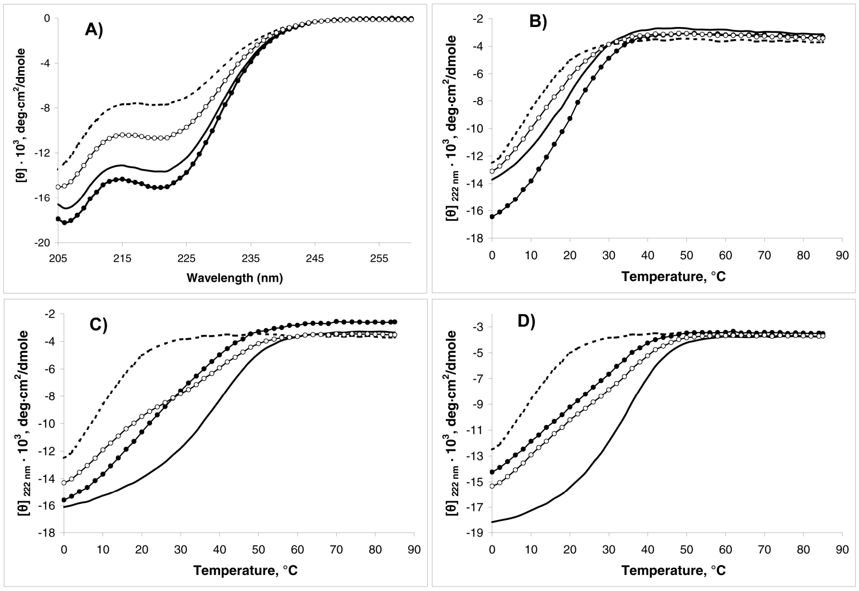

Supplementary Figure 6 Solution characterization of anti-JUN by CD. Format and presentation is the same as in Fig. **2**B-E for anti-SMAF. The target protein is cJun (in **A** and **B**), the closest off-target competitor is CHOP (in **C**), and the bZIP related to the target by sequence is ATF-7 (in **D**). T_m values are given in Supplementary Table 2.

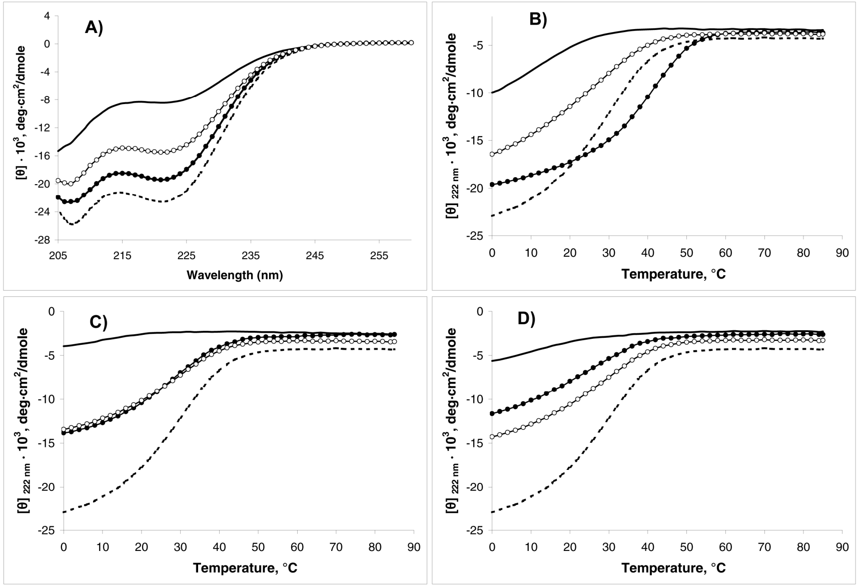

Supplementary Figure 7 Solution characterization of anti-FOS by CD. Format and presentation is the same as in Fig. **2**B-E for anti-SMAF. The target protein is Fos (in **A** and **B**), closest off-target competitor is BACH1 (in **C**), and bZIP related to the target by sequence is ATF-3 (in **D**). T_m values are given in Supplementary Table 2.

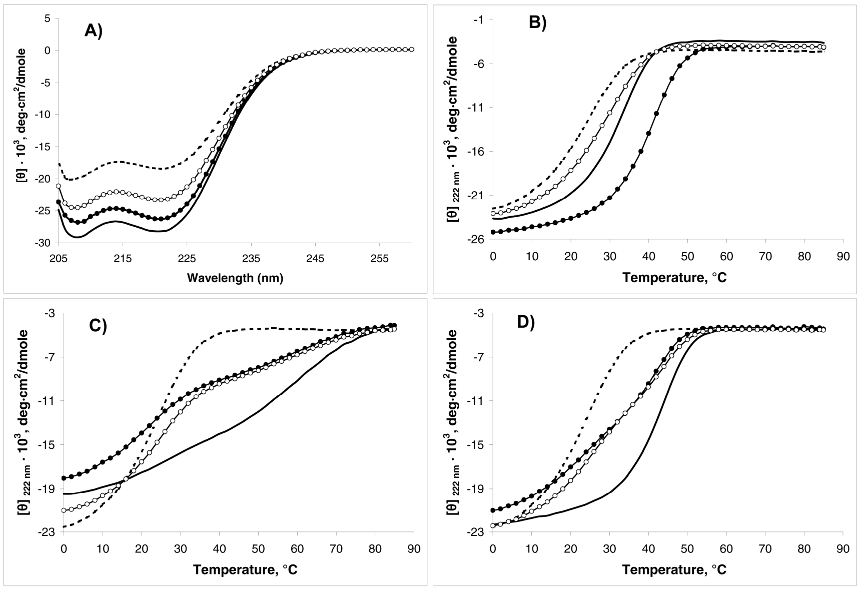

Supplementary Figure 8 Solution characterization of anti-ZF by CD. Format and presentation is the same as in Fig. **2**B-E for anti-SMAF. The target protein is ZF (in **A** and **B**), closest off-target competitor is NFE2 (in **C**), and the bZIP related to the target by sequence is XBP-1 (in **D**). T_m values are given in Supplementary Table 2.

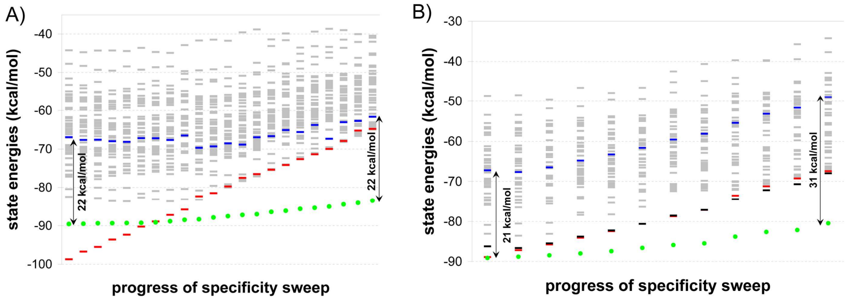

Supplementary Figure 9 Specificity sweep (**A**) and biased specificity sweep (**B**) diagrams for the design of a peptide to bind the leucine-zipper region of ZF. Green dots correspond to the design•target complex and red bars to the design•design complex. Blue bars in **A)** correspond to the energy of the design•XBP-1 complex, which contrary to the prediction of the model showed evidence of strong interaction on the microarray. As a way of addressing this issue, a biased specificity sweep was conducted for ZF, where the gap between the energies of the design•ZF and design•XBP-1 complexes was shifted by 19 kcal/mol. This is shown in **(B)** with blue bars corresponding to the actual model-predicted design•XBP-1 energy, while the black bars are the energies used in the biased specificity sweep. Whereas in the regular specificity sweep there is no competition with the design•XBP-1 state, due to its incorrectly predicted high energy, in the biased specificity sweep this competition is imposed. This procedure generated a successful, highly specific design: anti-ZF.

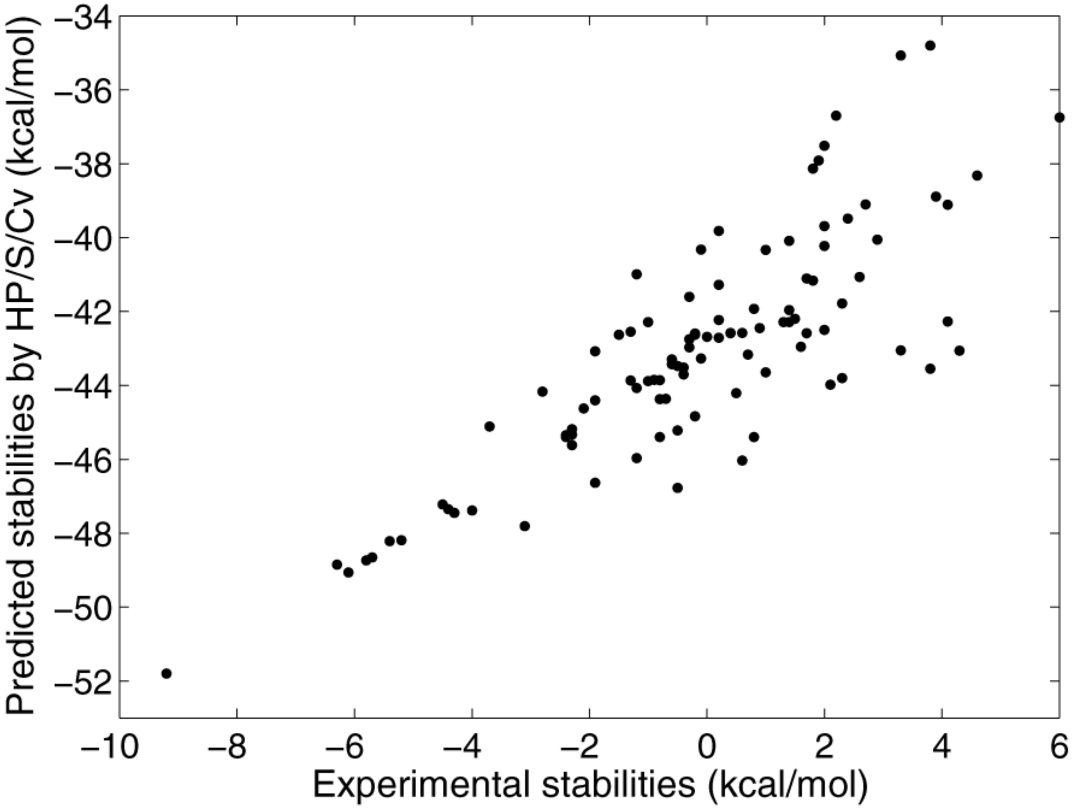

Supplementary Figure 10 Adjusting the 9 **a**-position point ECI in model HP/S/Cv to optimally fit 100 stabilities experimentally measured by Vinson and co-workers[22]. R for the final fit is 0.83.

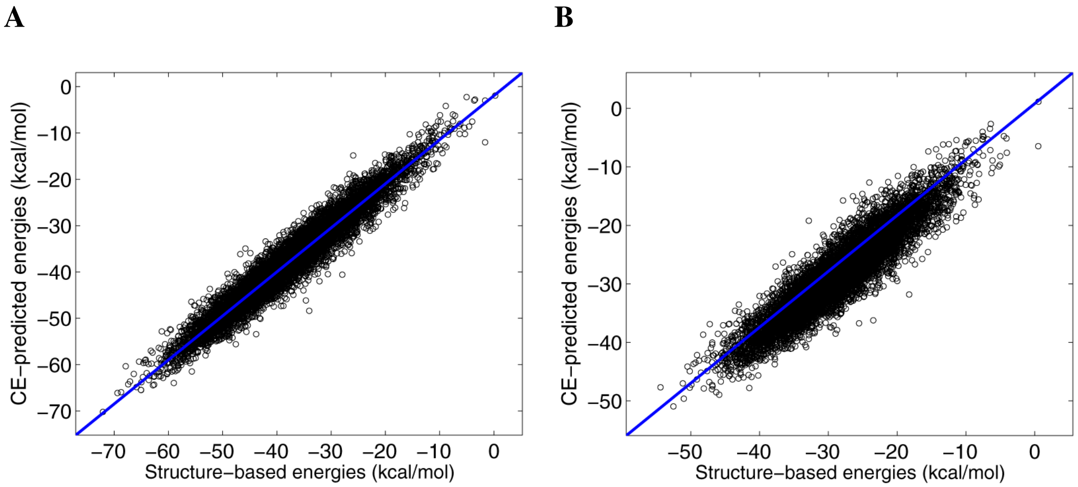

Supplementary Figure 11 The performance of cluster-expanded versions of models HP/S/Ca and HP/S/Cv (panels **A** and **B**, respectively) on a randomly generated set of 10,000 sequences not present in the training set. Root mean square deviations between CE-predicted and structure-based energies are 2.4 and 2.6 kcal/mol for HP/S/Ca and HP/S/Cv, respectively. The cluster expansions contain 2,544 ECI for HP/S/Ca and 2,470 ECI for HP/S/Cv.

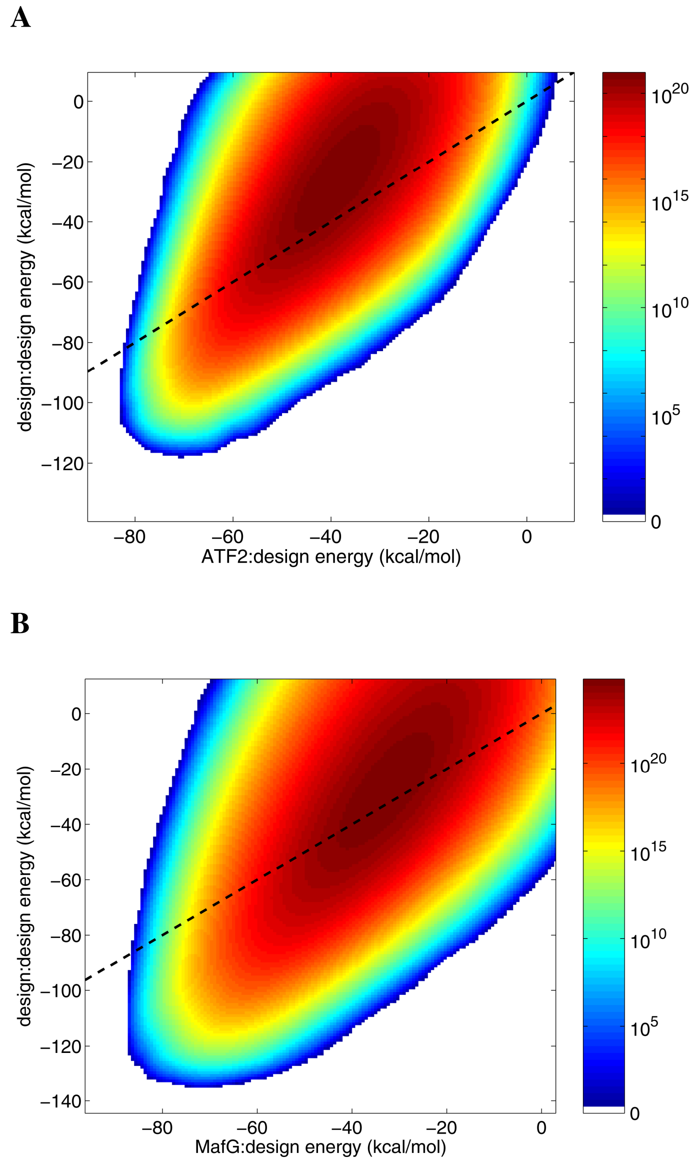

Supplementary Figure 12 2D energy histograms of two states – the design•target state and the design•design homodimer state. Color represents the total number of possible sequences in each bin (bin sizes are ~1 kcal/mol). The targets are ATF-2 and MafG in **(A)** and **(B),** respectively. The line where design•target and design•design scores are equal is shown. By optimizing only the design•target energy, sequences with high homodimerization propensity will be obtained in these examples. The specificity sweep procedure run with only one disfavoured state (design•design) locates the top boundary of this phase space.

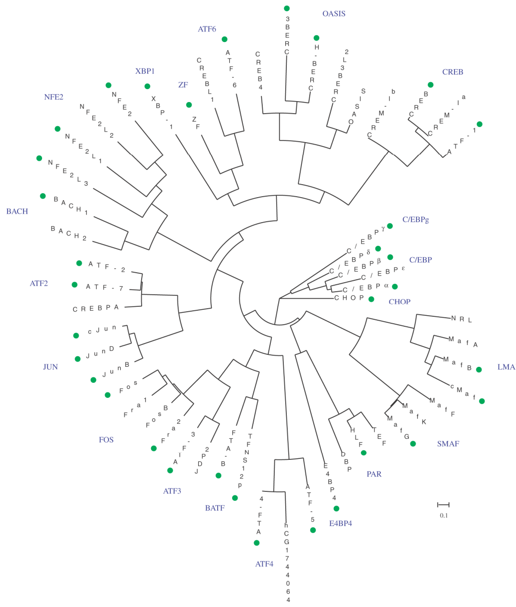

Supplementary Figure 13 Phylogentic tree constructed using the leucine-zipper regions of all human bZIP proteins. Protein names are in black and family names are in blue. Green dots indicate the 33 proteins used in the experiments in this study. The scale refers to amino-acid replacements per site.

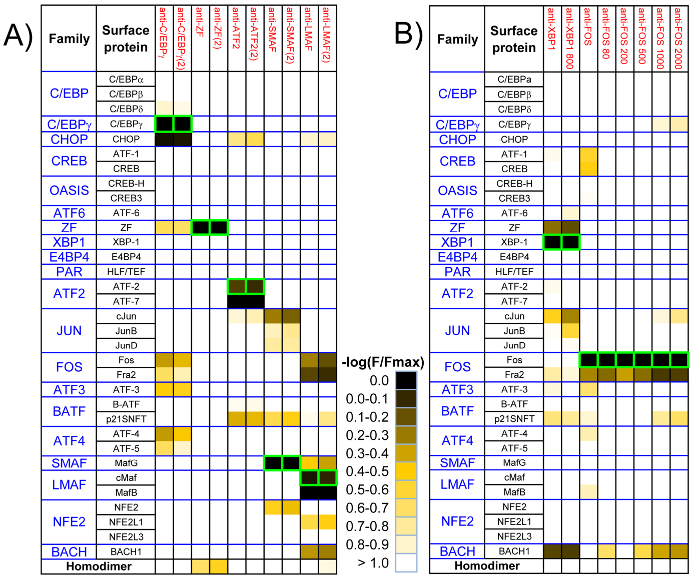

Supplementary Figure 14 Reproducibility of protein-microarray measurements of design interactions probed in duplicate in **(A)** and at different concentrations in **(B)** (probe concentration in nM is shown as part of the probe name in the top row and is 160 nM where not indicated). Data are displayed in the same format as for Supplementary Fig. 1.

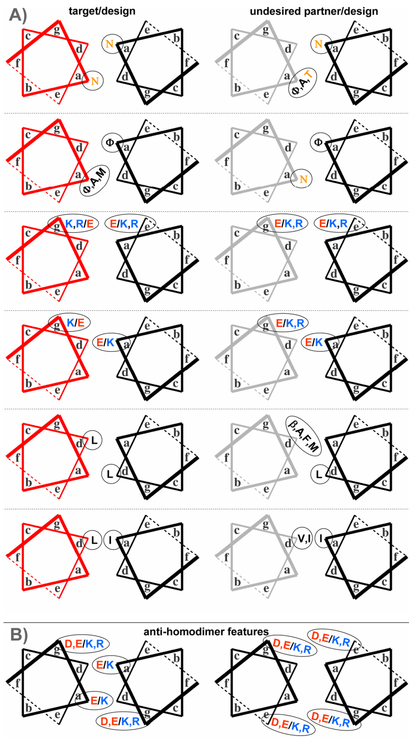

Supplementary Figure 15 Common specificity mechanisms in successful designed peptides. **A)** Specificity features used for discriminating between design•target and design•off-target interactions. The design is in black, the target in red and the undesired partner in gray. Amino acids listed with single-letter codes are the residues comprising the specificity pattern. Slashes delineate subgroups of residues, with corresponding subgroups delineated similarly at the interacting position. Φ designates hydrophobic residues Ile, Val or Leu and β stands for beta-branched residues Ile or Val. In the last row, the **a-d'** interaction is between an **a** residue and the more C-terminal **d**' residue on the opposite helix. **B)** Specificity features commonly used in designed peptides to disfavor the design•design homodimer, using the same notation.

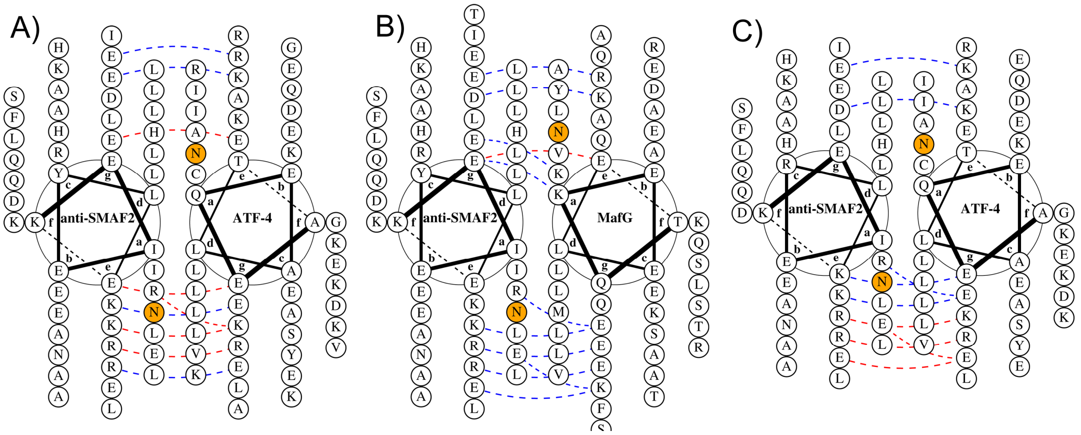

Supplementary Figure 16 Helical-wheel diagrams for anti-SMAF-2 complexes with ATF-4 and MafG. **(A)** The anti-SMAF-2•ATF-4 complex is predicted to be much weaker than the anti-SMAF-2•MafG complex shown in **(B)**, in large part due to the misaligned asparagines at **a** positions in anti-SMAF-2•ATF-4. **(C)** A different alignment of anti-SMAF-2•ATF-4, where the asparagines match up, may be more favorable, although it is not predicted to be much stronger computationally. Diagrams made with DrawCoil 1.0 (http://www.gevorggrigoryan.com/drawcoil/).

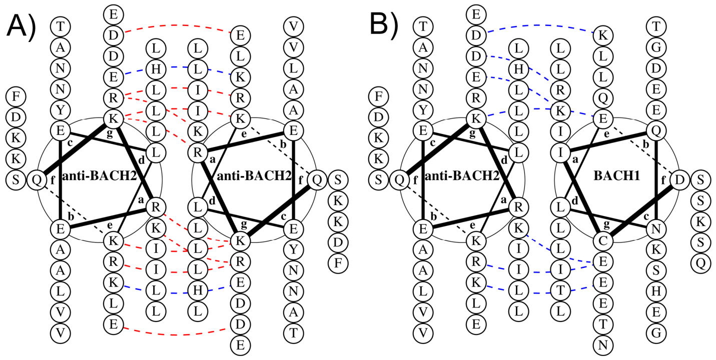

Supplementary Figure 17 Helical-wheel diagrams of the anti-BACH-2 homodimer complex, shown in **(A)**, and the anti-BACH-2•BACH1 complex shown in **(B)**. The strong anti-homodimerization features of anti-BACH-2 are concentrated at the N-terminus of the sequence, leaving open the possibility that this portion simply does not fold, while the remainder of the coiled coil forms a stable complex. Diagrams made with DrawCoil 1.0 (http://www.gevorggrigoryan.com/drawcoil/).

Supplementary Tables

Supplementary Table 1 All designed sequences tested. For each design, listed in columns are: the name of the design, the name of the bZIP target for that design, the family of the target bZIP, the round of design/testing in which this sequence was produced, the count of attempts to design a partner for the given target, the energy function used and the designed sequence. Note that designs are named after the family of the target rather than the individual protein. There were three rounds of experiments. Attempts are different than rounds because not all targets were attempted in the first (or second) rounds. An attempt involved testing one or two designs (in one case, three) for each target considered in a set of experiments. When the first experimental attempt to identify a specific design was unsuccessful, alternative solutions from the specificity sweep were selected for testing in subsequent rounds (constituting further attempts). In a few cases, listed in the footnotes, these additional designs were created with a modified procedure aimed at addressing experimentally identified shortcomings of previous designs.

Design name	Target	Family	Round	Attempt	Method	Design sequence
						fgabcdefgabcdefgabcdefgabcdefgabcdefgabcdefgabcdefgabc
anti-C/EBP-2	C/EBPα	C/EBP	2	1	HP/S/Ca	FENVTHEFILATLENENAKLRRLEAKLERELARLRNEVAWL
anti-C/EBP	C/EBPα	C/EBP	3	2	HP/S/Cv	AENQYVEDLIQYLEKENARLKKEVQRLVRELSYFRRRIAELA
anti-C/EBP-3	C/EBPα	C/EBP	3	2	HP/S/Cv	AENQSVEDIIAKKEDENAHLKNEVKTLINELETLRKKIEYLA
anti-C/EBPγ	C/EBPγ	C/EBPγ	2	1	HP/S/Ca	NDLDAYEREAEKLEKKNEVLRNRLAALENELATLRQEVASMKQELQS
anti-C/EBPγ-2	C/EBPγ	C/EBPγ	2	1	HP/S/Cv	RDLQNVEREIQSLEKKNESLKKKIASLENELATLKQEIAYFKRELAY
anti-CHOP	CHOP	CHOP	3	1	HP/S/Cv	DRLAVKENRVAVLKNENAKLRNIIANLKDRIAYFRRELAYLELEEEQLA
anti-CREB	CREB	CREB	2	1	HP/S/Cv	QLVAQLRSKVEQLVNRNQALKNKLEYLRQEIAETEQ
anti-CREB-2	CREB	CREB	3	2	HP/S/Cv[1]	NKVEQLKNKVEQLKNRNAALKNDLARLEREIAYAEE
anti-CREB-3	CREB	CREB	3	2	HP/S/Cv[1]	QKVESLKQKIEELKQRKAQLKNDIANLEKEIAYAET
anti-OASIS	CREB3	OASIS	2	1	HP/S/Cv	QKVEQLKNKVEQKLKENESLENKVAELKNRNEYLKNKIENLINDITNLENDVAR
anti-OASIS-2	CREB3	OASIS	2	1	HP/S/Cv	QKVAELKNRVAVKLNRNEQLKNKVEELKNRNAYLKNELATLENEVARLENDVAE
anti-OASIS-3	CREB3	OASIS	3	2	HP/S/Cv[5]	QKVAQLKNRVAYKLKENAKLENIVARLENDNANLEKDIANLEKDIANLERDVAR
anti-OASIS-4	CREB3	OASIS	3	2	HP/S/Cv[5]	QKVAQLKNIIAKKEDENAVLENLVAVLENENAYLEKELARLERDIARAERDVKV
anti-ATF6	ATF-6	ATF6	3	1	HP/S/Cv	EKIQELKRRLAYFRRENATLKNDNATLENELASVEAENEALRK
anti-ZF-2	ZF	ZF	2	1	HP/S/Cv	QKIAYLRDRIAALKAENEALRAKNEALRSKIEELKKEKEELRDKIAQKKDR
anti-ZF	ZF	ZF	3	2	HP/S/Cv[6]	NLVAQLENEVASLENENETLKKKNLHKKDLIAYLEKEIANLRKKIEE
anti-XBP1-2	XBP-1	XBP1	2	1	HP/S/Ca	SKYDALRNKLEALKNRNAQLRKENEQLRLEEAVLEVRNEVL
anti-XBP1	XBP-1	XBP1	2	1	HP/S/Cv	QKIEYLKDKIAELKDRNAVKRSENAQLRQAVATLEQKNEEL
anti-E4BP4-2	E4BP4	E4BP4	2	1	HP/S/Ca	QKRQELKQRLAVLENDNARLKNDLAQLEVEEAYIE
anti-E4BP4	E4BP4	E4BP4	2	1	HP/S/Cv	NKNNVKKNRLAVLENENATLRNELAWLRLELAAME
anti-E4BP4-3	E4BP4	E4BP4	3	2	HP/S/Cv[3]	EKNQELKNRLAVLENDNAALRNDLARLEREIAYME
anti-ATF2-2	ATF-2	ATF2	1	1	HP/S/Ca	QKLQTLRDLLAVLENRNQELKQLRQHLKDLLKYLEDELATLEKE
anti-ATF2-3	ATF-2	ATF2	2	2	HP/S/Cv	STVEELLRAIQELEKRNAELKNRKEELKNLVAHLRQELAAHKYE
anti-ATF2	ATF-2	ATF2	3	3	HP/S/Cv	NTVKELKNYIQELEERNAELKNLKEHLKFAKAELEFELAAHKFE
anti-ATF2-4	ATF-7	ATF2	3	3	HP/S/Cv	QKVEELKNKIAELENRNAVKKNRVAHLKQEIAYLKDELAAHEFE
anti-JUN	cJun	JUN	1	1	HP/S/Ca	SIAATLENDLARLENENARLEKDIANLERDLAKLEREEAYF
anti-FOS	Fos	FOS	1	1	HP/S/Ca	NEKEELKSKKAELRNRIEQLKQKREQLKQKIANLRKEIEAYK
anti-ATF3	ATF-3	ATF3	1	1	HP/S/Ca	ELTDELKNKKEALRKDNAALLNELASLENEIANLEKEIAYFK
anti-ATF3-2	ATF-3	ATF3	1	1	HP/S/Ca	NETEQLINKKEQLKNDNAALEKDAASLEKEIANLEKEIAYFK
anti-ATF3-3	ATF-3	ATF3	3	3	HP/S/Cv[7]	NILASLENKKEELKKLNAHLLKEIENLEKEIANLEKEIAYFK
anti-ATF4	ATF-4	ATF4	2	1	HP/S/Cv	KRIAYLRKKIAALKKDNANLEKDIANLENEIERLIKEIKTLENEVASHEQ
anti-ATF4-2	ATF-4	ATF4	2	1	HP/S/Cv	ARNAYLRKKIARLKKDNLQLERDEQNLEKIIANLRDEIARLENEVASHEQ
anti-BATF	p21SNFT	BATF	2	1	HP/S/Ca	NELESLENKKEELKNRNEELKQKREQLKQKLAALRNKLDAYKNRL
anti-BATF-2	p21SNFT	BATF	3	2	HP/S/Cv	NDIENLKDKIEELKQRKEELKQKIEYLKQKIEALRQKLAALKQRIA
anti-BATF-3	p21SNFT	BATF	3	2	HP/S/Cv	EKIEELKDKIAELRSRNAALRNKIEALKQKLEALRQKIEYLKDRIA
anti-PAR	HLF	PAR	3	1	HP/S/Cv	NRLQELENKNEVLEKRKAELRNEVATLEQELAAHRYELAAIEKEIA
anti-SMAF-2	MafG	SMAF	1	1	HP/S/Ca	KEIEYLEKEIERLKDLREHLKQDNAAHRQELNALRLEEAKLEFILAHLLST
anti-SMAF-3	MafG	SMAF	1	1	HP/S/Ca	KEIERLEKEIKTLINLLTTLRQDNAAHRKEAAALEKEEANLERDIQNLLRY
anti-SMAF	MafG	SMAF	2	2	HP/S/Cv	KEIANLEKEIASLEKKVAVLKQRNAAHKQEVAALRKEIAYVEDEIQYVEDE
anti-LMAF-2	cMaf	LMAF	3	1	HP/S/Cv	NKNETLKNINARLRNDVARLKNRIARLKDDIENVEDEIQYLE
anti-LMAF-3	cMaf	LMAF	3	1	HP/S/Cv	LENAQIKKEIAQLRKEVAQLKQKIEELKNDNARVEREIQYLE
anti-LMAF	cMaf	LMAF	3	1	HP/S/Ca	KDIANLKKEIAHLKNDLQRLESIRERLKFDILNHEQEEYALE
anti-NFE2	NFE2	NFE2	1	1	HP/S/Ca	QKRQQLKQKLAALRRDIENLQDEIAYKEDEIANLKDKIEQLLS
anti-NFE2-2	NFE2	NFE2	3	2	HP/S/Cv	QKIESLKDKLANKRDKIALLRSEVASFEKEIAYLEKEIANLEN
anti-NFE2-3	NFE2	NFE2	3	2	HP/S/Cv[4]	EKIEYLKDKLAHKRNEVAQLRKEVTHKVDELTSLENEVAQLLK
anti-BACH-2	BACH1	BACH	2	1	HP/S/Ca	QKREELKSRKAYLRKEIANLKKDILNLLDDLVAHEFELVTL
anti-BACH	BACH1	BACH	2	1	HP/S/Cv	QKIQYLKQRIAELRKKIANLRKDIANLEDDAAVKEDELVHL
anti-BACH-3	BACH1	BACH	3	2	HP/S/Cv[2]	EKIEYLKDRIAELRSKIAALRNDLTHLKNDKAHKENELAHLA

[1] The only strong off-target interaction for design anti-CREB, produced in round 2, was the design•design homodimer. However, the specificity sweep produced no solutions that were significantly more specific against the homodimer. Thus, in the next round we sought to remove design homodimerization by considering only the homodimer as a competitor. In the resulting designs anti-CREB-2 and anti-CREB-3,

homodimerization was indeed no longer a problem, but global specificity was reduced. This indicates that maintaining gaps to many states simultaneously can be important.

[2] The two strong off-target competitors for anti-BACH in round 2 were Fos and NFE2. The latter was deemed too close in sequence to effectively discriminate with our models. To improve specificity against Fos, a biased specificity sweep was used with a gap offset of -10 kcal/mol for Fos (making gaps with Fos more negative than they would be, which caused competition with Fos to be more stringent). However, anti-BACH-3 still interacted with Fos more strongly than with BACH-1.

[3] The initial two designs against E4BP4 were not very stable, and this was not predicted by the models. HP/S/Cv predicted that the most stable design against E4BP4 had a Lys at the N-terminal **d** position. To address this, we temporarily adjusted the ECI for Leu-Leu at **d**-**d'** in HP/S/Cv to be more favorable by 2 kcal/mol and reran the specificity sweep procedure. Anti-E4BP4-3 was picked from this list. Although this resulted in a more hydrophobic core, there was no detectable increase in stability according to the microarray assay.

[4] The only strong off-target competitor for anti-NFE2 was ATF-4, so in this design we used a biased specificity sweep approach with a gap offset of -3 kcal/mol for ATF-4 (making gaps with ATF-4 more negative). However this design interacted with Fos, which had not previously been a strong competitor.

[5] To eliminate the only significant competitor of anti-OASIS, p21SNFT, a biased specificity sweep was run with a gap offset of -10 kcal/mol for p21SNFT. This did indeed eliminate p21SNFT as a competitor, but MafG emerged as a new strong competitor.

[6] Because the only significant competitor for the first design, anti-ZF-2, was XBP-1, we applied a biased specificity sweep approach with a gap offset of -10 kcal/mol for XBP-1. This successfully removed XBP-1 as a competitor and resulted in a very specific and stable design.

[7] Significant competitors for designs against ATF-3 were Fos and ATF-4, whereas the models considered JUN and ATF2 families more likely to interact. To bias the specificity sweep against the relevant competitors, gap offsets of +8 and +2 kcal/mol for JUN and ATF2 families respectively were imposed (making gaps with JUN and ATF2 family members less important in the optimization).

Supplementary Table 2 Melting temperature (T_m) values estimated by fitting to CD-monitored melting curves. Corresponding 95% confidence intervals are given in brackets (see section Circular dichroism). Some measurements were made in duplicate to evaluate reproducibility; duplicate measurements are marked with a number two in parentheses.

bZIP•bZIP homodimers	**T_m (° C)**	**95% CI**		**design•design homodimers**	**T_m (° C)**	**95% CI**
CHOP	36.4	[35.8 36.9]		anti-SMAF	11.6	[11.1 12.1]
BACH1	8.4	[6.9 9.9]		anti-ATF2	5.2	[1.7 8.7]
XBP-1	42.0	[41.7 42.3]		anti-ATF4	48.6	[48 49.3]
NFE2	multiple transitions			anti-LMAF	3.0	[-3.4 9.3]
ZF	31.6	[31.3 31.8]		anti-ZF	22.1	[21.7 22.4]
MafB	19.8	[19.1 20.6]		anti-JUN	7.3	[6.6 8.1]
cMaf	43.1	[42.5 43.8]		anti-FOS	27.2	[26.8 27.6]
Fra2	<0	[-13.4 5.7]				
p21SNFT	33.0	[32.6 33.4]		**design•bZIP heterodimers**	**T_m (° C)**	
ATF-4	7.9	[6.1 9.7]		anti-ATF4:ATF-4	52.1	[51.4 52.8]
ATF-3	9.4	[6.4 12.3]		anti-ATF2:ATF-7	41.0	[40.4 41.6]
ATF-3(2)	6.6	[4.3 9]		anti-SMAF:MafG	37.9	[37 38.7]
Fos	10.6	[8.9 12.4]		anti-JUN:cJun	24.2	[23.4 24.9]
Fos(2)	9.0	[8.1 9.9]		anti-FOS:FOS	43.6	[42.7 44.4]
cJun	16.6	[16.0 17.3]		anti-ZF:ZF	43.0	[42.7 43.4]
cJun(2)	16.2	[15.7 16.8]				
ATF-7	31.4	[31 31.8]				
ATF-7(2)	31.7	[31.3 32.1]				
MafG	30.2	[29.7 30.8]				
MafG(2)	31.8	[31.5 32.2]				

Supplementary Table 3 Average background-corrected fluorescence values (top panel) and S_{array} values (bottom panel) from round 1 of array measurements. Peptides on the surface are in rows, those in solution in columns. Duplicate measurements are marked with a number two in parentheses. The anti-FOS peptide was tested at concentrations ranging from 80 nM to 2000 nM, as indicated in the probe names.

	ATF-2	cJun	Fos	Fra2	ATF-3	ATF-4	p21SNFT	MafG	NFE2	NFE2L1	BACH1	anti-ATF2-2	anti-ATF3	anti-ATF3-2	anti-JUN	anti-FOS	anti-SMAF-2	anti-SMAF-3	anti-NFE2	anti-FOS80	anti-FOS200	anti-FOS500	anti-FOS1000	anti-FOS2000
C/EBPα	-1210	-220	291	-790	4573	16459	2170	-341	-1513	92	-207	-819	1158	277	-406	-599	-294	80	719	204	270	542	1006	765
C/EBPβ	-2318	-543	-1388	-2407	7687	5320	2156	338	-4575	-3091	-721	-2532	-311	367	-283	357	-401	-1885	-2307	327	292	394	1885	2025
C/EBPδ	-3236	-540	-1080	-978	7598	15172	2626	-245	-1144	-575	-1533	-566	955	351	-118	-617	-131	-274	153	216	119	-174	-263	47
C/EBPγ	5156	346	733	262	21941	34209	5172	-8	-861	-717	82	8475	2588	390	616	2685	-112	1142	492	277	409	2204	6819	5538
CHOP	5110	997	5691	3996	24898	5879	18419	331	-980	-830	3778	14295	3111	438	2289	1453	-155	-139	380	285	317	1676	5433	3921
ATF-1	-1962	-947	-880	-861	-2213	-2297	-2073	-319	-3054	-2447	1971	-2297	-687	410	1454	-923	60	-1207	832	407	388	263	913	597
CREB	-6257	-1355	-1371	-2093	-4313	-3194	-3907	-671	-5053	-2797	3077	-2383	-290	420	756	-991	-316	-2506	-2083	420	374	-534	-2069	-1908
CREB-H	-933	-831	-6	-351	-235	-91	-376	-284	-708	-596	-210	3	-890	220	5	1466	-113	217	51	197	217	1359	4159	3986
CREB3	-821	-279	-1117	-1014	1397	-1810	438	-75	-816	-1099	-599	915	-1117	357	444	1225	38	212	39	346	330	927	4479	3427
ATF-6	-3780	-1124	-980	-1252	-1826	-1502	-2021	-867	-2016	-2267	-254	-992	-1229	302	-105	-897	-369	-995	-1414	289	199	-574	-908	-257
ZF	-790	296	-360	-385	3405	5529	1020	862	2730	21548	2353	4059	973	337	-48	-372	494	3841	-862	292	246	-124	-415	-416
XBP-1	-2049	-359	-727	-2537	445	-815	-1979	-294	-1705	-1383	696	-1393	-3462	335	-687	-904	-885	-970	-1292	300	296	464	1520	2020
E4BP4	-1943	-513	-932	-546	1080	-1776	306	116	-817	-1685	101	1511	-1435	306	532	-113	-154	-486	-475	248	205	302	1728	1681
ATF-2	6995	4899	5724	4636	20295	1121	5203	-266	-2236	3164	4399	6768	486	322	-303	-87	-332	433	5345	303	260	226	1282	1361
ATF-7	9594	8100	6785	7510	22271	4420	7512	-453	724	7212	6092	13903	828	299	223	462	58	1555	3605	241	223	556	2135	2013
cJun	14760	1997	27052	24951	24562	-320	11769	-334	-2590	-1941	42	532	806	285	4862	3658	1305	561	5047	267	419	2437	6728	5978
JunB	4759	449	16151	16857	18106	-758	9729	17	-219	-1815	-299	-457	-226	332	1163	1084	889	207	1225	289	273	908	3161	2901
JunD	9823	789	22889	22692	22719	-1332	11304	98	-712	-1082	203	-588	259	272	2164	1755	1268	390	2837	251	274	1211	4387	3817
Fos	13984	35015	2121	1451	6143	7327	704	-855	-1298	5427	2638	201	24396	4055	-197	35148	2324	4563	15804	842	3726	23274	38006	25564
Fra2	9788	19126	3893	609	9627	1023	266	-634	-847	1584	2030	-858	6044	1450	-107	17466	240	609	13442	512	1444	11485	26425	17567
ATF-3	19928	12050	2675	6100	195	11043	13952	181	-4022	-2556	647	-120	29694	969	1028	1568	-198	1084	-519	382	408	1836	5583	4559
ATF-4	1729	-1060	8751	-223	21845	-1508	14458	-338	-1788	27265	2517	8517	26002	595	1520	-547	43710	5986	45654	362	249	-547	-1360	-1113
ATF-5	-4832	-1941	-2288	-1926	-2946	-3322	3955	-945	-704	-997	1437	4261	-129	374	126	-1422	2217	1429	-2845	312	221	-958	-3448	-3212
B-ATF	2150	13378	463	-713	8148	4416	2425	-675	-52	3341	4338	3926	1459	322	-214	819	-118	371	360	232	254	1175	3755	3799
p21SNFT	9069	12668	298	-21	23989	8109	5699	1393	-1526	-536	3288	11316	6628	489	249	2910	26	-42	765	354	490	2749	7858	6503
HLF	-2699	-188	-1099	-829	-628	-3384	122	-474	-4778	-1520	21	-1036	-371	254	23	-634	-408	-1248	-2333	225	145	-126	-459	-203
MafG	-254	268	768	-532	3180	-193	2433	1388	11187	49005	25075	908	1654	568	595	1147	7203	11537	13977	274	235	1283	4001	3615
cMaf	-253	93	212	128	2222	1816	-1081	-39	-899	3789	5397	-1087	-167	392	35	848	283	2257	3369	334	337	1224	3534	2918
MafB	-734	-218	2279	1685	4347	-1943	-936	-472	-572	4157	11656	-968	-433	368	66	1441	324	1584	1353	360	399	1642	5263	4429
NFE2	-2475	-545	-444	-1246	-891	-115	-1827	346	15668	-1367	759	-1075	434	317	-177	161	5185	10083	35514	269	247	629	2240	1951
NFE2L1	99	-285	771	-13	-1683	3979	-770	38492	-329	4830	-126	66	3531	389	269	-75	13690	4758	1654	270	226	106	1112	1050
NFE2L3	-4487	-1629	-3241	-2831	-4049	-415	-3341	31186	13034	-3371	-1015	-1228	-1316	189	-1338	-1048	6395	-428	-1981	283	218	-589	-1905	-1728
BACH1	6186	457	1933	2078	-50	1253	896	18424	-618	332	2580	-788	2616	374	706	6630	3044	4954	11213	341	614	5078	14231	10864
anti-ATF2-2	735	-410	-874	-1497	-754	-731	3897	-171	-2764	13088	-1593	6187												
anti-ATF3	7223	1718	19633	15128	30646	16602	9409	3310	15014	44240	11233		-906											
anti-ATF3-2	579	562	13724	7513	8260	839	936	532	306	8928	295			259										
anti-JUN	2506	6966	2211	511	6447	7163	2592	926	674	15897	6820				804									
anti-FOS	-177	2685	39045	22696	4549	-975	4052	1183	-683	-6	17631					1829				270	299	941	3212	2953
anti-SMAF-2	-2070	1877	1930	-1085	-448	21908	-1262	7927	25607	42287	5227						-274							
anti-SMAF-3	-812	-280	-80	-744	-1135	-915	-802	-37	1143	11089	-95							6628						
anti-NFE2	67	-305	6307	3093	479	10427	45	2958	32984	4472	7008								21018					

	ATF-2	cJun	Fos	Fra2	ATF-3	ATF-4	p21SNFT	MafG	NFE2	NFE2L1	BACH1	anti-ATF2-2	anti-ATF3	anti-ATF3-2	anti-JUN	anti-FOS	anti-SMAF-2	anti-SMAF-3	anti-NFE2	anti-FOS80	anti-FOS200	anti-FOS500	anti-FOS1000	anti-FOS2000
C/EBPα	-0.4	-0.3	-0.2	-0.4	0.3	6.3	0.5	-0.6	-0.3	0.1	-0.9	-0.6	0.5	-0.9	-1.1	-1.0	-0.9	-0.3	0.0	-1.9	-0.1	-0.2	-0.5	-0.6
C/EBPβ	-0.8	-0.7	-1.2	-1.7	0.9	1.8	0.5	0.8	-1.9	-1.6	-1.2	-1.9	-0.5	0.2	-0.9	-0.2	-1.2	-1.8	-1.5	0.9	0.3	-0.4	-0.3	-0.2
C/EBPδ	-1.2	-0.7	-1.0	-0.6	0.9	5.7	0.7	-0.4	-0.2	-0.3	-1.7	-0.4	0.3	0.0	-0.5	-1.0	-0.5	-0.5	-0.3	-1.7	-2.4	-1.0	-1.0	-0.9
C/EBPγ	2.0	0.3	0.0	0.4	4.1	13.4	1.8	0.1	0.0	-0.4	-0.8	6.6	1.4	0.5	0.8	1.6	-0.4	0.6	-0.1	-0.3	2.1	1.5	1.3	1.1
CHOP	2.0	1.0	2.8	3.3	4.7	2.0	7.4	0.8	-0.1	-0.4	1.3	11.1	1.8	1.0	3.9	0.6	-0.6	-0.4	-0.2	-0.1	0.7	1.0	0.9	0.5
ATF-1	-0.7	-1.1	-0.9	-0.5	-1.2	-1.3	-1.3	-0.6	-1.1	-1.3	0.3	-1.7	-0.8	0.7	2.4	-1.2	0.0	-1.3	0.0	2.7	1.8	-0.5	-0.6	-0.7
CREB	-2.3	-1.5	-1.2	-1.5	-1.7	-1.6	-2.1	-1.3	-2.1	-1.5	0.9	-1.8	-0.5	0.8	1.1	-1.3	-1.0	-2.3	-1.4	3.0	1.5	-1.4	-1.5	-1.6
CREB-H	-0.3	-1.0	-0.4	-0.1	-0.8	-0.4	-0.6	-0.5	0.1	-0.3	-0.9	0.0	-0.9	-1.6	-0.3	0.6	-0.4	-0.2	-0.3	-2.1	-0.9	0.6	0.5	0.6
CREB3	-0.2	-0.4	-1.0	-0.6	-0.4	-1.1	-0.2	-0.1	0.0	-0.6	-1.1	0.8	-1.1	0.0	0.5	0.5	0.0	-0.2	-0.4	1.3	0.9	0.2	0.6	0.4
ATF-6	-1.4	-1.3	-1.0	-0.8	-1.2	-0.9	-1.3	-1.7	-0.6	-1.2	-0.9	-0.7	-1.1	-0.6	-0.5	-1.2	-1.1	-1.1	-1.1	0.0	-1.1	-1.4	-1.2	-1.0
ZF	-0.2	0.2	-0.6	-0.1	0.0	1.9	0.0	1.8	1.8	11.4	0.5	3.2	0.3	-0.2	-0.4	-0.8	1.2	2.7	-0.8	0.1	-0.4	-1.0	-1.0	-1.0
XBP-1	-0.7	-0.5	-0.8	-1.8	-0.7	-0.7	-1.3	-0.5	-0.4	-0.7	-0.4	-1.0	-2.7	-0.2	-1.6	-1.2	-2.5	-1.1	-1.0	0.2	0.4	-0.3	-0.4	-0.2
E4BP4	-0.7	-0.6	-0.9	-0.3	-0.5	-1.0	-0.3	0.3	0.0	-0.9	-0.7	1.2	-1.3	-0.6	0.7	-0.6	-0.6	-0.7	-0.6	-0.9	-1.1	-0.5	-0.3	-0.3
ATF-2	2.7	5.1	2.8	3.8	3.7	0.1	1.8	-0.5	-0.7	1.7	1.7	5.3	0.0	-0.4	-0.9	-0.6	-1.0	0.0	2.3	0.3	-0.2	-0.6	-0.5	-0.4
ATF-7	3.7	8.5	3.4	6.1	4.2	1.4	2.8	-0.9	0.8	3.8	2.6	10.8	0.3	-0.7	0.1	-0.1	0.0	0.9	1.4	-1.1	-0.8	-0.2	-0.2	-0.2
cJun	5.7	2.0	14.6	19.8	4.7	-0.5	4.6	-0.6	-0.9	-1.0	-0.8	0.5	0.2	-0.9	8.8	2.4	3.4	0.1	2.2	-0.5	2.2	1.8	1.3	1.3
JunB	1.9	0.4	8.6	13.4	3.2	-0.6	3.7	0.1	0.3	-1.0	-1.0	-0.3	-0.5	-0.3	1.8	0.3	2.3	-0.2	0.2	0.0	0.0	0.1	0.1	0.2
JunD	3.8	0.7	12.3	18.0	4.3	-0.9	4.4	0.3	0.1	-0.6	-0.7	-0.4	-0.1	-1.0	3.7	0.9	3.3	0.0	1.1	-0.9	0.0	0.5	0.5	0.5
Fos	5.4	37.1	0.8	1.3	0.6	2.6	-0.1	-1.7	-0.2	2.9	0.7	0.2	16.3	45.6	-0.7	27.0	6.2	3.3	7.6	12.5	52.9	24.0	11.4	8.4
Fra2	3.8	20.2	1.8	0.7	1.4	0.1	-0.3	-1.2	0.0	0.8	0.3	-0.6	3.8	13.5	-0.5	13.2	0.5	0.2	6.4	5.1	17.9	11.4	7.6	5.5
ATF-3	7.6	12.7	1.1	5.0	-0.7	4.1	5.5	0.4	-1.6	-1.4	-0.4	0.0	19.9	7.6	1.6	0.7	-0.7	0.5	-0.6	2.1	2.1	1.1	0.9	0.8
ATF-4	0.7	-1.2	4.5	0.0	4.1	-0.9	5.7	-0.6	-0.5	14.5	0.6	6.6	17.4	3.0	2.5	-0.9	119.3	4.4	22.6	1.7	-0.4	-1.4	-1.3	-1.3
ATF-5	-1.8	-2.2	-1.7	-1.3	-1.4	-1.7	1.3	-1.9	0.1	-0.5	0.0	3.3	-0.4	0.3	-0.1	-1.6	5.9	0.8	-1.8	0.5	-0.8	-1.8	-2.0	-2.1
B-ATF	0.9	14.1	-0.2	-0.4	1.0	1.4	0.6	-1.3	0.4	1.8	1.6	3.1	0.7	-0.4	-0.7	0.1	-0.5	0.0	-0.2	-1.3	-0.3	0.4	0.3	0.5
p21SNFT	3.5	13.4	-0.2	0.2	4.5	2.9	2.0	2.9	-0.4	-0.3	1.0	8.8	4.2	1.7	0.1	1.8	-0.1	-0.4	0.0	1.5	3.3	2.1	1.7	1.5
HLF	-1.0	-0.3	-1.0	-0.5	-0.9	-1.7	-0.4	-0.9	-2.0	-0.8	-0.8	-0.8	-0.6	-1.2	-0.3	-1.0	-1.2	-1.3	-1.5	-1.5	-2.0	-1.0	-1.0	-1.0
MafG	0.0	0.2	0.0	-0.2	-0.1	-0.4	0.6	2.9	6.0	26.0	13.2	0.7	0.8	2.6	0.8	0.4	19.5	8.8	6.7	-0.3	-0.6	0.5	0.4	0.4
cMaf	0.0	0.0	-0.3	0.3	-0.3	0.4	-0.9	0.0	0.0	2.0	2.2	-0.8	-0.4	0.5	-0.3	0.2	0.6	1.5	1.3	1.0	1.0	0.5	0.3	0.2
MafB	-0.2	-0.3	0.9	1.5	0.2	-1.1	-0.8	-0.9	0.1	2.2	5.7	-0.7	-0.6	0.2	-0.2	0.6	0.8	0.9	0.3	1.6	1.9	0.9	0.8	0.7
NFE2	-0.9	-0.7	-0.7	-0.8	-0.9	-0.4	-1.2	0.8	8.2	-0.7	-0.4	-0.8	0.0	-0.5	-0.7	-0.4	14.0	7.6	17.5	-0.5	-0.4	-0.1	-0.1	-0.2
NFE2L1	0.1	-0.4	0.0	0.2	-1.1	1.3	-0.8	79.2	0.2	2.6	-0.9	0.1	2.1	0.4	0.2	-0.6	37.3	3.4	0.5	-0.4	-0.7	-0.7	-0.5	-0.5
NFE2L3	-1.6	-1.8	-2.2	-2.0	-1.6	-0.5	-1.9	64.2	6.9	-1.8	-1.4	-0.9	-1.2	-2.0	-2.8	-1.3	17.3	-0.7	-1.4	-0.1	-0.9	-1.4	-1.5	-1.5
BACH1	2.4	0.4	0.7	1.8	-0.8	0.2	-0.1	38.0	0.1	0.2	0.6	-0.6	1.5	0.2	1.0	4.7	8.2	3.6	5.3	1.2	5.2	4.6	3.7	3.1
anti-ATF2-2	0.3	-0.5	-0.9	-1.0	-0.9	-0.6	1.2	-0.3	-1.0	6.9	-1.7	4.8												
anti-ATF3	2.8	1.7	10.5	12.1	6.0	6.3	3.6	6.9	7.9	23.5	5.5		-0.9											
anti-ATF3-2	0.3	0.5	7.2	6.1	1.1	0.0	0.0	1.2	0.6	4.7	-0.6			-1.2										
anti-JUN	1.0	7.3	0.8	0.6	0.7	2.5	0.7	2.0	0.7	8.4	3.0				1.2									
anti-FOS	0.0	2.8	21.3	18.0	0.3	-0.7	1.3	2.5	0.1	0.0	9.0					0.9				-0.4	0.4	0.2	0.2	0.2
anti-SMAF-2	-0.7	1.9	0.7	-0.7	-0.8	8.4	-1.0	16.4	13.2	22.4	2.1						-0.9							
anti-SMAF-3	-0.2	-0.4	-0.5	-0.4	-1.0	-0.7	-0.8	0.0	1.0	5.9	-0.9							4.9						
anti-NFE2	0.1	-0.4	3.1	2.6	-0.6	3.8	-0.4	6.2	16.8	2.4	3.1								10.2					

Supplementary Table 4 Average background-corrected fluorescence values (top panel) and S_{array} values (bottom panel) from round 2 of array measurements. Peptides on the surface are in rows, those in solution in columns. Duplicate measurements are marked with a number two in parentheses. The anti-XBP1 peptide was also tested at a concentration of 800 nM, as indicated in the probe name.

	C/EBPa	C/EBPb	C/EBPd	C/EBPg	CHOP	CREB	CREB3	ATF-6	ZF	XBP-1	E4BP4	ATF-2	cJun	Fos	ATF-3	ATF-4	p21SNFT	TEF	MafG	cMaf	NFE2	BACH1	anti-XBP1-2	anti-XBP1	anti-BATF	anti-SMAF	anti-E4BP4-2	anti-E4BP4	anti-C/EBPγ	anti-C/EBPγ-2	anti-ATF4	anti-ATF4-2	anti-BACH-2	anti-BACH	anti-ATF2-3	anti-ZF-2	anti-CREB	anti-C/EBP-2	anti-OASIS	anti-OASIS-2	anti-C/EBPγ(2)	anti-SMAF(2)	anti-XBP1800
C/EBPa	14379	10132	19625	3902	20179	-633	-453	-540	-2415	661	-751	445	-32	2536	3711	34359	13324	446	-192	-291	-1825	-1601	133	238	-622	-379	351	118	1011	8546	2675	4290	3027	820	-2789	-895	-101	22363	-1010	-749	905	478	238
C/EBPb	12040	3043	13984	3909	42049	-841	-1299	-1071	-1722	2158	-1934	-596	-560	-1108	4086	6427	6601	-1123	-676	-129	-5213	-1075	385	461	-971	-1004	558	192	1259	8497	-2170	-1822	-2526	-597	-1430	-1809	-450	11580	952	-1294	309	55	319
C/EBPd	15952	10389	15986	7235	16730	-240	255	-497	-4881	361	-416	-879	-444	-1297	7160	34679	24971	244	-72	-3719	-1078	-2390	257	503	-1583	-588	557	-293	3168	21820	4397	2624	4397	176	-294	-1414	-874	18934	-5	-1458	2858	-5	251
C/EBPg	13810	8788	24250	1623	22187	2081	1873	1415	-214	2398	3750	6527	356	640	22896	24109	18510	1652	-73	-13	-1967	56	422	520	1369	164	730	2937	23323	24328	1315	-389	3661	807	22134	-111	3935	26890	6183	6129	24063	2043	353
CHOP	19799	31078	23784	14533	5785	2709	4398	1671	9281	2844	8722	7309	1575	3997	23809	11390	26243	4399	20	1569	-1860	6763	282	495	24029	279	1064	37604	21184	18431	1951	3610	-974	1042	41197	1515	3048	30992	1782	10526	20660	911	361
ATF-1	-841	-1926	-3696	-1633	-819	15720	-1394	-631	-2320	3469	5413	-1315	-320	-532	112	-4294	-11330	-929	-112	-794	-4381	2919	684	736	-866	283	905	-119	-880	-1520	-695	-1609	-3360	642	946	-306	3149	-1469	-1944	524	-1121	1020	703
CREB	-1529	-3224	-3357	-1296	-641	17970	-319	-4369	-8696	1457	4004	-2088	-1269	-1561	-1441	-4409	-10523	-4102	-577	-1270	-6534	4000	259	482	-3341	-339	581	-1504	-524	-1899	-1782	-1786	-5286	-261	6396	-3751	2830	-1195	-320	-918	-956	419	650
CREB-H	310	-347	-102	216	26	2801	3174	2038	1727	2271	3409	66	73	-334	1993	840	3896	3424	-123	-351	-851	-426	467	537	223	101	837	1076	-451	223	358	-84	457	1077	1468	1127	2010	-811	2421	4962	-785	1200	408
CREB3	399	-1604	-821	138	103	2103	2520	269	1167	2201	877	-452	-583	-943	1259	-1027	4115	-165	-184	84	-1349	-515	377	550	-785	-108	749	117	-591	703	8138	4482	-662	-535	4802	528	1683	-1492	7749	10027	-1115	-114	399
ATF-6	-217	-1167	-1167	-670	-613	570	-208	14542	1511	9836	-147	-886	-423	-479	355	-717	-5641	-60	-331	191	-3878	-90	696	610	-1389	-213	653	526	-1008	-697	-899	-985	-1529	-680	-534	3825	-638	-934	-261	-375	-894	236	1158
ZF	133	-959	-1346	-420	682	-730	-318	3119	32237	22214	-437	705	261	-238	4145	8786	1040	701	31	-210	1888	3316	3913	1392	1146	319	558	572	4654	1968	5086	1821	-2628	-1017	30724	9988	-478	1162	-579	821	4418	1278	3886
XBP-1	669	49	-853	-181	-632	3971	271	26092	27480	31542	-162	222	67	-1328	3024	1618	-2074	2785	-173	-972	-3023	476	10565	2314	541	-227	646	360	-668	-1705	-1484	-429	-894	-1457	487	18014	20	-1757	1127	3027	-574	815	6190
E4BP4	244	-1226	1344	737	835	15649	2934	2081	1963	2245	40608	-361	-544	-811	4648	-3189	10001	2939	-320	-1819	-979	-74	478	510	-805	-618	855	5262	413	-352	-484	-1839	-56	143	7336	1712	230	-2182	1063	497	-1689	227	410
ATF-2	242	-447	-1214	2157	1323	1120	59	388	-555	3930	-562	4996	4632	3684	12382	1308	24723	959	65	660	-2829	6906	69	736	-830	-60	919	835	-229	4940	25341	4014	-941	2025	48887	1807	-378	-615	-451	262	-540	1473	640
ATF-7	4337	3878	3626	5025	6199	2765	898	1302	4957	2493	-37	7407	8616	6192	19158	9845	29216	2031	-232	694	1296	9042	316	383	-192	1640	486	1234	561	8720	14443	7965	244	433	53618	3740	580	3846	-956	3037	538	2281	374
cJun	1976	1018	2582	797	1446	3881	21	1615	6370	2653	-745	13287	2943	28144	23634	704	27604	2242	1	1494	-1682	1393	249	946	-1152	18512	497	1579	1206	9882	14654	3451	576	-428	25474	5199	1563	-417	1154	3427	514	22956	2842
JunB	642	-776	-286	-589	-139	2234	-576	1831	4287	2021	-1211	4807	716	18677	19483	-3499	22546	1889	-96	-117	-1277	-45	275	729	-1039	5859	591	496	-128	4820	13823	-659	-120	-583	12123	2124	169	-1490	67	3045	-815	7609	1651
JunD	690	-819	1030	101	779	3248	-277	1565	5963	1893	-1449	8136	829	22003	21914	-18	29892	1232	-245	1304	-858	-215	481	516	-1266	6489	454	453	139	4999	16156	1327	586	-377	8850	2718	-665	-1020	192	1699	258	7232	1082
Fos	4014	416	2099	885	3244	1392	-264	367	8015	997	-1	8114	29520	1778	3489	10139	-404	2895	-282	2130	-2478	5113	178	691	5771	3979	661	1347	8366	6282	29530	34437	3453	24319	49898	3533	5916	5173	3890	17550	7112	4833	915
Fra2	1438	-28	627	436	1302	2830	-426	1813	8316	3028	-1183	7411	17577	2955	5901	4285	2168	2200	-360	1269	-1697	2183	558	792	7880	1525	824	144	4515	13295	22082	10493	330	12409	53166	4148	4027	-1102	801	13052	3399	1443	1140
ATF-3	3521	4106	6043	13256	9384	-557	312	-1090	6442	3086	888	10483	9526	1961	676	15172	31526	797	151	482	-6967	-493	616	747	-387	1339	962	3528	6073	526	21316	22705	-4281	2880	50238	-325	605	4072	6282	18199	5734	1916	522
ATF-4	41351	14860	45224	45711	29556	162	836	-1396	27126	901	-852	1706	-483	5717	11747	-927	27759	-3262	54	10885	-1982	3517	-29	595	-588	747	748	282	8454	23208	39871	37369	622	3715	918	4099	-321	36728	944	796	6383	1329	294
ATF-5	11769	1232	13936	43585	-930	-2877	-845	-3744	-1675	-1932	-836	-2309	-1582	-2500	-2250	-4027	15658	-4280	-89	-895	-556	775	110	355	-2198	-633	522	-1703	4543	1857	5265	1630	-1829	137	-4757	-5863	-360	3613	-1074	-1727	3136	1061	72
B-ATF	4622	5606	8969	7972	16113	4414	1949	2879	7505	1769	2782	4071	16188	-582	8664	13362	19458	8602	-249	257	424	6755	307	469	14012	651	646	7437	503	-469	6057	1614	1874	4312	27785	1559	1262	3825	1871	4359	563	1650	449
p21SNFT	6622	4154	13175	4779	25657	2509	4765	1482	10063	2309	2341	7257	12525	375	19962	14457	26991	4459	1263	856	-3044	4764	725	831	15853	8521	869	8897	2080	4894	7768	7313	-1040	3809	48355	4508	7522	13474	10563	10585	1451	11301	1314
TEF	-582	-2005	-2087	-846	-327	-1793	-844	-3237	-2597	3077	-751	-1283	-935	-1822	123	-3493	-5322	3396	-419	-849	-5938	-398	60	515	-2356	-457	714	2917	-402	-646	-1846	-2058	-3865	-1713	-2792	-2797	-1150	-1515	-1024	-2561	-925	968	340
MafG	30	-714	307	-113	929	4843	-369	2886	6196	4110	113	589	1459	163	1757	1110	16893	2032	1970	69	17720	44305	560	573	6081	42793	673	2946	-603	1031	13716	584	4747	755	31517	2968	4128	-855	6806	11082	-324	42999	677
cMaf	460	222	-674	-200	-729	2295	-119	1455	2434	2665	11	1172	246	656	3639	5310	-191	1700	53	24097	-1070	9751	311	544	3	1748	619	1371	-480	11263	700	566	-142	3569	1127	1845	-397	-130	-213	802	-489	2598	426
MafB	418	-1435	-2047	-945	-1315	2019	-1270	1752	4784	3499	-523	834	23	1953	5564	-1037	-4966	2167	-154	27521	-1783	15628	606	658	-569	848	729	754	-1545	4030	382	129	-619	3601	-1693	1369	-1146	-2333	-2846	1042	-2180	1888	631
NFE2	-607	-1494	-1943	-387	-571	737	0	1107	3751	915	-1195	316	-411	-1276	-693	-719	-5788	1824	380	-558	19093	449	572	656	-766	10067	575	114	-379	-313	25019	3269	10477	30996	-3207	4144	-521	-1286	467	-112	-538	12839	1035
NFE2L1	540	-612	808	-765	-1143	6115	-197	1019	27090	1168	-298	1388	-110	1059	364	6787	-1870	1250	38273	1542	708	22	340	396	-1129	939	448	206	-894	-681	27209	1491	6634	2781	-1364	3577	-127	1463	8	858	-1276	1120	390
NFE2L3	-536	-1644	-1521	-1796	-1348	-2402	-1392	-3045	-2936	-866	-787	-2125	-1338	-1976	-2201	-1622	-15235	-3185	27392	-1132	12017	-1945	190	422	-1979	-1159	477	-1657	-1318	-1393	7553	-1925	-1925	201	-5329	-2656	-1138	-1718	-1970	-2437	-1654	569	189
BACH1	485	-190	-961	160	456	7972	377	3421	15754	4293	1412	5134	523	1517	1600	2708	5126	3448	13684	8475	-2609	3086	10529	1647	12	3092	827	5134	1349	1077	7648	1427	4770	15577	-694	5641	5151	-1300	395	4117	952	4106	4252
anti-XBP1-2	577	-482	-723	83	-277	3063	-158	6120	15814	8919	-310	28	554	-193	2805	731	-1079	3236	-60	-424	-353	9744	277																				
anti-XBP1	932	-701	-865	-532	-1010	3871	-204	6672	11306	5130	-1152	-652	990	-325	1343	1316	-3135	3086	-221	-2219	-486	2714		406																			455
anti-BATF	1552	3091	1613	6935	25631	2435	1450	62	28914	3470	-812	1959	-426	12467	5325	4116	20417	9230	10299	-85	-1484	858			-1486																		
anti-SMAF	14	-449	-441	319	-406	5857	-151	1891	4048	2717	-291	887	4517	1786	3155	1873	25246	2111	14168	2407	16335	5105				4741																5383	
anti-E4BP4-2	752	-324	-142	73	-285	4926	-53	3900	2104	2189	1219	395	507	-648	3557	-672	-3406	4597	-702	-6	-1181	-734					594																
anti-E4BP4	994	-111	-707	167	2327	4962	470	3062	2764	2629	5120	54	451	415	2806	218	7575	8804	-23	43	-4	1533						12172															
anti-C/EBPγ	3702	7158	16173	22418	16943	3990	2730	3094	27028	2991	738	1480	2046	5762	12269	11299	24112	2822	305	-1612	-457	3705							1560												1752		
anti-C/EBPγ-2	15069	12318	40113	14941	13520	4375	5280	1591	12426	3464	1396	9184	5305	4767	6109	32503	24454	9770	414	32749	5733	5480								10250													
anti-ATF4	10508	2320	22113	2202	3285	6850	16657	1201	24672	4354	3072	20937	9518	16635	20245	38931	27373	2252	6694	5583	30085	24527									3541												
anti-ATF4-2	12447	897	16506	1646	4608	2106	11699	810	7739	1446	-528	6264	1867	19899	17575	37258	27212	542	-173	1428	10552	5146										4570											
anti-BACH-2	1722	-1164	-288	-743	-535	143	-758	-72	-1315	598	-1776	-839	-299	-245	1300	-3506	-11212	3	4	-552	-629	2208											22601										
anti-BACH	4253	808	770	306	-526	6946	1034	1307	863	2160	465	1622	19	14562	4288	930	7472	2119	-201	6904	31130	33014												8223									
anti-ATF2-3	397	-285	2357	3461	4947	11953	3664	5249	28725	2959	4362	32285	2933	19785	16925	5706	24497	1653	2297	52	-787	437													18633								
anti-ZF-2	-610	-367	284	113	249	6620	2013	18946	24890	23268	2000	2821	2112	2914	3294	8337	10087	526	1477	886	3045	11656														5163							
anti-CREB	-932	-991	-1725	1185	41	12013	1676	2728	479	2587	1746	-1018	328	1438	815	-1579	15076	3523	612	-219	-1507	3385															16780						
anti-C/EBP-2	33588	21296	36955	27320	25906	2011	1682	2094	18057	1834	-842	3314	547	9064	17207	44466	28553	4661	-149	2874	2558	-156																-1467					
anti-OASIS	2627	6575	10765	6089	-325	5052	27430	1417	1278	2129	8390	-238	959	3742	13676	2059	21807	1830	3717	-495	-205	-480																	269				
anti-OASIS-2	1858	1113	1578	5851	1886	3453	15076	1726	4944	2320	3346	2668	1646	3005	16413	-527	20343	1975	2120	896	-2149	3221																		-102			

	C/EBPα	C/EBPβ	C/EBPδ	C/EBPγ	CHOP	CREB	CREB3	ATF-6	ZF	XBP-1	E4BP4	ATF-2	cJun	Fos	ATF-3	ATF-4	p21SNFT	TEF	MafG	cMaf	NFE2	BACH1	anti-XBP1-2	anti-XBP1	anti-BATF	anti-SMAF	anti-E4BP4-2	anti-E4BP4	anti-C/EBPγ	anti-C/EBPγ-2	anti-ATF4	anti-ATF4-2	anti-BACH-2	anti-BACH	anti-ATF2-3	anti-ZF-2	anti-CREB	anti-C/EBP-2	anti-OASIS	anti-OASIS-2	anti-C/EBPγ(2)	anti-SMAF(2)	anti-XBP1800
C/EBPα	12.3	8.8	8.9	3.4	14.4	-1.3	-0.8	-0.8	-1.3	-1.2	-0.8	-0.4	-0.5	0.5	-0.1	9.7	0.0	-0.6	-0.5	-0.3	-0.3	-1.5	-1.6	-2.3	0.1	-1.0	-2.7	-0.5	0.5	1.8	-0.7	1.4	1.3	0.0	-1.2	-0.8	-0.4	31.8	-1.0	-0.9	0.5	-1.0	-1.9
C/EBPβ	10.2	2.7	6.3	3.4	30.6	-1.4	-1.8	-1.0	-1.1	-0.2	-2.1	-0.9	-1.1	-1.1	0.0	1.4	-0.4	-1.1	-2.3	-0.2	-1.7	-1.3	0.2	-0.7	-0.3	-1.7	-0.8	-0.4	0.7	1.8	-1.7	-1.7	-1.0	-1.0	-1.0	-1.1	-0.8	16.9	0.5	-1.2	0.0	-1.5	-1.3
C/EBPδ	13.8	9.1	7.2	6.6	11.8	-1.1	0.0	-0.8	-1.7	-1.4	-0.4	-1.1	-1.0	-1.2	0.9	9.8	0.7	-0.7	0.0	-3.1	0.0	-1.8	-0.7	-0.3	-1.0	-1.2	-0.8	-0.9	2.3	6.1	-0.3	0.6	1.8	-0.5	-0.9	-1.0	-1.3	27.1	-0.3	-1.3	1.9	-1.6	-1.8
C/EBPγ	11.8	7.7	11.1	1.2	15.9	-0.3	1.9	-0.1	-0.9	-0.1	4.2	2.9	-0.2	-0.4	5.7	6.6	0.3	-0.1	0.0	-0.1	-0.4	-0.8	0.4	-0.2	2.3	-0.4	0.7	2.1	19.7	7.0	-1.0	-1.0	1.5	0.0	2.4	-0.6	4.5	38.0	4.4	2.8	17.4	0.8	-1.0
CHOP	17.3	26.9	10.9	13.8	3.7	0.0	4.8	0.0	0.7	0.2	9.6	3.3	1.1	1.1	6.0	2.9	0.8	0.9	0.3	1.2	-0.3	1.8	-0.5	-0.4	27.0	-0.2	3.8	33.8	17.9	5.0	-0.8	1.1	-0.4	0.2	5.2	-0.1	3.4	43.7	1.1	5.3	14.9	-0.5	-1.0
ATF-1	-1.6	-1.6	-2.1	-2.0	-1.2	4.9	-1.9	-0.9	-1.3	0.6	6.0	-1.3	-0.8	-0.9	-1.2	-1.7	-1.5	-1.1	-0.2	-0.7	-1.3	0.3	2.3	1.4	-0.2	-0.2	2.3	-0.7	-1.2	-1.5	-1.4	-1.6	-1.3	-0.1	-0.7	-0.6	3.6	-1.0	-1.7	-0.2	-1.0	-0.4	1.6
CREB	-2.3	-2.7	-2.0	-1.7	-1.1	5.7	-0.7	-2.3	-2.3	-0.7	4.4	-1.7	-1.8	-1.3	-1.7	-1.8	-1.5	-2.2	-1.9	-1.1	-2.2	0.7	-0.7	-0.5	-2.9	-0.9	-0.6	-2.0	-0.8	-1.6	-1.6	-1.7	-2.1	-0.8	0.1	-1.7	3.2	-0.7	-0.5	-1.0	-0.9	-1.1	1.2
CREB-H	-0.6	-0.2	-0.4	-0.2	-0.6	0.0	3.3	0.2	-0.6	-0.1	3.8	-0.6	-0.4	-0.8	-0.6	-0.2	-0.6	0.5	-0.2	-0.3	0.1	-1.0	0.8	-0.1	1.0	-0.4	1.7	0.4	-0.8	-0.9	-1.2	-0.8	0.2	0.2	-0.6	-0.2	2.2	-0.1	1.6	2.2	-0.8	-0.2	-0.6
CREB3	-0.5	-1.3	-0.8	-0.3	-0.5	-0.3	2.6	-0.5	-0.7	-0.2	1.0	-0.9	-1.1	-1.1	-0.9	-0.8	-0.6	-0.8	-0.5	0.0	-0.1	-1.1	0.1	0.0	-0.1	-0.7	0.9	-0.5	-0.9	-0.8	0.5	1.5	-0.2	-1.0	-0.1	-0.4	1.8	-1.1	5.5	5.0	-1.0	-1.7	-0.7
ATF-6	-1.1	-0.9	-0.9	-1.1	-1.0	-0.8	-0.5	5.1	-0.6	4.8	-0.1	-1.1	-0.9	-0.9	-1.1	-0.7	-1.2	-0.8	-1.0	0.1	-1.1	-0.9	2.4	0.5	-0.8	-0.8	0.0	-0.1	-1.3	-1.2	-1.4	-1.3	-0.6	-1.1	-0.9	0.6	-1.0	-0.3	-0.4	-0.7	-0.9	-1.3	5.0
ZF	-0.7	-0.7	-1.0	-0.8	-0.1	-1.3	-0.7	0.6	4.7	12.9	-0.4	-0.3	-0.2	-0.7	0.0	2.1	-0.8	-0.5	0.3	-0.2	1.2	0.4	25.0	6.4	2.0	-0.2	-0.8	-0.1	3.6	-0.3	-0.1	0.1	-1.0	-1.4	3.7	2.4	-0.8	2.6	-0.7	-0.1	3.0	-0.1	25.4
XBP-1	-0.2	0.1	-0.8	-0.6	-1.0	0.4	0.0	9.7	3.9	19.1	-0.1	-0.5	-0.4	-1.2	-0.3	0.0	-1.0	0.3	-0.4	-0.9	-0.8	-0.7	71.8	13.4	1.3	-0.8	0.0	-0.3	-1.0	-1.5	-1.6	-1.0	-0.3	-1.7	-0.8	4.8	-0.2	-1.4	0.6	1.1	-0.6	-0.7	42.6
E4BP4	-0.6	-1.0	0.3	0.3	0.0	4.8	3.1	0.2	-0.5	-0.2	44.7	-0.8	-1.1	-1.0	0.2	-1.4	-0.2	0.3	-1.0	-1.6	0.0	-0.9	0.8	-0.3	-0.1	-1.2	1.9	4.2	0.0	-1.1	-1.4	-1.7	0.0	-0.5	0.3	0.0	0.0	-2.0	0.5	-0.2	-1.4	-1.3	-0.6
ATF-2	-0.6	-0.3	-0.9	1.7	0.4	-0.6	-0.2	-0.5	-0.9	0.9	-0.6	2.0	4.1	1.0	2.5	-0.1	0.7	-0.4	0.5	0.5	-0.7	1.8	-2.0	1.4	-0.1	-0.6	2.5	0.2	-0.6	0.6	4.3	1.3	-0.4	0.9	6.4	0.0	-0.7	0.1	-0.6	-0.4	-0.6	0.1	1.1
ATF-7	3.1	3.4	1.4	4.5	4.0	0.0	0.7	-0.1	0.0	0.0	0.0	3.3	8.1	2.1	4.6	2.4	1.0	0.0	-0.6	0.5	1.0	2.7	-0.3	-1.2	0.5	1.3	-1.5	0.5	0.1	1.9	1.9	3.3	0.1	-0.3	7.1	0.6	0.5	6.3	-1.0	1.1	0.2	1.0	-0.9
cJun	1.0	1.0	0.9	0.4	0.5	0.4	-0.3	0.0	0.2	0.1	-0.8	6.5	2.4	11.8	5.9	-0.3	0.9	0.1	0.2	1.2	-0.2	-0.3	-0.8	3.0	-0.5	20.1	-1.4	0.8	0.6	2.2	2.0	1.0	0.3	-0.9	2.9	1.0	1.7	0.4	0.6	1.4	0.2	24.8	17.6
JunB	-0.3	-0.6	-0.5	-1.0	-0.7	-0.2	-1.0	0.1	-0.1	-0.3	-1.3	1.9	0.2	7.6	4.7	-1.5	0.6	-0.1	-0.1	-0.2	-0.1	-0.9	-0.6	1.4	-0.4	6.0	-0.5	-0.2	-0.5	0.6	1.8	-1.1	0.0	-1.0	1.0	0.1	0.0	-1.1	-0.2	1.2	-0.8	7.1	8.7
JunD	-0.2	-0.6	0.1	-0.3	0.0	0.2	-0.6	0.0	0.2	-0.4	-1.6	3.7	0.3	9.1	5.4	-0.5	1.0	-0.3	-0.7	1.0	0.1	-0.9	0.9	-0.2	-0.6	6.7	-1.8	-0.2	-0.3	0.7	2.3	-0.1	0.3	-0.9	0.5	0.3	-1.0	-0.4	-0.1	0.4	0.0	6.7	4.4
Fos	2.8	0.5	0.6	0.4	1.8	-0.5	-0.6	-0.5	0.5	-1.0	0.0	3.7	29.1	0.2	-0.2	2.5	-0.9	0.3	-0.8	1.7	-0.6	1.1	-1.3	1.1	7.1	3.9	0.1	0.6	6.8	1.1	5.3	16.9	1.5	17.9	6.5	0.5	6.9	8.1	2.6	9.1	5.0	4.0	3.2
Fra2	0.5	0.1	-0.1	0.0	0.4	0.0	-0.8	0.1	0.6	0.4	-1.3	3.3	17.1	0.7	0.6	0.8	-0.7	0.1	-1.1	1.0	-0.3	0.0	1.4	1.8	9.4	1.2	1.6	-0.5	3.5	3.4	3.6	4.6	0.2	8.8	7.0	0.7	4.6	-0.5	0.3	6.6	2.3	0.1	4.9
ATF-3	2.4	3.6	2.5	12.5	6.4	-1.3	0.1	-1.0	0.3	0.4	1.0	5.0	9.0	0.2	-1.0	4.0	1.1	-0.4	0.8	0.3	-2.4	-1.1	1.8	1.5	0.3	1.0	2.9	2.6	4.8	-0.8	3.5	10.9	-1.7	1.6	6.6	-0.6	0.5	6.6	4.4	9.5	4.0	0.6	0.2
ATF-4	37.0	12.9	21.0	44.2	21.3	-1.0	0.7	-1.2	3.8	-1.0	-0.9	0.3	-1.0	1.9	2.3	-0.8	0.9	-1.9	0.4	9.0	-0.4	0.5	-2.7	0.4	0.1	0.3	0.9	-0.3	6.9	6.6	7.5	18.4	0.3	2.2	-0.7	0.7	-0.6	51.6	0.5	-0.1	4.5	-0.1	-1.5
ATF-5	9.9	1.2	6.2	42.2	-1.3	-2.1	-1.3	-2.1	-1.1	-2.9	-0.9	-1.9	-2.1	-1.7	-1.9	-1.7	0.1	-2.3	-0.1	-0.8	0.2	-0.6	-1.7	-1.4	-1.6	-1.2	-1.2	-2.2	3.5	-0.4	-0.1	0.0	-0.7	-0.5	-1.5	-2.3	-0.7	6.0	-1.0	-1.5	2.1	-0.4	-3.1
B-ATF	3.4	4.9	3.9	7.4	11.4	0.6	1.9	0.5	0.4	-0.5	3.1	1.6	15.7	-0.9	1.4	3.5	0.4	2.4	-0.7	0.2	0.6	1.8	-0.4	-0.6	16.1	0.2	0.0	6.2	0.0	-1.1	0.1	0.0	0.8	2.7	3.3	-0.1	1.3	6.2	1.1	1.9	0.2	0.3	-0.3
p21SNFT	5.2	3.7	5.9	4.2	18.4	-0.1	5.2	0.0	0.9	-0.1	2.6	3.3	12.0	-0.5	4.8	3.8	0.8	0.9	5.0	0.7	-0.8	1.0	2.6	2.1	18.1	9.0	2.0	7.5	1.4	0.6	0.5	3.0	-0.4	2.3	6.3	0.8	8.9	19.5	7.6	5.3	0.9	11.4	6.2
TEF	-1.4	-1.6	-1.4	-1.3	-0.8	-1.7	-1.3	-1.9	-1.3	0.4	-0.8	-1.3	-1.4	-1.4	-1.2	-1.5	-1.2	0.5	-1.4	-0.8	-2.0	-1.0	-2.1	-0.2	-1.8	-1.1	0.6	2.1	-0.7	-1.2	-1.7	-1.9	-1.6	-1.9	-1.2	-1.4	-1.6	-1.1	-1.0	-1.9	-0.9	-0.5	-1.1
MafG	-0.8	-0.5	-0.2	-0.5	0.1	0.8	-0.7	0.5	0.2	1.1	0.2	-0.3	1.0	-0.6	-0.7	-0.2	0.2	0.0	7.6	0.0	7.6	16.4	1.4	0.2	7.4	47.2	0.2	2.1	-0.9	-0.6	1.8	-0.5	2.0	0.0	3.8	0.3	4.8	-0.2	4.8	5.6	-0.4	47.8	1.4
cMaf	-0.4	0.3	-0.7	-0.6	-1.1	-0.2	-0.4	0.0	-0.4	0.1	0.1	0.0	-0.3	-0.3	-0.1	1.1	-0.8	-0.1	0.4	20.0	0.0	2.9	-0.3	0.0	0.8	1.4	-0.3	0.6	-0.8	2.7	-1.1	-0.5	0.0	2.1	-0.7	0.0	-0.7	0.8	-0.4	-0.1	-0.6	1.4	-0.5
MafB	-0.5	-1.1	-1.3	-1.3	-1.6	-0.3	-1.7	0.1	0.0	0.7	-0.5	-0.2	-0.5	0.2	0.4	-0.8	-1.1	0.1	-0.4	22.8	-0.3	5.2	1.7	0.8	0.1	0.4	0.7	0.1	-1.7	0.3	-1.2	-0.7	-0.2	2.1	-1.1	-0.1	-1.6	-2.2	-2.4	0.1	-1.8	0.6	1.1
NFE2	-1.4	-1.2	-1.3	-0.8	-1.0	-0.8	-0.3	-0.2	-0.2	-1.0	-1.3	-0.5	-0.9	-1.2	-1.5	-0.7	-1.2	-0.1	1.7	-0.5	8.2	-0.7	1.5	0.8	-0.1	10.7	-0.7	-0.5	-0.7	-1.1	4.3	0.9	4.4	23.0	-1.3	0.7	-0.9	-0.8	0.1	-0.6	-0.6	13.2	4.1
NFE2L1	-0.4	-0.4	0.0	-1.2	-1.4	1.2	-0.5	-0.2	3.8	-0.9	-0.3	0.1	-0.6	-0.2	-1.1	1.5	-0.9	-0.3	144.0	1.2	0.7	-0.9	-0.1	-1.1	-0.5	0.5	-1.8	-0.4	-1.2	-1.2	4.8	0.0	2.8	1.5	-1.0	0.5	-0.4	3.0	-0.2	-0.1	-1.1	-0.3	-0.7
NFE2L3	-1.3	-1.3	-1.1	-2.2	-1.6	-2.0	-1.9	-1.8	-1.4	-2.2	-0.8	-1.8	-1.8	-1.5	-1.9	-1.0	-1.8	-1.9	103.1	-1.0	5.3	-1.6	-1.2	-0.9	-1.4	-1.8	-1.6	-2.1	-1.5	-1.4	0.4	-1.8	-0.8	-0.4	-1.6	-1.3	-1.6	-1.4	-1.7	-1.9	-1.4	-0.9	-2.2
BACH1	-0.4	-0.1	-0.8	-0.3	-0.2	1.9	0.1	0.7	1.9	1.2	1.6	2.1	0.0	0.0	-0.8	0.3	-0.5	0.5	51.6	7.0	-0.6	0.3	71.5	8.3	0.8	2.9	1.6	4.1	0.8	-0.6	0.4	-0.1	2.0	11.3	-0.9	1.1	6.0	-0.8	0.0	1.7	0.5	3.1	28.1
anti-XBP1-2	-0.3	-0.3	-0.7	-0.3	-0.8	0.1	-0.5	1.8	1.9	4.2	-0.3	-0.6	0.0	-0.7	-0.4	-0.3	-0.9	0.4	0.0	-0.4	0.3	2.9	-0.6																				
anti-XBP1	0.0	-0.5	-0.8	-0.9	-1.3	0.4	-0.5	2.0	1.1	1.7	-1.2	-1.0	0.5	-0.8	-0.8	-0.1	-1.0	0.4	-0.6	-1.9	0.2	0.2		-1.1																			-0.2
anti-BATF	0.6	2.8	0.4	6.3	18.4	-0.1	1.4	-0.6	4.1	0.6	-0.9	0.4	-0.9	4.9	0.4	0.7	0.4	2.6	38.9	-0.1	-0.2	-0.5			-0.9																		
anti-SMAF	-0.8	-0.3	-0.6	-0.1	-0.9	1.1	-0.5	0.1	-0.2	0.1	-0.3	-0.2	4.0	0.2	-0.3	0.1	0.7	0.0	53.4	1.9	7.1	1.1				4.7																4.6	
anti-E4BP4-2	-0.2	-0.2	-0.4	-0.4	-0.8	0.8	-0.4	0.9	-0.5	-0.2	1.4	-0.4	0.0	-0.9	-0.2	-0.7	-1.0	0.9	-2.4	-0.1	0.0	-1.1					-0.5																
anti-E4BP4	0.1	0.0	-0.7	-0.3	1.1	0.8	0.2	0.6	-0.4	0.1	5.7	-0.6	-0.1	-0.5	-0.4	-0.4	-0.4	2.5	0.1	0.0	0.4	-0.3						10.5															
anti-C/EBPγ	2.5	6.3	7.3	21.5	12.0	0.4	2.8	0.6	3.8	0.3	0.9	0.2	1.5	1.9	2.5	2.9	0.7	0.3	1.4	-1.4	0.3	0.6							1.0												1.1		
anti-C/EBPγ-2	13.0	10.7	18.6	14.2	9.4	0.6	5.8	0.0	1.3	0.6	1.6	4.3	4.8	1.5	0.6	9.1	0.7	2.8	1.8	27.2	2.8	1.3								2.4													
anti-ATF4	8.8	2.1	10.1	1.7	1.9	1.5	18.8	-0.1	3.4	1.2	3.4	10.6	9.0	6.7	4.9	11.0	0.9	0.1	25.4	4.6	12.7	8.7									-0.5												
anti-ATF4-2	10.6	0.9	7.4	1.2	2.8	-0.3	13.1	-0.3	0.5	-0.7	-0.5	2.7	1.4	8.2	4.1	10.5	0.9	-0.5	-0.4	1.1	4.7	1.1										1.5											
anti-BACH-2	0.7	-0.9	-0.5	-1.2	-1.0	-1.0	-1.2	-0.6	-1.1	-1.2	-1.9	-1.1	-0.8	-0.7	-0.8	-1.5	-1.5	-0.7	0.2	-0.5	0.2	0.0											9.4										
anti-BACH	3.0	0.8	0.0	-0.1	-1.0	1.6	0.9	-0.1	-0.7	-0.2	0.6	0.2	-0.5	5.8	0.1	-0.2	-0.4	0.0	-0.5	5.7	13.1	12.0												5.7									
anti-ATF2-3	-0.5	-0.1	0.8	3.0	3.1	3.4	3.9	1.5	4.1	0.3	4.8	16.6	2.4	8.1	3.9	1.2	0.7	-0.1	8.9	0.0	0.1	-0.7													1.9								
anti-ZF-2	-1.4	-0.2	-0.2	-0.3	-0.4	1.4	2.0	6.8	3.4	13.6	2.2	0.9	1.6	0.7	-0.2	2.0	-0.2	-0.5	5.8	0.7	1.7	3.7														1.0							
anti-CREB	-1.7	-0.8	-1.2	0.7	-0.5	3.5	1.6	0.5	-0.8	0.1	2.0	-1.2	-0.2	0.0	-1.0	-0.9	0.1	0.5	2.5	-0.2	-0.2	0.5															20.1						
anti-C/EBP-2	29.9	18.5	17.1	26.3	18.6	-0.3	1.6	0.2	2.3	-0.4	-0.9	1.1	0.0	3.4	4.0	12.7	0.9	1.0	-0.3	2.3	1.5	-0.9																-1.0					
anti-OASIS	1.6	5.8	4.7	5.5	-0.8	0.8	31.2	-0.1	-0.6	-0.2	9.3	-0.8	0.5	1.0	2.9	0.1	0.5	-0.1	14.2	-0.5	0.4	-1.0																	0.0				
anti-OASIS-2	0.8	1.1	0.4	5.3	0.8	0.2	17.0	0.1	0.0	-0.1	3.7	0.8	1.1	0.7	3.7	-0.6	0.4	0.0	8.2	0.7	-0.4	0.4																		-0.6			

Supplementary Table 5 Average background-corrected fluorescence values (top panel) and S_{array} values (bottom panel) from round 3 of array measurements. Peptides on the surface are in rows, those in solution in columns. Duplicate measurements are marked with a number two in parentheses.

	C/EBPα	C/EBPδ	C/EBPγ	CHOP	CREB	CREB3	ATF-6	ZF	XBP-1	E4BP4	ATF-2	ATF-7	cJun	Fos	ATF-3	ATF-4	p21SNFT	HLF	MafG	cMaf	NFE2	BACH1	anti-CREB-2	anti-CREB-3	anti-BACH-3	anti-E4BP4-3	anti-C/EBP	anti-C/EBP-3	anti-NFE2-2	anti-NFE2-3	anti-OASIS-3	anti-OASIS-4	anti-ZF	anti-ATF3-3	anti-ATF2	anti-ATF2-4	anti-CHOP	anti-ATF6	anti-LMAF-2	anti-LMAF-3	anti-LMAF	anti-PAR	anti-BATF-2	anti-BATF-3	anti-ATF2(2)	anti-LMAF(2)	anti-ZF(2)
C/EBPα	13210	14794	5579	20538	-3573	-349	-1110	-3046	129	-162	-1032	1516	111	377	1030	14650	5213	-257	-376	-1249	-1939	-1976	-101	-640	2143	175	19484	4422	-355	155	174	242	-25	5395	-1254	-340	11954	104	-48	-787	-872	-19	-1112	-2431	-843	-306	-94
C/EBPβ	13656	12534	8039	43557	-5424	-836	-2332	-934	1921	-283	-1335	2728	-258	-499	2757	6848	6411	434	-872	-1006	-6727	-2370	48	-197	245	305	20832	1479	-402	125	64	-2135	-468	5149	-628	-46	13914	163	-83	-1110	-978	123	-1572	-2798	-388	-644	-206
C/EBPδ	16058	12663	11335	19226	-3982	127	-1355	-3096	-60	-576	-1908	-900	-48	-583	3976	15766	10374	1443	-667	-4241	-1143	-2252	-323	-317	140	84	27625	4766	-866	164	172	-698	-22	5497	-927	-471	11358	124	-106	-3456	-1595	-71	-1297	-254	-775	-1321	-50
C/EBPγ	12622	18023	3251	18316	-547	3901	-105	-730	1940	3345	5637	9824	1301	2072	17973	32062	11232	3209	247	-673	-262	-351	698	35	1274	1640	28736	2178	181	248	517	1410	586	16082	1132	3701	18072	139	443	-449	359	350	2470	143	1288	622	603
CHOP	18137	17305	12237	6193	998	5479	195	2076	2039	8968	6155	13037	3221	7857	21974	6803	31993	36937	592	-238	725	3533	1177	128	2534	3108	25219	19180	2	417	455	6441	72	7075	3530	2912	20927	165	1999	330	3041	1427	1918	5556	4241	2871	35
ATF-1	-785	-2285	-380	-1290	19530	-1428	-1519	-1798	3431	5916	-1325	-1590	-276	-786	-4065	-988	-3790	-1022	-267	-1377	-4343	1983	544	227	764	232	-1572	-221	-332	229	-98	-1156	-145	-799	388	-120	-818	165	-186	-437	-458	154	-1143	-1439	297	-183	-22
CREB	-2492	-3500	-1550	-1431	24166	284	-4971	-5891	934	5504	-3179	-1697	-1444	-290	-2973	-2645	-4637	-4761	-656	-1624	-11556	1839	584	121	106	-22	-2866	-568	-101	199	-115	-256	-54	-1186	562	-407	-1353	157	-459	-397	-238	98	-3065	-6040	669	-656	108
CREB-H	-429	-71	622	-338	1520	4298	632	189	2412	3255	-525	-412	100	-399	-791	1050	1012	421	-275	-423	119	-819	356	263	508	1786	-599	-327	-792	155	888	5117	68	-1646	-269	-90	-764	160	54	-832	-749	-10	18	1351	-418	-441	88
CREB3	-50	422	358	-1656	-775	4662	-1059	656	2226	1811	-1822	-1422	-352	-989	-1797	52	-253	-980	-140	-698	230	-1547	338	-19	-21	1745	-360	-420	-512	225	1468	14325	-11	-1139	-705	-486	-1661	159	-212	-1038	-508	47	1320	1985	-310	-216	21
ATF-6	-522	-1050	-572	-908	-1652	-890	15606	632	10367	148	-1838	-924	-804	-1048	-2662	-727	-2853	-371	-258	-673	-2123	-914	15	-358	-1300	498	-556	-317	-402	185	-95	4	517	-1232	-907	-398	-1869	1467	-345	-430	-839	70	-3597	-3331	-430	-905	389
ZF	-1218	-1837	-235	164	-3135	-929	1321	6025	13890	-316	-286	397	1034	308	-50	6677	2208	-995	241	-372	2886	780	140	-232	-170	786	59	-330	-27	272	192	-935	44045	9265	249	256	627	965	586	-285	-706	319	-404	1838	-94	-44	33820
XBP-1	418	-781	221	-728	1185	-101	23320	13397	23973	768	-1655	-696	637	-543	-725	297	-2151	60	-228	-1510	-1632	-164	354	-570	-1104	1057	-653	-322	-744	227	-15	3068	1181	-212	-729	-494	-2719	2181	-756	-2186	-2028	71	-2021	-526	-264	-1098	895
E4BP4	-37	1346	1345	-108	16860	3140	670	1192	2770	35244	-1528	-700	-720	-555	-1721	-376	2473	967	-363	-1238	222	-528	-167	-321	157	807	1630	-260	-956	140	376	2519	-46	-1318	-853	-797	117	149	-221	279	-695	-51	-2017	-654	-1405	-696	-12
ATF-2	382	-604	4215	1218	-1842	-466	-477	103	3979	-407	4630	9622	6360	6200	10201	1436	7412	737	-594	-515	-1568	3863	-146	-350	912	202	11515	105	-20	257	-43	-982	-94	2288	15893	566	3454	219	-25	13479	1278	173	1509	2444	16848	2267	10
ATF-7	4211	3217	7323	7111	-73	830	5	2473	2308	156	9273	13071	12902	10117	16815	5917	11722	1509	564	-39	3279	5888	270	-162	850	572	18691	1782	90	293	146	293	158	3167	24425	8311	9653	172	384	5742	579	674	4919	4116	22663	1376	177
cJun	1272	1988	1501	1820	1703	106	179	751	2520	39	14318	23434	4173	35886	24256	548	24110	5642	31	-95	-1657	-734	864	1241	-341	557	12589	297	-588	134	1799	1136	2225	17397	2563	4664	4619	239	-292	-53	-1184	518	4792	3539	2955	155	1858
JunB	-30	97	155	-296	-207	-676	460	1210	2248	-606	5202	11126	997	20803	16463	107	25629	2138	-247	-1269	-1216	-1397	228	623	-428	703	8171	-399	-538	305	933	-2126	754	8353	831	1839	1213	254	24	-873	-559	261	6590	5779	829	-117	787
JunD	697	1078	714	388	1006	-587	164	1325	1735	-277	7662	17369	1622	27825	21844	333	23364	2556	-170	645	189	-445	254	405	-225	636	10636	-221	-216	523	1179	-1050	903	11596	302	1393	1713	228	24	-120	288	162	4922	4002	948	440	755
Fos	3548	1704	2049	4125	-820	-33	282	1737	586	59	7564	12781	33396	3087	1165	7057	-61	635	-351	1059	-1141	2666	2361	34630	18745	1533	415	1192	2169	1060	637	2170	570	35040	-535	5698	16117	184	16476	35641	10263	634	10662	10178	198	11655	432
Fra2	1461	615	1241	1409	401	-893	623	2158	2269	-201	6753	11612	20027	4411	5185	3244	-1136	1150	-222	984	-383	899	1440	18815	8467	835	-123	-7	1297	644	-252	-1659	191	20465	-1011	4584	9977	205	8673	31957	15006	398	8320	8848	207	14515	222
ATF-3	4066	4646	15837	8668	-3592	645	-1484	-274	911	333	14559	18779	12798	3479	-1831	9263	22943	1429	-45	-57	-5603	-660	867	608	1745	1093	5389	1015	-103	387	1449	7955	92	21730	536	5781	20725	153	935	2968	1006	2400	4513	2636	434	1915	78
ATF-4	35862	33317	47228	34395	-3495	1130	-2093	17038	676	-218	2659	10814	111	11242	9814	-762	23445	8053	-304	8586	-76	660	38	-328	1385	597	19941	1411	51	766	85	15012	833	43682	341	-152	33309	199	-124	-19	1262	356	6633	4306	614	1881	802
ATF-5	12591	10963	46412	-1321	-6166	-2218	-4080	-3706	-2362	-613	-2976	-1683	-1713	-2562	-3205	-2370	5510	603	-1266	-1964	1466	-878	-65	-553	-355	233	1098	-226	-1004	212	-475	-802	20	-504	-480	-478	-2249	97	-588	-1210	184	-15	-4659	-954	-269	297	-40
B-ATF	4400	7028	10871	18099	2221	2150	1758	2509	2100	2209	4181	4390	19466	544	6528	6194	6636	14240	-235	-488	1714	4512	331	-140	4697	714	7387	847	-427	214	-224	-71	88	1219	2302	13	18218	191	11858	412	1	324	7149	8749	2440	1212	116
p21SNFT	5925	10041	6911	24888	-189	5459	869	2258	1949	2567	7246	9491	14415	709	15837	7808	8758	14212	1928	-408	-1489	3238	2173	279	4965	976	15340	1843	-370	328	41	8408	719	7028	7298	5692	33127	223	6614	1209	2774	440	7082	6828	6479	3477	606
HLF	75	595	639	4668	-171	-455	-496	630	3818	1647	-1210	48	877	12	-798	1520	3625	11523	-214	-876	-1612	-145	134	-419	142	589	6304	2294	-194	271	-187	-264	86	29	-472	-252	3446	240	615	-72	-497	281	-2535	-122	71	-467	49
MafG	477	1097	1218	968	2225	536	1270	3136	4015	1596	-183	2281	2627	556	467	1876	6846	589	5847	-52	21971	29120	1777	783	397	964	146	-124	-406	355	2598	5215	365	22642	-119	266	-476	211	660	17393	6121	-17	15294	12397	70	6919	359
cMaf	-297	-885	-1	-791	-1619	-863	342	595	2572	-313	-564	-658	497	738	-332	3776	-1602	-131	-322	16014	-196	4327	92	1256	3009	184	-454	-358	4060	170	-127	-592	-63	1310	-490	2	-980	162	1045	25571	20835	196	2919	-1284	-317	15397	12
MafB	-162	-1296	-128	-1323	-766	-1336	513	2527	2994	-202	-123	-1807	580	3470	100	-87	-2950	-623	-270	21421	1380	11119	79	1531	3524	340	-2087	-462	195	330	-101	-1852	71	-727	-7	-318	32	246	786	20432	24035	169	4354	-568	-464	19611	62
NFE2	-386	-1859	-141	-1908	-2632	-500	-371	-1048	759	-358	-1662	-1153	-420	-960	-2428	655	-3446	-1089	1234	-1039	19407	-1453	415	587	25615	281	-386	-264	108	420	120	-520	4001	8995	-1356	-477	-2691	178	495	2026	663	170	-123	1418	-775	1078	3373
NFE2L1	-132	202	-588	-1192	2936	-21	-968	8911	990	-608	158	796	-329	1390	-1961	4173	-2215	-711	38564	812	2517	-909	200	543	1861	268	-793	-647	309	349	188	546	416	10573	-806	-610	-2601	136	33	638	4858	139	-1771	1862	-433	5060	432
NFE2L3	-1097	-1365	-1336	-1704	-6600	-2039	-3745	-2930	-1561	-868	-3043	-2223	-1553	-2323	-4125	111	-5146	-3135	43491	-1372	22894	-3604	-191	-139	-220	-306	-2199	-407	-599	1	-389	-2437	322	-2263	-347	-891	-1743	102	-558	-2066	-1532	44	-1858	-3155	-662	-947	158
BACH1	-343	-979	529	602	7604	487	2064	3666	3163	1691	4290	5348	780	2171	-1058	2162	2421	2250	16171	3893	-2252	2300	2436	4184	11791	1573	52	-54	1463	532	68	402	853	6761	-802	-194	-1100	834	445	5197	8827	233	3182	5345	-214	8570	640
anti-CREB-2	3426	565	1771	-181	9292	2177	349	167	2697	1097	-424	369	1299	3562	1454	456	6703	53	1376	-376	3325	4956	1282																								
anti-CREB-3	-24	6	714	-1003	10743	3594	1934	17	2107	891	-412	-339	4205	39554	5508	1248	1344	-219	1092	9720	8723	24989		852																							
anti-BACH-3	655	-18	673	-959	3107	508	326	487	3012	345	136	-574	-152	12211	1437	1599	2733	-486	-413	1191	27546	10812			4499																						
anti-E4BP4-3	-127	407	1407	-109	3974	4395	2146	83	2914	2975	-822	-882	668	157	785	881	-1046	1803	-627	-882	1406	452				1629																					
anti-C/EBP	20584	21469	21568	20690	-1977	2616	-302	143	2680	2505	3524	9706	2582	-167	890	4579	5508	13049	-467	-601	431	-1633					5674																				
anti-C/EBP-3	10762	10968	4879	15697	658	-317	919	193	1939	106	498	5439	2067	5125	6282	4427	5787	11024	-594	-1586	2412	-238						-399																			
anti-NFE2-2	-858	-1003	315	-1012	586	-1254	1558	-380	3692	-801	-873	-855	7	2470	-549	896	-2332	-63	-604	2531	1582	597							21301																		
anti-NFE2-3	-379	-1652	-1037	-2910	-666	-1247	-132	-562	1999	-320	-2642	-2156	-322	1305	-3494	2187	-3802	-1929	-511	-1201	10108	-234								924																	
anti-OASIS-3	5572	12381	5385	-374	3533	19185	2237	1671	1480	9622	2064	4019	7855	7248	8315	3467	2813	435	11150	169	6655	4291									-964																
anti-OASIS-4	2211	4412	4144	2218	5247	15999	3511	1592	2890	5416	-632	788	1174	2350	7525	6101	7237	633	4754	-560	5339	-377										26871															
anti-ZF	365	-1154	432	-2420	47	-786	2592	20272	2834	-148	-1599	-1241	2008	780	-2762	1802	-2181	-1487	-90	-1228	29941	767											7836														7695
anti-ATF3-3	7029	6925	11064	4067	2507	2810	3335	8056	3412	486	3243	4351	9894	22313	13767	16659	7978	1679	17906	1767	24378	8858												10723													
anti-ATF2	547	1841	8594	9825	18552	2679	2197	4016	1880	187	35112	32056	6294	3430	4127	4296	27166	7674	-52	508	965	172													-794										-600		
anti-ATF2-4	-199	20	8048	856	1293	-567	494	326	2497	-640	3706	15049	3614	10982	10694	1822	13543	-484	-113	-363	1590	-873														-243											
anti-CHOP	13368	10774	18768	18869	911	1353	279	1139	3383	4315	6226	9176	3639	14944	16488	12488	34190	19272	27	386	4326	-263															9341										
anti-ATF6	334	-292	385	-407	1419	-530	14359	2531	4570	97	-871	-628	411	-432	-265	810	-1630	-306	-173	-373	1763	174																1966									
anti-LMAF-2	5432	1872	2815	2753	8001	2075	-307	1250	2023	225	118	257	382	29369	2351	2313	20610	7392	-356	6391	7589	5217																	3977								
anti-LMAF-3	-54	-562	307	-774	3296	138	1235	356	2796	1806	1869	976	858	18033	1971	1228	325	1830	9261	29158	7536	6535																		20935							
anti-LMAF	140	267	70	-413	2122	-70	1108	399	1865	-428	111	-590	-90	7381	103	1686	625	-374	2183	13286	4397	4953																			2456					2647	
anti-PAR	-311	-793	647	-213	657	-687	907	1590	2415	-292	-1249	761	2200	2456	6405	2066	-2123	365	-908	-1596	-315	-82																				538					
anti-BATF-2	3976	3050	3833	1992	1257	8034	-925	-1143	5107	310	2782	4861	4139	12061	2702	5525	5226	415	8680	3679	1333	6846																					-2386				
anti-BATF-3	5996	6996	5492	5902	9898	14557	-250	1768	7118	8465	8728	7153	5984	15296	5414	8966	11336	5909	12477	-1995	11290	10739																						-824			

	C/EBPα	C/EBPδ	C/EBPγ	CHOP	CREB	CREB3	ATF-6	ZF	XBP-1	E4BP4	ATF-2	ATF-7	cJun	Fos	ATF-3	ATF-4	p21SNFT	HLF	MafG	cMaf	NFE2	BACH1	anti-CREB-2	anti-CREB-3	anti-BACH-3	anti-E4BP4-3	anti-C/EBP	anti-C/EBP-3	anti-NFE2-2	anti-NFE2-3	anti-OASIS-3	anti-OASIS-4	anti-ZF	anti-ATF3-3	anti-ATF2	anti-ATF2-4	anti-CHOP	anti-ATF6	anti-LMAF-2	anti-LMAF-3	anti-LMAF	anti-PAR	anti-BATF-2	anti-BATF-3	anti-ATF2(2)	anti-LMAF(2)	anti-ZF(2)
C/EBPα	12.7	8.5	3.0	13.0	-1.3	-0.5	-0.7	-1.7	-1.4	-0.6	-0.7	0.4	-0.7	-0.7	-0.1	6.7	0.3	-0.5	-0.5	-0.8	-0.8	-1.5	-1.2	-1.7	1.2	-1.1	8.5	20.3	-0.3	-1.0	0.1	0.1	-0.8	0.0	-1.8	-0.9	3.8	-1.7	-0.2	-0.6	-0.9	-1.4	-0.7	-1.2	-1.7	-0.8	-1.5
C/EBPβ	13.2	7.2	4.7	27.8	-1.8	-0.9	-1.4	-0.7	-0.3	-0.8	-0.8	1.1	-1.0	-1.1	0.4	2.6	0.5	-0.1	-1.8	-0.6	-2.0	-1.7	-0.8	-0.7	-0.5	-0.7	9.1	7.3	-0.5	-1.3	-0.1	-1.6	-2.7	-0.1	-0.6	0.2	4.5	-0.4	-0.3	-0.8	-1.0	-0.4	-0.9	-1.3	-0.7	-1.1	-2.1
C/EBPδ	15.6	7.3	7.0	12.1	-1.4	0.0	-0.9	-1.7	-1.5	-1.3	-1.2	-0.9	-0.8	-1.1	0.8	7.3	1.3	0.5	-1.3	-3.4	-0.6	-1.6	-1.9	-1.0	-0.6	-1.3	12.3	21.8	-1.5	-0.9	0.1	-0.6	-0.8	0.0	-1.2	-1.4	3.6	-1.3	-0.4	-2.7	-1.5	-1.7	-0.8	-0.5	-1.5	-1.7	-1.2
C/EBPγ	12.2	10.5	1.3	11.6	-0.4	3.6	-0.2	-0.6	-0.3	5.5	3.2	5.0	0.2	-0.1	5.3	15.9	1.4	1.5	1.1	-0.3	-0.4	-0.5	1.2	-0.2	0.4	2.4	12.8	10.4	0.9	-0.1	0.6	0.9	1.7	1.9	2.8	14.3	6.0	-0.9	1.1	-0.3	0.1	1.3	0.3	-0.4	2.6	0.1	2.5
CHOP	17.7	10.0	7.6	3.7	0.0	5.1	-0.1	0.6	-0.2	15.4	3.5	6.8	1.7	2.1	6.5	2.6	5.4	21.3	2.0	0.1	-0.2	1.9	2.7	0.0	1.6	5.9	11.1	85.3	0.5	1.4	0.5	4.5	-0.4	0.3	7.4	11.3	7.1	-0.4	5.3	0.3	2.4	9.0	0.1	1.1	8.4	2.1	-0.7
ATF-1	-1.3	-1.7	-1.2	-1.1	5.4	-1.5	-1.0	-1.1	0.6	10.0	-0.8	-1.3	-1.0	-1.2	-1.8	-1.5	-1.4	-1.0	-0.2	-0.9	-1.4	0.9	0.7	0.2	0.0	-0.9	-1.4	-0.2	-0.3	-0.3	-0.3	-0.9	-1.3	-1.1	1.3	-0.1	-0.8	-0.3	-0.6	-0.3	-0.6	-0.1	-0.7	-0.9	0.6	-0.7	-1.1
CREB	-3.0	-2.5	-2.0	-1.2	6.8	0.1	-2.7	-3.0	-0.9	9.3	-1.9	-1.4	-1.9	-1.0	-1.4	-2.4	-1.6	-3.1	-1.2	-1.1	-3.2	0.8	0.9	0.0	-0.7	-1.5	-2.0	-1.7	0.2	-0.6	-0.3	-0.3	-0.9	-1.2	1.7	-1.1	-1.0	-0.6	-1.4	-0.3	-0.4	-0.5	-1.3	-2.2	1.4	-1.1	-0.3
CREB-H	-0.9	-0.4	-0.5	-0.5	0.2	4.0	0.1	-0.2	0.0	5.4	-0.4	-0.7	-0.7	-1.0	-0.7	-0.4	-0.5	-0.1	-0.3	0.0	-0.3	-0.8	0.2	0.3	-0.3	2.8	-0.9	-0.7	-1.4	-1.0	1.2	3.5	-0.4	-1.3	0.1	0.1	-0.8	-0.5	0.0	-0.6	-0.8	-1.3	-0.4	-0.1	-0.8	-0.9	-0.5
CREB3	-0.5	-0.1	-0.7	-1.3	-0.5	4.3	-0.7	0.0	-0.1	2.8	-1.1	-1.2	-1.0	-1.2	-1.0	-1.0	-0.7	-0.9	0.1	-0.3	-0.3	-1.2	0.1	-0.3	-0.8	2.7	-0.8	-1.1	-0.7	-0.4	2.0	10.1	-0.8	-1.2	-0.8	-1.4	-1.1	-0.5	-0.7	-0.8	-0.6	-0.9	0.0	0.1	-0.6	-0.7	-0.8
ATF-6	-1.0	-1.0	-1.3	-0.8	-0.7	-1.0	7.9	0.0	4.9	-0.1	-1.1	-1.0	-1.4	-1.3	-1.3	-1.4	-1.2	-0.6	-0.2	-0.3	-0.9	-0.8	-0.9	-1.1	-2.0	-0.3	-0.9	-0.6	-0.5	-0.7	-0.3	-0.1	1.4	-1.2	-1.2	-1.1	-1.2	29.4	-1.1	-0.3	-0.9	-0.7	-1.4	-1.4	-0.8	-1.3	1.3
ZF	-1.7	-1.5	-1.1	-0.1	-1.2	-1.0	0.5	2.5	7.0	-0.9	-0.2	-0.2	0.0	-0.8	-0.5	2.5	-0.3	-0.9	1.1	0.0	0.4	0.2	-0.5	-0.8	-0.9	0.4	-0.6	-0.7	0.4	0.1	0.1	-0.7	181.7	0.7	1.1	1.4	-0.3	17.9	1.5	-0.2	-0.8	1.1	-0.5	0.1	-0.2	-0.5	190.4
XBP-1	-0.1	-0.8	-0.8	-0.7	0.1	-0.2	11.8	5.8	13.2	1.0	-1.0	-0.8	-0.3	-1.1	-0.7	-0.8	-1.1	-0.3	-0.1	-1.0	-0.7	-0.4	0.2	-1.5	-1.8	1.1	-0.9	-0.7	-1.2	-0.3	-0.2	2.1	4.2	-1.0	-0.8	-1.5	-1.5	45.7	-2.2	-1.7	-1.9	-0.7	-1.0	-0.6	-0.5	-1.5	4.1
E4BP4	-0.5	0.5	0.0	-0.3	4.6	2.9	0.2	0.2	0.2	61.4	-1.0	-0.8	-1.3	-1.1	-1.0	-1.2	-0.2	0.2	-0.5	-0.8	-0.3	-0.6	-1.4	-1.0	-0.6	0.5	0.1	-0.4	-1.7	-1.2	0.4	1.7	-0.9	-1.2	-1.1	-2.6	-0.5	-0.7	-0.7	0.2	-0.8	-1.6	-1.0	-0.7	-2.8	-1.1	-1.0
ATF-2	-0.1	-0.7	2.0	0.5	-0.8	-0.6	-0.4	-0.3	1.0	-1.0	2.7	4.9	4.1	1.4	2.8	-0.2	0.7	0.1	-1.1	-0.1	-0.7	2.1	-1.4	-1.0	0.1	-1.0	4.7	1.2	0.4	-0.1	-0.2	-0.8	-1.1	-0.6	31.3	2.5	0.7	0.9	-0.2	10.5	0.9	0.0	0.0	0.2	33.5	1.6	-0.9
ATF-7	3.7	1.6	4.2	4.3	-0.3	0.7	-0.2	0.8	-0.1	-0.1	5.4	6.9	9.1	2.9	4.9	2.1	1.5	0.5	1.9	0.3	0.5	3.3	-0.1	-0.6	0.0	-0.1	8.1	8.6	0.7	0.3	0.1	0.1	-0.1	-0.4	47.8	31.5	3.0	-0.2	0.9	4.5	0.3	3.6	1.0	0.7	45.0	0.8	0.1
cJun	0.8	0.8	0.1	0.9	0.2	0.0	-0.1	0.0	0.1	-0.3	8.3	12.6	2.4	12.5	7.3	-0.7	3.9	3.0	0.5	0.2	-0.7	-0.7	1.7	2.4	-1.1	-0.1	5.2	2.1	-0.9	-1.2	2.5	0.7	8.5	2.1	5.6	17.9	1.1	1.3	-0.9	0.0	-1.2	2.5	1.0	0.5	5.9	-0.3	9.6
JunB	-0.5	-0.3	-0.8	-0.4	-0.3	-0.8	0.1	0.3	-0.1	-1.4	3.0	5.8	0.0	6.9	4.8	-0.9	4.2	0.9	-0.2	-0.8	-0.6	-1.1	-0.2	1.1	-1.2	0.2	3.2	-1.0	-0.8	0.4	1.2	-1.6	2.4	0.5	2.2	7.3	-0.1	1.7	-0.1	-0.7	-0.7	0.6	1.5	1.2	1.7	-0.6	3.5
JunD	0.2	0.3	-0.4	0.0	0.0	-0.7	-0.1	0.3	-0.4	-0.8	4.4	9.3	0.5	9.5	6.5	-0.8	3.7	1.1	0.0	0.9	-0.3	-0.5	-0.1	0.6	-1.0	0.0	4.3	-0.2	0.0	2.4	1.6	-0.8	3.0	1.1	1.2	5.6	0.1	1.1	-0.1	-0.1	0.0	-0.1	1.0	0.7	1.9	-0.1	3.3
Fos	3.1	0.7	0.5	2.4	-0.5	-0.2	0.0	0.5	-1.1	-0.2	4.4	6.7	24.7	0.3	-0.1	2.7	-0.7	0.0	-0.5	1.3	-0.6	1.3	6.3	75.3	16.7	2.2	-0.4	6.0	5.5	7.5	0.8	1.4	1.6	5.2	-0.4	21.7	5.3	0.1	44.5	27.7	8.4	3.3	2.6	2.4	0.4	10.1	1.5
Fra2	1.0	0.0	-0.1	0.7	-0.1	-1.0	0.1	0.7	-0.1	-0.7	3.9	6.0	14.5	0.8	1.2	0.7	-0.9	0.3	-0.1	1.2	-0.4	0.3	3.5	40.8	7.1	0.5	-0.7	0.7	3.5	3.6	-0.5	-1.3	0.1	2.7	-1.4	17.6	3.1	0.5	23.3	24.8	12.4	1.6	2.0	2.1	0.4	12.7	0.3
ATF-3	3.6	2.4	10.2	5.3	-1.3	0.5	-0.9	-0.4	-0.9	0.3	8.5	10.0	9.0	0.4	-1.0	3.9	3.7	0.5	0.3	0.3	-1.7	-0.7	1.7	1.1	0.9	1.1	1.9	5.2	0.2	1.2	2.0	5.5	-0.3	2.9	1.6	22.0	7.0	-0.6	2.4	2.3	0.6	16.0	0.9	0.3	0.9	1.3	-0.5
ATF-4	35.4	19.7	32.2	21.9	-1.3	1.0	-1.3	7.5	-1.1	-0.7	1.5	5.6	-0.7	3.3	2.7	-1.4	3.7	4.4	-0.3	7.9	-0.3	0.1	-0.8	-1.0	0.5	0.0	8.7	7.0	0.6	4.7	0.0	10.5	2.7	6.8	1.3	-0.2	11.6	0.4	-0.5	0.0	0.9	1.3	1.5	0.8	1.2	1.2	3.6
ATF-5	12.1	6.2	31.6	-1.1	-2.1	-2.2	-2.3	-2.0	-2.9	-1.4	-1.8	-1.4	-2.1	-1.8	-1.5	-2.2	0.4	0.0	-2.8	-1.4	0.0	-0.8	-1.1	-1.5	-1.1	-0.9	-0.1	-0.2	-1.8	-0.5	-0.9	-0.7	-0.6	-1.1	-0.3	-1.4	-1.3	-1.9	-1.7	-0.9	0.0	-1.3	-1.7	-0.7	-0.5	-0.2	-1.2
B-ATF	3.9	3.9	6.7	11.4	0.4	1.9	0.7	0.8	-0.2	3.5	2.4	2.0	14.1	-0.7	1.6	2.3	0.6	8.0	-0.2	-0.1	0.1	2.5	0.1	-0.6	3.6	0.2	2.8	4.5	-0.5	-0.5	-0.5	-0.1	-0.4	-0.7	5.0	0.4	6.1	0.2	32.0	0.3	-0.2	1.1	1.6	2.0	4.9	0.6	-0.3
p21SNFT	5.5	5.7	3.9	15.8	-0.3	5.1	0.3	0.7	-0.3	4.2	4.2	4.9	10.2	-0.6	4.6	3.1	1.0	8.0	5.4	0.0	-0.7	1.7	5.7	0.3	3.9	0.9	6.5	8.9	-0.4	0.6	-0.1	5.9	2.3	0.3	14.7	21.7	11.5	1.0	17.8	1.0	2.1	1.9	1.6	1.5	12.9	2.7	2.5
HLF	-0.4	0.0	-0.5	2.8	-0.3	-0.6	-0.4	0.0	0.9	2.6	-0.8	-0.4	-0.1	-0.9	-0.7	-0.2	0.0	6.4	-0.1	-0.4	-0.7	-0.4	-0.5	-1.2	-0.6	-0.1	2.3	10.9	0.0	0.1	-0.4	-0.3	-0.4	-1.0	-0.3	-0.6	0.7	1.4	1.5	0.0	-0.6	0.8	-1.1	-0.5	0.2	-0.9	-0.7
MafG	0.0	0.3	-0.1	0.4	0.4	0.4	0.5	1.1	1.0	2.5	-0.2	0.8	1.2	-0.7	-0.3	0.0	0.6	0.0	15.5	0.3	5.1	17.4	4.5	1.4	-0.4	0.8	-0.6	0.2	-0.5	0.9	3.7	3.6	0.8	3.0	0.4	1.4	-0.7	0.7	1.7	13.5	4.9	-1.4	4.0	3.1	0.2	5.8	1.1
cMaf	-0.8	-0.9	-0.9	-0.8	-0.7	-0.9	0.0	0.0	0.1	-0.9	-0.4	-0.8	-0.4	-0.6	-0.6	1.0	-1.0	-0.4	-0.4	14.5	-0.4	2.4	-0.6	2.5	2.1	-1.0	-0.8	-0.8	9.8	-0.9	-0.3	-0.5	-1.0	-0.7	-0.4	0.4	-0.9	-0.4	2.7	19.9	17.3	0.2	0.4	-0.8	-0.6	13.5	-0.9
MafB	-0.6	-1.1	-1.0	-1.1	-0.5	-1.4	0.1	0.9	0.4	-0.7	-0.1	-1.5	-0.3	0.4	-0.4	-1.0	-1.2	-0.7	-0.2	19.2	0.0	6.5	-0.7	3.1	2.5	-0.7	-1.6	-1.3	0.9	0.6	-0.3	-1.4	-0.4	-1.1	0.6	-0.8	-0.5	1.5	2.0	15.9	20.0	0.0	0.8	-0.6	-0.9	17.4	-0.6
NFE2	-0.9	-1.5	-1.0	-1.5	-1.0	-0.6	-0.4	-0.8	-1.0	-1.0	-1.0	-1.1	-1.1	-1.2	-1.2	-0.6	-1.3	-1.0	3.6	-0.6	4.5	-1.2	0.3	1.0	23.1	-0.8	-0.8	-0.4	0.7	1.5	0.0	-0.5	15.8	0.6	-2.0	-1.4	-1.5	-0.1	1.2	1.6	0.4	0.0	-0.4	-0.1	-1.5	0.5	18.1
NFE2L1	-0.6	-0.2	-1.4	-1.0	0.6	-0.1	-0.7	3.8	-0.9	-1.4	0.0	0.0	-1.0	-0.4	-1.1	1.2	-1.1	-0.8	99.5	1.0	0.3	-0.8	-0.3	0.9	1.0	-0.8	-1.0	-2.1	1.2	0.8	0.1	0.3	1.0	0.9	-1.0	-1.9	-1.5	-1.0	0.0	0.5	3.9	-0.2	-0.9	0.1	-0.8	4.1	1.5
NFE2L3	-1.6	-1.2	-1.9	-1.3	-2.2	-2.1	-2.1	-1.6	-2.4	-1.9	-1.9	-1.7	-1.9	-1.7	-1.8	-0.9	-1.7	-2.2	112.1	-0.9	5.3	-2.5	-1.5	-0.6	-1.0	-2.2	-1.7	-1.0	-0.9	-2.5	-0.7	-1.8	0.6	-1.4	-0.1	-2.9	-1.2	-1.8	-1.6	-1.6	-1.5	-0.9	-0.9	-1.4	-1.3	-1.3	-0.1
BACH1	-0.8	-0.9	-0.6	0.1	1.9	0.3	0.9	1.4	0.5	2.6	2.5	2.5	-0.2	-0.1	-0.8	0.2	-0.2	1.0	42.0	3.8	-0.9	1.1	6.5	8.9	10.2	2.3	-0.6	0.5	3.8	2.5	-0.1	0.2	2.8	0.2	-1.0	-0.3	-0.9	14.9	1.1	4.1	7.2	0.4	0.5	1.1	-0.4	7.3	2.7
anti-CREB-2	3.0	0.0	0.3	-0.4	2.4	1.9	0.0	-0.2	0.2	1.6	-0.3	-0.2	0.2	0.5	0.0	-0.7	0.6	-0.3	4.0	0.0	0.5	2.7	3.0																								
anti-CREB-3	-0.5	-0.4	-0.4	-0.9	2.9	3.3	0.8	-0.3	-0.2	1.2	-0.3	-0.6	2.4	13.9	1.3	-0.3	-0.4	-0.5	3.2	8.9	1.8	14.9		1.6																							
anti-BACH-3	0.2	-0.4	-0.5	-0.9	0.6	0.4	0.0	-0.1	0.4	0.3	0.0	-0.8	-0.9	3.7	0.0	-0.1	-0.2	-0.6	-0.6	1.4	6.5	6.3			3.4																						
anti-E4BP4-3	-0.6	-0.1	0.0	-0.3	0.9	4.1	0.9	-0.3	0.3	4.9	-0.5	-0.9	-0.3	-0.8	-0.2	-0.5	-0.9	0.7	-1.2	-0.4	0.0	0.0				2.4																					
anti-C/EBP	20.1	12.6	14.2	13.1	-0.8	2.4	-0.3	-0.2	0.2	4.1	2.0	5.0	1.2	-0.9	-0.2	1.4	0.4	7.3	-0.8	-0.2	-0.2	-1.3					2.0																				
anti-C/EBP-3	10.3	6.2	2.5	9.9	-0.1	-0.4	0.3	-0.2	-0.3	-0.1	0.2	2.6	0.8	1.0	1.5	1.3	0.4	6.1	-1.1	-1.1	0.3	-0.4						-1.0																			
anti-NFE2-2	-1.3	-1.0	-0.7	-0.9	-0.1	-1.3	0.6	-0.5	0.8	-1.7	-0.6	-0.9	-0.8	0.0	-0.6	-0.5	-1.1	-0.4	-1.1	2.6	0.1	0.1							49.6																		
anti-NFE2-3	-0.9	-1.4	-1.7	-2.1	-0.5	-1.3	-0.2	-0.6	-0.3	-0.9	-1.6	-1.7	-1.0	-0.4	-1.6	0.2	-1.4	-1.5	-0.9	-0.7	2.2	-0.4								6.2																	
anti-OASIS-3	5.1	7.1	2.8	-0.5	0.8	18.1	1.0	0.5	-0.6	16.5	1.1	1.8	5.2	1.8	2.2	0.8	-0.2	-0.1	29.1	0.5	1.3	2.3									-1.6																
anti-OASIS-4	1.7	2.3	2.0	1.2	1.3	15.1	1.6	0.4	0.3	9.2	-0.4	0.0	0.1	0.0	1.9	2.2	0.7	0.0	12.6	-0.2	1.0	-0.5										18.9															
anti-ZF	-0.1	-1.1	-0.6	-1.8	-0.3	-0.9	1.2	9.0	0.3	-0.6	-1.0	-1.1	0.8	-0.6	-1.3	0.0	-1.1	-1.2	0.2	-0.8	7.1	0.2											31.7														42.6
anti-ATF3-3	6.6	3.8	6.8	2.4	0.5	2.5	1.5	3.4	0.6	0.5	1.8	2.0	6.8	7.5	3.9	7.8	0.8	0.6	46.4	1.9	5.7	5.1												0.9													
anti-ATF2	0.1	0.7	5.1	6.1	5.1	2.4	1.0	1.5	-0.3	0.0	20.5	17.5	4.0	0.4	0.9	1.3	4.5	4.1	0.3	0.8	-0.1	-0.2													-0.9										-1.2		
anti-ATF2-4	-0.7	-0.3	4.7	0.3	0.1	-0.7	0.1	-0.2	0.1	-1.4	2.1	8.0	2.0	3.2	2.9	0.0	1.9	-0.6	0.2	0.0	0.1	-0.8														-0.5											
anti-CHOP	12.9	6.1	12.2	11.9	0.0	1.2	0.0	0.2	0.6	7.2	3.6	4.7	2.0	4.7	4.8	5.6	5.8	10.9	0.5	0.7	0.7	-0.4															2.9										
anti-ATF6	-0.1	-0.5	-0.7	-0.5	0.1	-0.6	7.2	0.9	1.3	-0.2	-0.6	-0.8	-0.4	-1.0	-0.5	-0.6	-1.0	-0.5	0.0	0.0	0.1	-0.2																40.8									
anti-LMAF-2	5.0	0.8	1.0	1.5	2.1	1.8	-0.3	0.3	-0.2	0.1	0.0	-0.3	-0.5	10.1	0.3	0.2	3.2	4.0	-0.5	6.0	1.5	2.9																	10.6								
anti-LMAF-3	-0.5	-0.7	-0.7	-0.7	0.7	0.0	0.5	-0.1	0.2	2.8	1.0	0.1	-0.1	5.9	0.2	-0.3	-0.6	0.7	24.2	26.1	1.5	3.7																		16.3							
anti-LMAF	-0.3	-0.2	-0.9	-0.5	0.4	-0.2	0.4	-0.1	-0.3	-1.1	0.0	-0.8	-0.8	1.9	-0.4	-0.1	-0.6	-0.6	6.0	12.1	0.8	2.7																			1.9					1.9	
anti-PAR	-0.8	-0.8	-0.5	-0.4	-0.1	-0.8	0.3	0.4	0.0	-0.8	-0.8	0.0	0.9	0.0	1.6	0.1	-1.1	-0.1	-1.9	-1.1	-0.4	-0.3																				2.6					
anti-BATF-2	3.5	1.5	1.7	1.0	0.1	7.5	-0.7	-0.8	1.7	0.2	1.6	2.3	2.4	3.6	0.4	1.9	0.3	-0.1	22.7	3.6	0.0	3.9																					-1.1				
anti-BATF-3	5.5	3.8	2.9	3.6	2.6	13.7	-0.3	0.5	2.9	14.5	5.1	3.6	3.8	4.8	1.3	3.7	1.5	3.1	32.5	-1.4	2.5	6.3																						-0.7			

Supplementary Table 6 Calculated S_{array} scores for the complete set of 33 human bZIP measurements. Peptides on the surface are in rows, those in solution are in columns.

	C/EBPα	C/EBPβ	C/EBPδ	C/EBPγ	CHOP	ATF-1	CREB	CREB-H	CREB3	ATF-6	ZF	XBP-1	E4BP4	ATF-2	ATF-7	cJun	JunB	JunD	Fos	Fra2	ATF-3	ATF-4	ATF-5	B-ATF	p21SNFT	HLF	MafG	cMaf	MafB	NFE2	NFE2L1	NFE2L3	BACH1
C/EBPα	5.9	8.0	7.0	6.2	6.1	-0.6	-1.1	0.4	0.4	-0.5	-1.0	-1.1	0.3	0.0	0.3	0.4	-0.3	-0.1	0.3	-0.1	0.5	7.5	2.2	2.0	0.9	0.2	-0.5	0.0	-0.4	0.2	1.4	0.3	-0.5
C/EBPβ	2.8	3.8	2.2	5.0	10.7	-1.2	-1.3	0.1	-0.3	-0.3	-0.9	0.6	-0.8	-0.2	0.5	0.0	-0.1	-0.2	-0.5	0.0	0.9	2.8	0.7	3.9	0.8	-0.1	-0.1	0.2	-0.2	-0.6	-0.6	-0.4	-1.1
C/EBPδ	6.9	10.0	6.2	8.7	6.2	-0.9	-1.4	-0.5	1.5	-0.8	-1.6	-2.2	0.0	-0.8	-0.7	-0.2	-1.1	-0.9	-0.2	0.1	1.1	9.6	1.5	3.9	2.2	-0.4	-0.3	-1.3	-1.6	0.1	0.5	0.0	-1.6
C/EBPγ	3.3	7.0	7.0	1.4	5.4	-0.1	0.0	-0.5	1.9	0.3	-0.8	0.0	1.2	1.5	2.3	0.0	0.1	0.2	-0.1	1.6	5.9	13.6	24.4	8.8	1.9	0.3	0.1	0.1	-0.1	-0.6	-0.6	0.4	-0.9
CHOP	9.5	20.1	9.7	20.0	1.6	1.1	0.4	1.4	4.3	0.5	0.5	0.0	8.2	3.3	3.6	1.3	2.9	2.3	4.9	9.1	7.3	6.4	-0.3	30.5	5.1	16.6	1.3	-0.4	0.2	0.6	-0.1	-0.4	3.6
ATF-1	-0.6	-1.0	-0.9	-0.8	-0.8	11.6	5.9	-1.8	-1.2	-0.4	-0.8	1.3	3.2	-0.7	-0.9	-0.3	-0.3	-0.5	-0.8	-0.7	-0.9	-0.9	0.0	-0.4	-1.1	-0.8	-0.1	0.6	-0.2	-0.5	-0.3	-0.7	1.4
CREB	-1.4	-1.6	-1.3	-1.4	-0.9	19.4	9.0	8.1	0.0	-2.3	-2.3	0.8	3.2	-2.2	-1.1	-1.1	-1.4	-2.0	-1.4	-2.0	-1.8	-2.1	-2.5	-0.6	-1.8	-2.0	-1.9	-0.7	-1.4	-2.2	-0.8	-2.7	1.6
CREB-H	-0.5	-0.8	-0.7	-0.1	-0.9	1.9	1.2	6.7	4.8	0.6	-0.5	0.5	3.6	-0.2	-0.8	-0.3	-0.1	-0.6	-0.3	-0.5	-0.3	-0.8	0.9	-0.5	-0.4	-0.8	-0.1	-0.6	-0.3	0.5	0.0	0.4	-1.3
CREB3	0.2	-0.2	0.2	0.0	-0.2	-0.6	-0.4	3.0	1.8	-0.2	0.0	-0.2	0.1	-0.3	-0.8	0.0	-0.7	-0.1	-0.6	-1.0	0.1	0.0	0.6	-0.4	0.0	-0.1	0.0	0.7	0.0	0.6	-0.2	-0.1	-0.9
ATF-6	-1.1	-0.8	-0.7	-0.8	-0.9	-0.3	-0.3	-0.1	-1.2	8.1	0.4	10.5	-0.4	-0.9	-1.1	-1.0	-0.7	-0.7	-1.2	-0.8	-1.1	-0.9	0.0	-0.7	-1.2	-1.0	-0.3	-2.1	-1.4	-0.8	-2.6	-1.6	-1.4
ZF	-0.9	-0.9	-1.3	-0.6	-1.0	-0.8	-0.8	0.0	-1.3	1.0	7.3	19.5	0.2	-0.6	-0.3	0.4	0.7	0.4	-0.4	-0.2	-0.5	1.2	-0.2	-0.8	-0.5	-0.8	0.3	0.5	0.3	6.7	18.8	0.0	1.5
XBP-1	-2.2	-0.8	-1.7	-1.3	-1.6	1.3	1.0	-0.4	-1.5	12.5	8.4	32.0	-1.0	-1.0	-0.9	-0.3	0.0	0.0	-0.9	-0.6	-1.2	-1.3	-1.3	-1.4	-1.3	-1.1	-0.2	-1.1	-1.5	-1.8	-1.7	-0.6	-1.2
E4BP4	-0.4	-0.2	-0.2	-0.2	-0.3	14.5	7.3	2.5	3.7	0.6	-0.2	-0.1	31.0	-1.0	-1.0	-0.2	-0.3	-0.6	-1.1	-0.6	-0.2	-0.8	-1.5	-0.9	0.0	-0.2	0.5	-0.3	-0.1	-0.7	-1.1	0.0	0.0
ATF-2	0.6	0.1	-0.4	3.9	0.5	-0.7	-0.4	-0.6	-0.3	-0.3	-0.2	1.2	-1.8	2.0	1.6	4.2	4.0	4.0	2.9	6.6	3.6	0.2	0.5	1.1	1.2	0.5	0.2	1.3	0.9	0.2	2.2	-0.4	3.9
ATF-7	1.5	2.1	0.5	5.5	1.9	-0.3	-0.2	0.0	0.4	0.0	0.4	0.0	-0.4	2.7	2.8	9.8	5.0	6.7	4.8	13.3	4.7	1.6	-1.0	0.8	1.5	0.5	0.5	0.5	0.3	3.5	5.0	0.6	5.7
cJun	-0.2	0.8	0.4	1.0	0.1	1.5	1.1	0.1	0.0	0.0	0.0	0.1	-0.1	7.9	7.6	2.9	1.1	0.9	25.2	59.4	8.3	-0.9	-0.5	28.1	3.7	2.0	-0.3	0.8	0.1	-1.8	-0.3	0.0	-0.3
JunB	0.3	0.1	0.2	-0.3	0.0	-0.1	-0.1	-2.3	-1.0	0.2	0.1	-0.6	-0.9	2.3	2.6	0.4	-0.2	0.1	16.3	29.4	4.1	-0.5	0.5	18.0	3.2	0.9	-0.7	0.9	0.0	-0.3	-0.9	-0.1	0.1
JunD	0.0	0.1	0.3	0.4	-0.3	0.2	0.0	-0.6	-0.4	0.2	0.0	-0.2	-0.7	4.2	5.0	0.5	-0.1	-0.1	20.8	39.7	5.9	-0.9	-0.1	23.5	3.4	1.2	-0.1	-0.6	-0.2	-0.5	-0.3	-0.1	-0.5
Fos	1.3	0.0	0.5	2.1	1.0	1.3	0.3	0.4	0.5	-0.2	0.8	-0.3	0.5	3.3	3.7	25.2	22.3	20.3	1.5	2.3	0.8	2.6	1.2	-0.4	-0.4	1.0	0.5	2.2	4.8	-0.1	4.1	0.6	2.9
Fra2	-0.6	-1.0	-1.0	-1.0	0.0	0.9	0.5	-0.7	-0.8	0.4	0.1	0.3	-0.3	3.5	2.8	15.2	15.2	14.9	1.9	1.0	1.5	0.0	-0.3	-1.9	-0.9	0.4	0.3	0.0	3.4	-0.7	1.0	-0.4	0.7
ATF-3	1.2	3.9	0.7	14.0	3.7	0.0	-0.5	0.6	1.0	0.1	-0.4	1.6	0.6	5.0	5.3	7.3	8.7	7.1	1.8	5.2	-0.1	3.5	-0.4	1.8	3.8	0.7	0.6	1.0	2.7	-0.4	-0.6	-1.3	-0.2
ATF-4	15.1	7.3	7.9	23.1	6.5	-0.3	-0.6	1.1	0.6	-1.3	5.1	-0.9	-0.8	0.2	0.6	-0.7	-0.9	-0.9	2.9	0.9	2.5	-1.2	-0.1	3.3	1.6	2.2	-0.2	7.4	0.4	0.7	13.1	3.6	0.0
ATF-5	2.7	0.2	1.9	23.0	-1.1	-2.2	-2.5	-1.3	-1.2	-1.8	-1.5	-1.9	-1.5	-1.5	-1.6	-2.2	-2.3	-2.0	-1.8	-1.1	-1.6	-1.1	-1.6	0.5	0.4	0.0	-3.1	-0.6	-1.6	1.5	0.7	-1.3	0.2
B-ATF	1.4	4.2	1.4	9.6	4.3	1.3	1.1	0.3	2.4	0.9	0.3	-0.2	2.3	1.6	0.5	13.6	19.1	16.8	-0.3	-1.5	1.3	1.7	3.4	0.0	0.5	5.9	0.2	-2.2	0.2	0.7	3.2	1.1	3.2
p21SNFT	1.1	3.3	2.5	4.8	6.0	-0.7	-0.1	1.1	4.3	0.1	0.7	-0.2	2.3	2.7	2.2	11.7	13.4	10.4	0.0	0.4	4.8	2.2	1.8	1.3	1.2	5.8	2.0	-0.1	0.6	-0.6	0.7	-0.3	1.5
HLF	-0.3	0.0	-0.2	-0.5	0.7	-0.1	-0.5	0.2	-0.3	-0.7	0.0	0.0	0.6	-0.9	-1.0	-0.5	0.2	-0.6	-1.0	-0.9	-1.1	-0.3	-0.3	1.3	-0.2	1.5	-0.9	-0.9	-1.6	0.0	-0.4	-0.3	-0.3
MafG	-0.2	-0.3	0.0	0.0	0.2	1.2	0.8	-1.3	0.6	-0.2	0.1	0.8	1.6	0.2	-0.1	1.0	1.7	1.2	0.6	-0.7	0.0	-0.1	1.3	-0.7	0.6	-0.8	3.7	-0.2	0.4	18.0	26.6	46.7	26.2
cMaf	-0.6	-0.6	-1.1	-0.5	-0.8	0.5	0.3	-0.4	-0.9	0.0	-0.5	-0.8	-0.7	-0.2	-1.0	-0.2	0.7	0.2	0.0	-0.3	-0.3	2.0	0.2	-0.8	-1.0	-0.9	0.0	20.7	10.0	-0.4	3.1	0.7	4.3
MafB	-1.7	-1.2	-1.5	-0.9	-1.4	0.5	0.4	-0.5	-1.7	0.0	0.3	0.6	-0.5	-0.3	-1.0	-0.5	0.4	0.5	1.6	2.3	-0.3	-0.9	-0.8	-0.6	-1.0	-1.5	-0.5	20.0	6.3	0.1	4.1	0.0	8.0
NFE2	-0.8	-0.9	-1.1	-0.5	-0.7	-0.2	-0.5	-0.5	-0.3	0.4	-0.3	-0.4	-0.6	-0.7	-1.1	-1.1	-1.0	-1.0	-0.9	-0.8	-1.0	-0.4	0.3	-1.8	-1.3	-0.9	1.2	-0.4	-0.2	31.7	0.0	14.5	-0.9
NFE2L1	-0.8	-1.5	-0.5	-2.4	-1.7	2.2	1.5	-0.6	0.3	-0.3	9.4	-0.8	-2.0	0.1	0.0	-1.8	-0.8	-0.4	0.3	0.2	-1.1	2.4	0.8	-1.1	-0.7	-0.4	37.3	1.4	1.7	3.0	3.4	0.4	-0.5
NFE2L3	-0.6	-1.6	-0.7	-0.9	-0.9	-2.3	-1.3	0.1	-0.8	-1.8	-1.2	-1.7	-0.6	-1.4	-1.1	-1.4	-1.7	-1.5	-1.7	-1.5	-1.4	-0.7	-0.6	-0.7	-1.4	-1.4	45.3	0.0	-0.8	27.8	-1.1	0.7	-1.6
BACH1	0.0	-0.4	-0.5	0.9	-0.2	6.2	3.6	0.0	0.3	1.9	1.7	2.3	0.9	1.8	0.7	0.2	0.9	0.9	0.9	0.8	-0.2	0.1	2.3	0.6	0.0	1.4	17.8	7.8	7.8	-0.2	0.9	0.1	2.4

Supplementary Notes

39. Acharya, A., Ruvinov, S. B., Gal, J., Moll, J. R. & Vinson, C. A heterodimerizing leucine zipper coiled coil system for examining the specificity of a position interactions: amino acids I, V, L, N, A, and K. Biochemistry 41, 14122-31 (2002).
40. O'Shea, E. K., Rutkowski, R. & Kim, P. S. Mechanism of specificity in the Fos-Jun oncoprotein heterodimer. Cell 68, 699-708 (1992).
41. Amoutzias, G. D. et al. One billion years of bZIP transcription factor evolution: conservation and change in dimerization and DNA-binding site specificity. Mol Biol Evol 24, 827-35 (2007).
42. Acharya, A., Rishi, V., Moll, J. & Vinson, C. Experimental identification of homodimerizing B-ZIP families in Homo sapiens. J Struct Biol 155, 130-9 (2006).
43. Vinson, C. et al. Classification of human B-ZIP proteins based on dimerization properties. Mol Cell Biol 22, 6321-35 (2002).
44. John, D. M. & Weeks, K. M. van't Hoff enthalpies without baselines. Protein Sci 9, 1416-9 (2000).
45. Chen, J. R., Chang, B. H., Allen, J. E., Stiffler, M. A. & MacBeath, G. Predicting PDZ domain-peptide interactions from primary sequences. Nat Biotechnol 26, 1041-5 (2008).
46. Kortemme, T. & Baker, D. Computational design of protein-protein interactions. Curr Opin Chem Biol 8, 91-7 (2004).
47. Hou, T., Zhang, W., Case, D. A. & Wang, W. Characterization of domain-peptide interaction interface: a case study on the amphiphysin-1 SH3 domain. J Mol Biol 376, 1201-14 (2008).
48. Hou, T., Chen, K., McLaughlin, W. A., Lu, B. & Wang, W. Computational analysis and prediction of the binding motif and protein interacting partners of the Abl SH3 domain. PLoS Comput Biol 2, e1 (2006).
49. Rahi, S. J., Virnau, P., Mirny, L. A. & Kardar, M. Predicting transcription factor specificity with all-atom models. Nucleic Acids Res (2008).

50. Siggers, T. W. & Honig, B. Structure-based prediction of C2H2 zinc-finger binding specificity: sensitivity to docking geometry. Nucleic Acids Res 35, 1085-97 (2007).
51. Paillard, G., Deremble, C. & Lavery, R. Looking into DNA recognition: zinc finger binding specificity. Nucleic Acids Res 32, 6673-82 (2004).
52. Morozov, A. V., Havranek, J. J., Baker, D. & Siggia, E. D. Protein-DNA binding specificity predictions with structural models. Nucleic Acids Res 33, 5781-98 (2005).
53. Smith, C. A. & Kortemme, T. Backrub-like backbone simulation recapitulates natural protein conformational variability and improves mutant side-chain prediction. J Mol Biol 380, 742-56 (2008).
54. Friedland, G. D., Linares, A. J., Smith, C. A. & Kortemme, T. A simple model of backbone flexibility improves modeling of side-chain conformational variability. J Mol Biol 380, 757-74 (2008).
55. Aloy, P. & Russell, R. B. Interrogating protein interaction networks through structural biology. Proc Natl Acad Sci U S A 99, 5896-901 (2002).
56. Apgar, J. R., Gutwin, K. N. & Keating, A. E. Predicting helix orientation for coiled-coil dimers. Proteins 72, 1048-65 (2008).
57. Matys, V. et al. TRANSFAC: transcriptional regulation, from patterns to profiles. Nucleic Acids Res 31, 374-8 (2003).
58. Spaller, M. R. Act globally, think locally: systems biology addresses the PDZ domain. ACS Chem Biol 1, 207-10 (2006).
59. Tonikian, R. et al. A specificity map for the PDZ domain family. PLoS Biol 6, e239 (2008).
60. Noyes, M. B. et al. Analysis of homeodomain specificities allows the family-wide prediction of preferred recognition sites. Cell 133, 1277-89 (2008).
61. Berger, M. F. et al. Variation in homeodomain DNA binding revealed by high-resolution analysis of sequence preferences. Cell 133, 1266-76 (2008).
62. Tarassov, K. et al. An in vivo map of the yeast protein interactome. Science 320, 1465-70 (2008).
63. Remy, I. & Michnick, S. W. A highly sensitive protein-protein interaction assay based on Gaussia luciferase. Nat Methods 3, 977-9 (2006).
64. Ahn, S. et al. A dominant-negative inhibitor of CREB reveals that it is a general mediator of stimulus-dependent transcription of c-fos. Mol Cell Biol 18, 967-77 (1998).
65. McClain, D. L., Gurnon, D. G. & Oakley, M. G. Importance of potential interhelical salt-bridges involving interior residues for coiled-coil stability and quaternary structure. J Mol Biol 324, 257-70 (2002).
66. Moitra, J., Szilak, L., Krylov, D. & Vinson, C. Leucine is the most stabilizing aliphatic amino acid in the d position of a dimeric leucine zipper coiled coil. Biochemistry 36, 12567-73 (1997).
67. Oakley, M. G. & Kim, P. S. A buried polar interaction can direct the relative orientation of helices in a coiled coil. Biochemistry 37, 12603-10 (1998).
68. Gonzalez, L., Jr., Woolfson, D. N. & Alber, T. Buried polar residues and structural specificity in the GCN4 leucine zipper. Nat Struct Biol 3, 1011-8 (1996).